



This is to certify that the

dissertation entitled

PHOTOREDUCTION OF INACTIVE DNA PHOTOLYASE:
CORRELATED TRIPLET-DOUBLET RADICAL PAIR
POLARIZATION OF TRYPTOPHAN IN THE ENZYME
presented by

Craig Michael Essenmacher

has been accepted towards fulfillment of the requirements for

Ph. D. degree in Chemistry

Major professor

MSU is an Affirmative Action/Equal Opportunity Institution

O-12771

PHOTOREDUCTION OF INACTIVE DNA PHOTOLYASE: CORRELATED TRIPLET-DOUBLET RADICAL PAIR POLARIZATION OF TRYPTOPHAN IN THE ENZYME

By

Craig Michael Essenmacher

A DISSERTATION

Submitted to
Michigan State University
in partial fulfillment of the requirements
for the degree of

DOCTOR OF PHILOSOPHY

Department of Chemistry

1995

ABSTRACT

PHOTOREDUCTION IN DNA PHOTOLYASE: CORRELATED TRIPLET-DOUBLET RADICAL PAIR POLARIZATION OF TRYPTOPHAN IN THE ENZYME

By

Craig Michael Essenmacher

UV radiation has many harmful effects on DNA, the most significant of which is the formation of pyrimidine dimers between adjacent thymines that occur in the nucleotide sequence. All organisms have mechanisms to repair these dimers. One of the most interesting is that carried out by DNA photolyase, which repairs pyrimidine dimers through a visible light-initiated photoreaction.

During isolation of the enzyme, one electron oxidation of the flavin produces the semiquinone form of the chromophore. The enzyme can be photoreactivated to its active form by electron transfer from an amino acid side chain to the flavin semiquinone. The electron transfer reaction generates a protein bound radical that can be reduced by an exogenous electron donor to form the active enzyme.

Time resolved electron paramagnetic resonance was used to detect the transient radical and to study the photoreactivating reaction. In agreement with previous optical studies, we have identified the donor to the flavin semiquinone as tryptophan-306 by using specific deuteration, ¹⁵N labeling, and site directed mutagenesis. Previous studies have indicated that the flavin semiquinone is reduced by hydrogen atom transfer from trp-306. Utilizing spin density calculations, we have identified the transient tryptophan radical as a

cation radical, from which we conclude that electron transfer occurs in the photoreactivating reaction.

We have also found that the transient tryptophan radical is formed initially in a spin polarized state. Spin polarization results from a non-Boltzman distribution of the electron spin energy levels. The transient tryptophan radical in photolyase has certain transitions in emission, which is hallmark of a spin polarized radical. Spin polarization results from interactions between two radicals in a radical pair. The polarization in photolyase is distinct from other radical pairs because the transitions alternate between emission and absorption, and arises from a doublet-triplet radical pair. This pattern has been observed for doublet-doublet radical pairs and is explained by the presence of an exchange interaction between the radicals during the observation time by EPR. We propose that spin polarization in photolyase reflects the same phenomenom but the interaction arises from a triplet-doublet radical pair.

ACKNOWLEDGEMENTS

I greatly appreciate the financial and emotional support my parents and family gave to me during my years as a graduate student at Michigan State University. This work would not have been possible without their continuing support.

I would also like to thank Dr. Aziz Sancar and Dr. Sang-Tae Kim for their contributions to this project. All of the enzyme used in this study was provided by them. They provided enzyme to me whenever it was needed, and their hard work made my research much easier to accomplish. They also had very helpful discussions with me about the intricacies of the enzyme, and many of the projects could not have been done without their help.

Dr. Curt Hoganson, Dr. Kurt Warnecke, Dr. Matt Espe, and Dr. Mike Atamian were also very helpful to me during my graduate career. I would like to thank Dr. Kurt Warnecke for helpful discussions about electron transfer, and Dr. Matt Espe for his help with EPR theory and computers. I also appreciate the discussions I had with Dr. Curt Hoganson concerning photosynthesis and electronics. Dr. Curt Hoganson was the person responsible for setting up the time-resolved EPR instrumentation, and without his help the experiments here could not have been performed. His help to me during graduate school made my work much easier to perform, and it is greatly appreciated. I want to thank Dr. Mike Atamian training me to use EPR instrumentation, and for his preliminary work on this project.

Finally, I would like to thank my advisor Dr. G.T. Babcock for his help to me during my graduate school career. Many times during graduate school I was lost and confused, but I was allowed to struggle until I was able to solve the problem myself. Knowing when to help me and when to let me solve the problem myself gave me the ability to think independently without always relying on others. For this I am deeply grateful. I would also like to thank him for making me computer lab manager during my time in his lab. At the time I was told I was the new computer manager, I absolutely did not want the responsibility because I completely computer illiterate. By the time I left the lab, I was highly skilled in computer software, programming, and hardware. If I had not been forced to do this job, I would not have gained the valuable knowledge I have acquired through this experience. I also appreciate the time that Dr. Babcock spent with me and his patience to improve my writing skills. Through his help, I have become a much more proficient writer. Finally, I would like to thank him for making my years at Michigan State enjoyable and rewarding.

TABLE OF CONTENTS

List of Tables		viii
List of Figures		ix
-		
I. Chapter 1 Introduction		
A. Photolyase		1
B. Electron Spin Polarization	on	16
C. Correlated Radical Pair I	Polarization	20
D. References		29
II. Chapter 2 The Identification of	a Transient Tryptophan Radical	
•	n Reaction of DNA Photolyase	
		31
A. Introduction		
B. Materials and Methods		
C. Results		
D. Discussion		
E. References		
	oreduction occurs through electron	
	hydrogen atom transfer	
A. Introduction		
B. Materials and Methods		
C. Results		
D. Discussion		
E. References		96
IV. Chapter 4 The Photoreduction	Mechanism in DNA Photolyase:	
Correlated Triplet-D	Oublet Radical Pair Polarization	
Arising From Difference	ences in Hyperfine Frequencies	98
A. Introduction		
B. Materials and Methods		
C. Results		
D. Discussion		

E. References		151
V. Chapter 5 Simulation of the Tra	ansient Tryptophan EPR Signal	
	Photoreduction of Inactive Photolyase	153
A. Introduction		
B. Materials and Methods		
C. Results and Discussion		166
D. References		
VI. Appendix Listing of program	to simulate spin polarized EPR spectra.	176

LIST OF TABLES

Table 5.1 Parameters used to simulate the spectra in Figure 5.3a and Figure 5.3b169

LIST OF FIGURES

J	Mechanism of pyrimidine dimer repair in ultraviolet induced damaged DNA. PRE is the photoreactivating enzyme, and pyr pyr is a pyrimidine dimer in damaged DNA
	enzyme, and pyr pyr is a pyrimidme dimer in damaged DIVA.
Figure 1.2.	The four isomers of pyrimidine dimers.
Figure 1.3.	Possible DNA photolyase chromophores in the enzyme8
Figure 1.4.	Proposed mechanism for pyrimidine dimer repair by DNA photolyase10
Figure 1.5.	Three oxidation states of flavin adenine dinucleotide
Figure 1.6.	Proposed mechanism of photoreactivation of inactive DNA photolyase15
_	Depiction of populations of spin energy levels and EPR stick diagrams for a boltzman and spin polarized manifold.
J	Diagram of relative populations of a doublet-doublet radical pair's energy levels and the corresponding EPR stick diagram for a) CIDEP, b) CRPP, and c) interacting CIDEP-CRPP type polarizations.
Figure 2.1.	Proposed photoreduction mechanism in DNA photolyase
•	Block diagram and timing sequence for kinetic trace acquisition. a) shows the experimental setup for obtaining kinetic traces and b) shows the timing sequence that was used. The switching of the flashlamp and the WAAG board are done by a trigger pulse from the CTM-05 timing card.
	Block diagram and the timing sequence for the gated integrator setup. a) shows a block diagram of the gated integrator and b) shows the timing sequence that was used40

•	flavin radical EPR spectrum in DNA Experimental conditions were: 6.3 mW	
•	Experimental conditions were: 6.3 mW	
-	power, 9.22226 Ghz microwave frequency,	
•	constant, 3290 G centerfield, 100 G sweep,	42
2.8 G moduli	lation amplitude.	42
Figure 2.5 Kinetic trace	e of the transient radical at 3290 G. The trace in	
•	with the flashlamp as the excitation source	
,	verages. The trace in b) was taken with the YAG	
	1000 averages. Experimental conditions were:	
	rowave power, 9.22226 Ghz microwave	
	5 μs time constant, 3290 G microwave field,	
	odulation amplitude.	45
 2.0 0		
Figure 2.6. Power depen	ndence of the transient EPR signal	
-	tolyase. Experimental conditions	
•	26 Ghz microwave frequency, 35 µs time	
	B G modulation amplitude. Photolyase samples	
	with the flashlamp.	47
	F	
Figure 2.7. Light satura	ation plot for the transient radical in	
•	lyase. Experimental conditions were:	
6.3 mW mici	rowave power, 9.22226 Ghz microwave	
frequency, 3	5 μs time constant, 3290 G magnetic field,	
and 2.8 G m	odulation amplitude. Light intensity was	
measured by	exciting the sample with the flashlamp and	
placing neuti	ral density filters in front of the cavity.	50
Figure 2 & Transient FI	PR spectra in DNA photolyase. a) is a	
•	mple and b) contains tryptophan that is	
-	at the positions indicated by the asterisks	
	a) is the average of 5 scans and b) is the average of	
	xperimental conditions were: 6.3 mW	
	power, 9.22226 Ghz microwave frequency,	
•	constant, 3290 G centerfield, 100 G sweep,	
•	lation amplitude, and 1000 second scans. Boxcar	
	vere: 3 averages per point, 1 Hz flash repetition rate,	
	48 µs aperture, trigger rate of 1 Hz, and	
	g of greater than 10 Hz.	52
Ac-coupling	5 OI SI SULLI HIGH IV III.	52
Figure 2.9 Integrated to	ransient spectra for a) wild type and b)	
	photolyase samples.	57
acatorated p		
Figure 2.10 Proposed	reaction mechanism for photolyase that is derived	
-	experimental results reported here.	60

Figure 3.1.	Possible photoreduction mechanisms in photolyase67
Figure 3.2.	Calculated electron spin densities for the cation and neutral tryptophan radicals.
Figure 3.3.	Isotopically labeled samples of DNA photolyase. Isotopic labeling of the samples is described in Kim, S.T.; Sancar, A.; Essenmacher, C. and Babcock, G.T. Proc. Natl. Acad. Sci. USA 1993, 90, 8023. Experimental conditions were: 6.3 mW microwave power, 9.22226 GHz microwave frequency, 1000 sec scan, 40 scans, 2.8 G modulation amplitude, 35 µs time constant, 3220-3350 G microwave field, 3 averages, 1 Hz repetition rate, 4 µs delay, 48 µs aperture, and AC-coupling of greater than 10 Hz73
Figure 3.4.	Tryptophan mutants of DNA photolyase. Samples preparation is described in Kim, S.T.; Sancar, A.; Essenmacher, C. and Babcock, G.T. <i>Proc. Natl. Acad. Sci. USA</i> 1993 , <i>90</i> , 8023. Experimental conditions were: 6.3 mW microwave power, 9.22226 GHz microwave frequency, 1000 sec scan, 40 scans, 2.8 G modulation amplitude, 35 µs time constant, 3220-3350 G microwave field, 3 averages, 1 Hz repetition rate, 4 µs delay, 48 µs aperture, and AC-coupling of greater than 10 Hz.
Figure 3.5.	Angles used for calculation of hyperfine coupling constants for β-methylene protons of tryptophan.
Figure 3.6.	Tryptophan numbering scheme82
Figure 3.7.	Possible geometries for tryptophan β-methylene protons.
Figure 3.8.	Proposed mechanism for photoreduction in photolyase based on the experimental results presented in this chapter.
Figure 4.1.	Integrated transient spectra for a)wild type and b) deuterated photolyase samples.
Figure 4.2.	Magnetic states of triplet-doublet radical pair and the energy levels and state mixing in the coupled basis set that are formed from interactions within the radical pair.
Figure 4.3.	Triplet-doublet state mixing from precessional frequency differences in the radical pair in the absence of an exchange interaction.

Figure 4.4.	EPR stick diagrams for net and multiplet effect electron spin polarization in the presence and absence of an exchange interaction.	119
Figure 4.5.	Triplet-doublet state mixing from precessional frequency differences in the radical pair in the presence of an exchange interaction with a doublet precursor.	122
Figure 4.6.	Triplet-doublet state mixing in the presence of an exchange interaction with a doublet precursor at later reaction times.	126
Figure 4.7.	Hyperfine state mixing in a triplet-doublet radical pair with a doublet precursor.	130
_	Triplet-doublet state mixing with a quartet precursor in the resence of an exchange interaction.	134
Figure 4.9.	Reaction mechanisms for spin polarization in inactive photolyase.	137
Figure 4.10.	Possible mechanisms for recombination during DNA photolyase photoreduction.	146
Figure 4.11.	Mechanism for photoreduction in photolyase that includes doublet precursor spin polarization.	149
Figure 5.1.	Simulation of EPR spectra that are in thermal equilibrium.	158
Figure 5.2	Simulation of a spin polarized radical.	160
Figure 5.3.	Comparison of simulated and experimental spectra: (a) shows the natural abundance spectra and (b) shows the α-ring deuterated spectra. The top spectrum in each figure is the experimental spectrum and the lower spectrum is the simulated one.	168
Figure 5.4.	Comparison of simulated and experimental absorption spectra for photolyase. (a) is the natural abundance spectrum and (b) is the deuterated spectra. The top spectrum in each figure is the experimental spectrum and the bottom one is the simulated one.	173

Chapter 1

Introduction

Photolyase

Ultraviolet radiation from sunlight has deleterious effects upon cell survival rates in biological organisms. The most significant target of UV radiation is DNA¹, and all organisms have mechanisms to remove the harmful photoproducts that are formed as a result of irradiation of the cells^{2,3}. One mechanism that organisms use to reverse the effects of UV-damage to DNA is photoreactivation. Figure 1.1 shows a diagram of the basic biological mechanism^{4,5}. The photoreactivating enzyme (PRE) binds to damaged DNA (pyr \leadsto pyr), and a subsequent photon of visible light repairs the DNA followed by dissociation of the enzyme.

The most abundant of the DNA photoproducts that form upon UV-irradiation of cells is pyrimidine dimers. Pyrimidine is excited to a singlet state with an excited state lifetime of 10⁻¹² seconds^{1,6}. The excited state may decay to the triplet or directly react with a nearby pyrimidine. In DNA, unlike isolated bases, pyrimidine dimer formation can occur from either the triplet or the excited singlet state^{1,6}. Four isomers of pyrimidine dimers are shown in Figure 1.2, but the cis-syn isomer is the predominate product in double-stranded DNA^{1,6}.

DNA photolyase is an enzyme that is capable of repairing UV-induced pyrimidine dimers in DNA⁶. This class of enzymes has a molecular weight of approximately 50,000.

Figure 1.1. Mechanism of pyrimidine dimer repair in ultraviolet induced damaged DNA. PRE is the photoreactivating enzyme, and pyryr is a pyrimidine dimer in damaged DNA.

$$PRE + pyr + pyr$$

Sancar, A. Photolyase:

In Advances in Electron Transfer Chemistry; Mariano, P.E., Ed.; JAI Press: London, 1992; Vol. 2, pp. 215-272.

Figure 1.1

Figure 1.2. The four isomers of pyrimidine dimers.

cis-anti (racemic)

CH3

trans-anti

ĆH3

ΗŃ

Figure 1.2

The active enzyme contains two chromophores, flavin adenine dinucleotide in its doubly reduced form^{7,8} and either methenyltetrahydrofolate (MTHF)⁹ or 8-hydroxy-5-deazaflavin (8-HDF)^{10,11,12}. Figure 1.3 shows the molecular structure for each of these species. Figure 1.3a shows the structure for the doubly reduced flavin chromophore. This molecule can have one of two ionic forms, the singly protonated anion or the doubly protonated neutral molecule. The ionic character of the flavin chromophore in the active form of the enzyme has been proposed to be the doubly protonated neutral form of the molecule^{7,8,13}, but this assignment will be discussed later in Chapter 3. Figure 1.3b and Figure 1.3c show the molecular structures for MTHF and 8-HDF. These chromophores act as additional light harvesting chromophores in the active enzyme to enhance the absorption cross section of the enzyme, but they are not necessary for the photoreactivating mechanism to occur⁹.

Pyrimidine dimer repair by DNA photolyase has been proposed to occur by electron transfer^{13,14,15} as shown in Figure 1.4. The photoreactivating enzyme, DNA photolyase, binds to the pyrimidine dimer. Photoexcitation of either MTHF or the flavin chromophore results in an excited flavin singlet state. This state can arise from either direct photoexcitation of the flavin molecule or by photoexcitation of the folate chromophore followed by electronic energy transfer to the flavin. Electron transfer from the excited singlet flavin species to the pyrimidine dimer results in dimer splitting and dissociation of the photoreactivating enzyme^{13,14,15}.

When DNA photolyase is isolated *in vitro*, one electron oxidation of the flavin chromophore occurs. This form of the enzyme is inactive in dimer repair and dark

Figure 1.3. Possible DNA photolyase chromophores in the enzyme.

a) FADH₂

$$\begin{array}{c|c} H_3C & \begin{array}{c} R & H \\ N & N \\ \end{array} \\ H_3C & \begin{array}{c} H & N \\ N & N \\ \end{array} \\ \end{array}$$

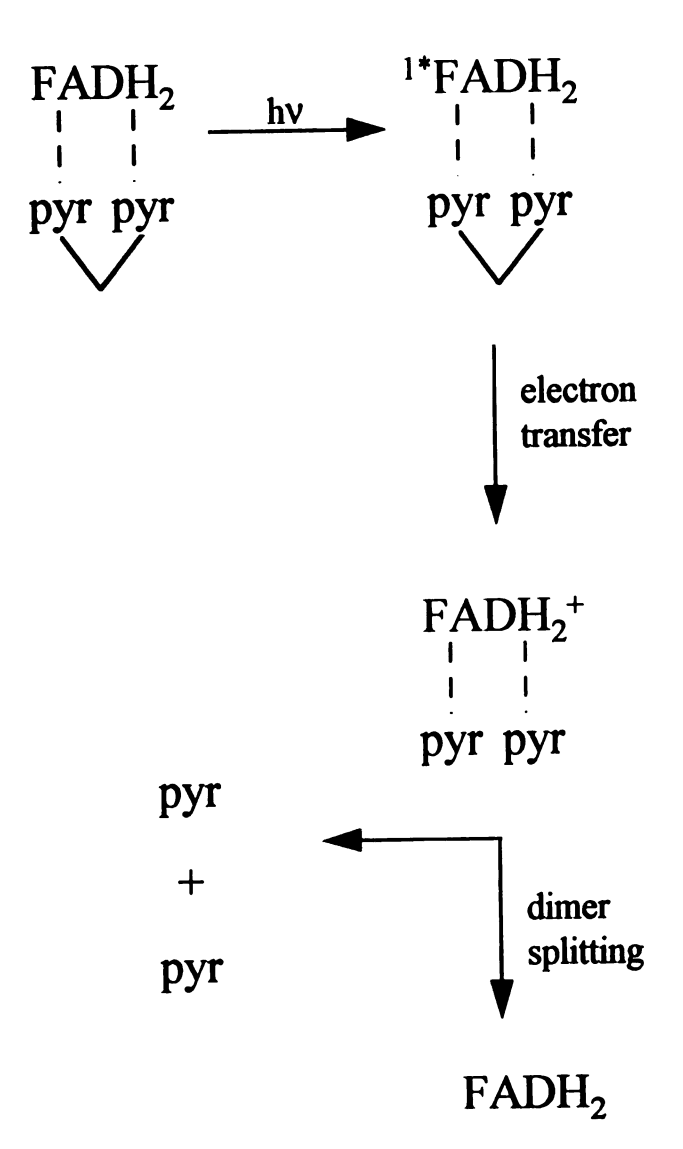
b) MTHF

C) 8-HDF

Sancar, A. *Photolyase:* In *Advances in Electron Transfer Chemistry*; Mariano, P.E. Ed.; JAI Press: London, **1992**; Vol. 2, pp. 215-272.

Figure 1.3

Figure 1.4. Proposed mechanism for pyrimidine dimer repair by DNA photolyase.



Heelis, P.F.; Okamura, T. and Sancar, A. *Biochemistry* 1990, 29, 5694.

Figure 1.4

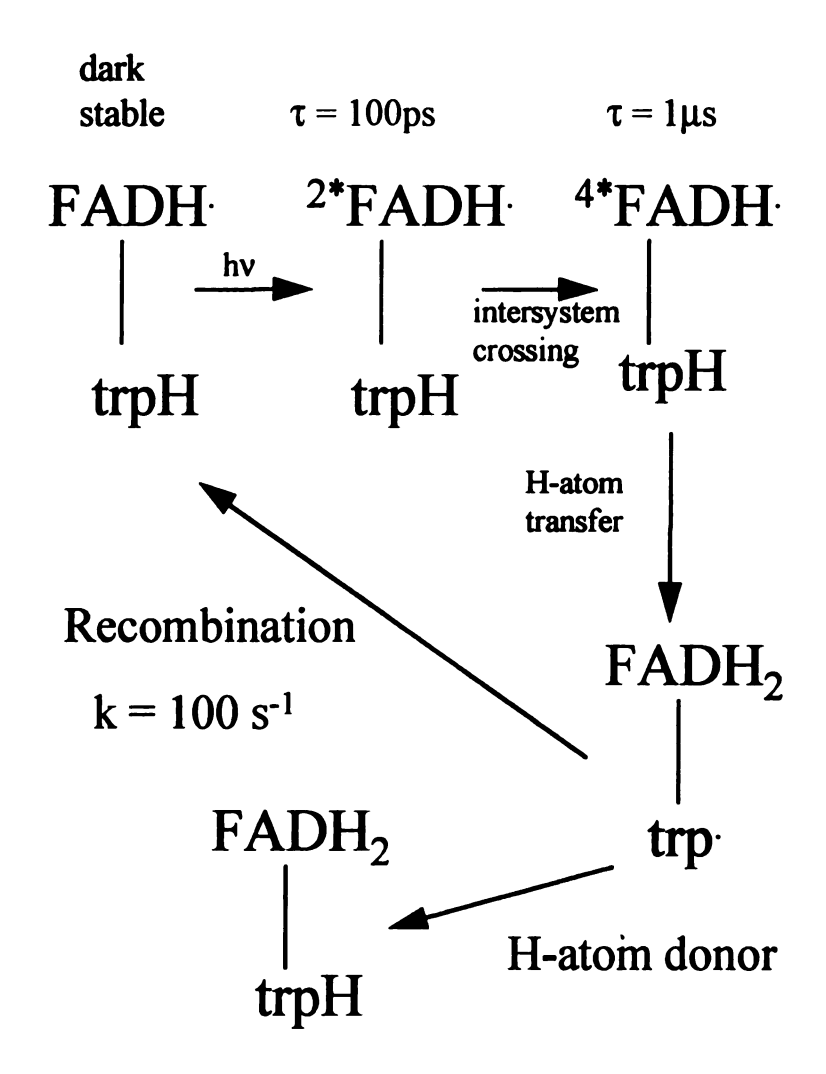
stable 16,17. The enzyme can be reactivated to the active form of the enzyme, capable of dimer repair, by photoexcitation of the inactive enzyme with visible light¹³. The three oxidation states of the flavin chromophore are shown in Figure 1.5. Figure 1.5a shows the oxidized form of the flavin, FAD. Figure 1.5b shows the singly protonated semiguinone form of the flavin, FADH. Figure 1.5c shows the doubly protonated reduced form of the enzyme that is proposed to be the active state of photolyase, FADH₂^{15,18}. A model for this reaction has been proposed and is shown in Figure 1.6¹³. Photoexcitation of either the flavin chromophore or MTHF results in an excited doublet state flavin with a lifetime of 10⁻¹⁰ seconds^{13,19}. This excited state is formed by direct photoexcitation of FADH or by excitation of MTHF followed by electronic energy transfer to FADH. In this model, the doublet flavin excited state (2°FADH') intersystem crosses to the quartet (4°FADH') which is postulated to have a lifetime of a microsecond 13,19. Hydrogen atom transfer from an amino acid donor to ⁴ FADH produces a neutral amino acid radical and FADH₂¹³. The identity of the amino acid donor has been determined to be tryptophan by optical spectroscopy^{13,20}; a further discussion of the amino acid donor will follow in Chapters 2 and 3. If no exogenous donors are present, the hydrogen atom transfer products recombine to form the inactive FADH-containing enzyme¹³ In the presence of exogenous donors, the external donor donates a hydrogen atom to the amino acid to form the active FADH₂-containing enzyme¹³.

Recently, the three dimensional crystal structure for DNA photolyase has been reported²¹. The structure shows that trp₃₀₆, implicated by optical spectroscopy to be the internal amino acid donor to FADH during photoreduction of the inactive enzyme²⁰, is

Figure 1.5. Three oxidation states of flavin adenine dinucleotide.

Figure 1.5

Figure 1.6. Proposed mechanism of photoreactivation of inactive DNA photolyase.



Heelis, P.F.; Okamura, T. and Sancar, A. *Biochemistry* **1990**, *29*, 5694.

Figure 1.6

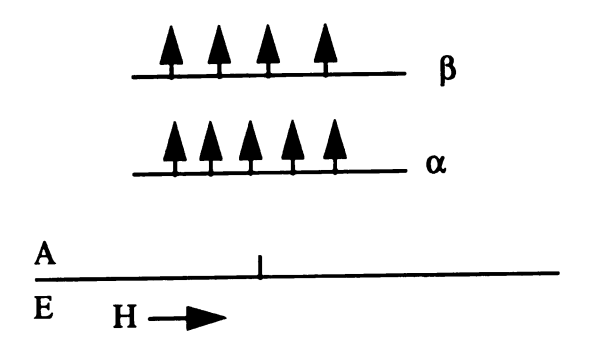
more than 13 Å away from FADH²¹. Two tryptophan residues, trp₃₅₉ and trp₃₈₂, lie between FADH and trp₃₀₆, and these intervening tryptophan residues may be intermediates during photoreduction of the inactive enzyme considering the distance between trp₃₀₆ and FADH is large²¹. The crystal structure also shows that trp₃₀₆ is near the protein surface and is accessible to the solvent²¹. This observation is consistent with the proposed mechanism for photoreduction of photolyase¹³ that is shown in Figure 1.6. In order to reduce the inactive FADH-containing enzyme to the active form (FADH₂), an exogenous hydrogen atom donor to trp₃₀₆ is necessary. Because trp₃₀₆ is near the protein surface, an external hydrogen atom donor has access to the internal donor and may be able to reduce trp₃₀₆ to form the active enzyme (see Figure 1.6).

Electron Spin Polarization

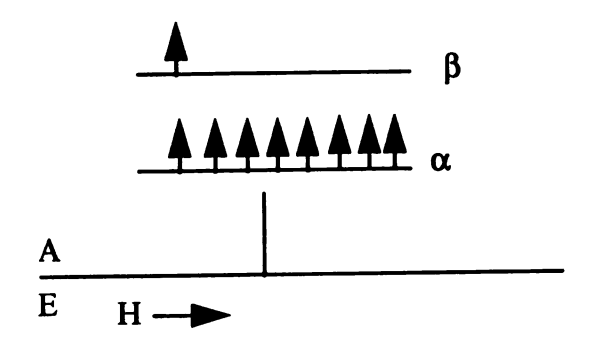
Electron spin polarization that arises from a pair of interacting doublet radicals has been observed in photosynthetic reaction centers^{22,23}. Spin polarization results in emissive and enhanced absorptive transitions in the EPR spectrum^{24,25}. Transitions in the EPR spectrum are proportional to the difference in population between the two energy levels that are involved in a particular transition. In a non-spin polarized EPR spectrum, the energy difference between an α and a β electron spin energy level is small. As a result, the difference in population between these two energy levels is also small due to the thermal equilibration of the levels. Figure 1.7a shows an EPR transition that arises from energy levels that are in Boltzman equilibria. The transition is low in intensity because the

Figure 1.7. Depiction of populations of spin energy levels and EPR stick diagrams for a boltzman and spin polarized manifold.

a) Boltzman equilibrium



b) Absorptive spin polarization



c) Emissive spin polarization

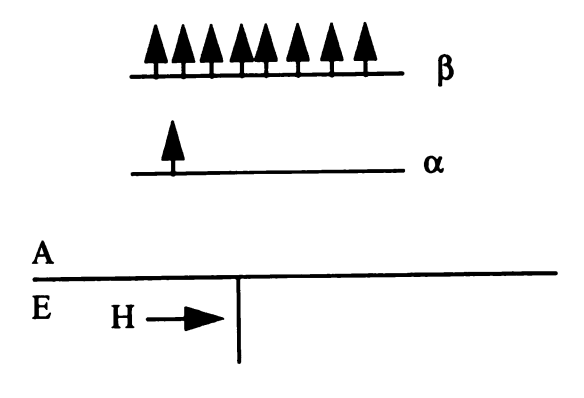


Figure 1.7

population difference between the electron spin energy levels is correspondingly small. Another characteristic of EPR transitions in a thermally equilibrated EPR spectrum is that all the transitions are in absorption. Boltzman equilibrium requires that the β electron spin energy level, which is lower in energy, must have a greater population than the higher energy α electron spin energy level. A transition between the two energy levels will be absorptive due to the greater population of the lower electron spin energy level.

Electron spin polarized EPR spectra typically have transitions that are enhanced in intensity compared to a spectrum that is determined by Boltzman equilibrium^{24,25}. The transitions may be absorptive or emissive depending on the relative populations of the two electron spin energy levels. Figure 1.7b shows the relative populations and the corresponding EPR transition that is expected for an enhanced absorptive spin polarized EPR spectrum. The population of the lower energy β electron spin energy level is much greater than that of the α electron spin energy level. The result of the large population difference between the electron spin energy levels in Figure 1.7b is that the transition is absorptive, and the intensity is much greater than what would be expected for a transition that is determined by a Boltzman distribution (compare Figure 1.7a to Figure 1.7b).

Figure 1.7c shows the relative populations of the electron spin energy levels for a spin polarized radical that is in emission. The higher energy α electron spin energy level has a much larger population than the β electron spin energy level. This large population difference results in an intense emissive transition. The intensity of the transition is much larger than the intensity of a transition that arises from a radical whose electron spin energy levels show a Boltzman population distribution (compare Figure 1.7a to Figure

1.7c) because the population difference between the electron spin energy levels is much larger in a spin polarized manifold^{24,25}.

Correlated Radical Pair Polarization

Photosynthetic reaction centers show electron spin polarization with a polarization pattern that alternates between emissive and absorptive transitions 22,26,27 . The experimental spectrum has been explained by a Correlated Radical Pair Polarization (CRPP) mechanism 22,26,27 . The spin polarized EPR spectrum arises from a pair of doublet radicals that are interacting through the electronic exchange interaction 26,27 . The coupled basis set of the radical pair has four eigenfunctions for a doublet-doublet radical pair. These eigenfunctions are represented as $|T_+>$, $|T_0>$, and $|T_->$ for the triplet states and $|T_->$ for the singlet state. State mixing between $|S_0>$ and $|T_0>$ occurs because of a difference in magnetic frequency between the two radicals of the pair. Equation 1.1 shows the mixed states that occur as a result of the magnetic frequency differences between the two members of the radical pair.

"S₀" =
$$|S_0| + \lambda |T_0| = |T_0| - \lambda |S_0|$$
 equation 1.1

"S₀" is the state that is of primarily singlet character and "T₀" is predominately triplet character. The parameter λ in equation 1.1 is the amount of state mixing that occurs. λ is

given in equation 1.2 as the sum of the difference in g-values and the hyperfine coupling frequencies of the two radicals of the radical pair.

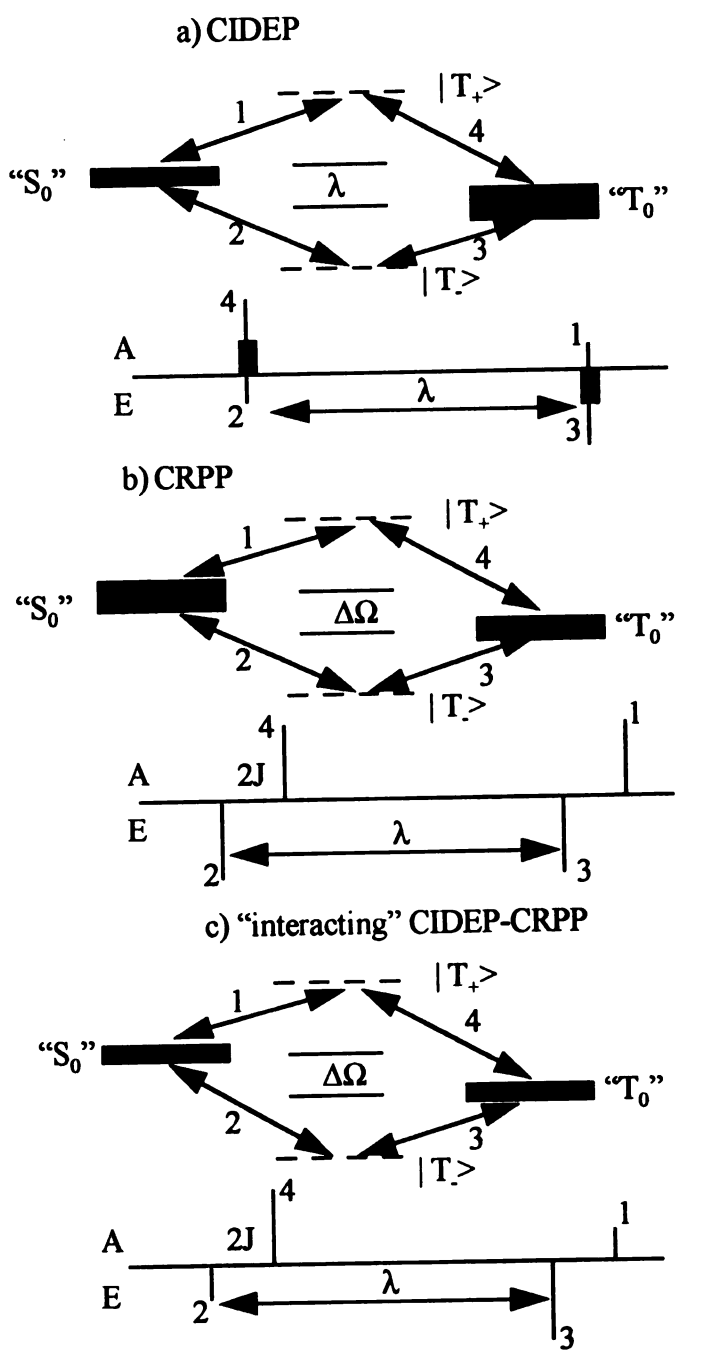
$$\lambda = g_{l}\beta H - g_{ll}\beta H + \sum_{k} A_{lk} m_{lk} - \sum_{k} A_{llk} m_{llk}$$
 equation 1.2

g is the electronic g-value of each radical, β is the Bohr magnetron, and H is the external magnetic field. A is the nuclear hyperfine frequency coupling constant and m is the electron spin quantum number.

Figure 1.8a shows the energy level diagram and the resulting EPR transitions for a doublet-doublet radical pair that was interacting but where the exchange interaction has decreased to zero during the EPR observation time period²⁶. The states denoted "S₀" and "T₀" are the mixed states that are formed by the perturbation that is shown in equations 1.1 and 1.2. $|T_+\rangle$ and $|T_-\rangle$ are the pure triplet states in the coupled basis set of the radical pair. The splitting ΔE between the "S₀" and "T₀" energy levels is equal to the perturbation in equation 1.2. ΔE is shown in equation 1.3 as the sum of the difference in magnetic frequency and the exchange interaction of the doublet-doublet radical pair²⁶. In Figure 1.8a, the exchange interaction has decreased to zero so the difference in energy between "S₀" and "T₀" is simply the difference in magnetic frequencies of the two radical pair members for the pure CIDEP case in this figure²⁶.

In photosynthetic reaction centers, the exchange interaction has been predicted to be a positive quantity²⁶. For neutral radicals, the exchange interaction should be negative (singlet lies lower in energy than the triplet)²⁵. When the radical pair is ionic, a positive

Figure 1.8. Diagram of relative populations of a doublet-doublet radical pair's energy levels and the corresponding EPR stick diagram for a) CIDEP, b) CRPP, and c) interacting CIDEP-CRPP type polarizations.



Norris, J.R.; Morris, A.L.; Thurnauer, M.C. and Tang, J. J. Chem. Phys. 1990, 92, 4239.

Figure 1.8

exchange interaction (singlet is higher in energy than the triplet) has been predicted^{25,28}. The radical pair in photosynthetic reaction centers are ionic; therefore, the exchange interaction that arises from the doublet-doublet radical pair in reaction centers should be positive. Figure 1.8a shows the energy level diagram for a radical pair that was interacting with a positive exchange interaction that has decreased to zero before the EPR observation time²⁶. "S₀" is higher in energy than "T₀" in the figure because of the positive exchange interaction²⁶.

The initial population of each state in Figure 1.8a is determined by the precursor state of the doublet-doublet radical pair due to electron spin conservation²⁶. If the radical pair is formed from a singlet precursor state, the only states that will have any initial population are the states that contain singlet character²⁶. Only "S₀" and "T₀" contain singlet character in Figure 1.8a. Therefore, only these states are initially populated. The pure triplet states in Figure 1.8a, $|T_+\rangle$ and $|T_-\rangle$, do not receive any initial population because these states do not contain any singlet character.

The transitions in Figure 1.8a are determined by the usual EPR spectroscopy selection rules ($\Delta m_I = 0 \Delta m_s = \pm 1$) where m_I is the nuclear quantum number and m_s is the electron spin quantum number. Because the exchange interaction is zero at the time of observation by EPR, transitions 1 and 3 in the figure occur at the same external magnetic field. The same is true for transitions 2 and 4. The intensity of an EPR transition is proportional to the product of the probability that a particular transition will occur and the population difference between the two levels involved in a particular transition. Since the transitions in Figure 1.8a are to the pure triplet states, $|T_+\rangle$ and $|T_-\rangle$, the transitional

probability is proportional to the amount of triplet character in the mixed " S_0 " and " T_0 " states. Transitions from " T_0 " will have a higher transition probability because this mixed state contains more triplet character than " S_0 ". The population difference is also greater from transitions that originate from " T_0 " in the CIDEP case that is illustrated in the figure. Initially with a singlet precursor, " S_0 " will receive more of the initial population because this state contains more singlet character than " T_0 ". As the radical pair evolves away from its initial spin distribution, " T_0 " receives more of the population. As a result, the transitions that arise from the " T_0 " state will show a greater EPR intensity than the transitions that arise from " S_0 " for the CIDEP case depicted in this figure S_0 ".

The low field absorptive peak in the EPR stick diagram arises from transitions 2 and 4 in the energy level diagram. Transition 2 ("S₀" to | T. >) is emissive, while transition 4 ("T₀" to | T₊ >) is absorptive. These transitions occur at the same magnetic field, so the EPR spectrum will only show the net addition of these two EPR transitions. The transition that originates from "T₀" (transition 4) will be more intense as discussed above. The net result is an absorptive peak in the EPR spectrum. The high field emissive peak in the EPR stick diagram arises from transitions 1 and 3. Transition 1 ("S₀" to | T₊ >) will be absorptive and transition 3 ("T₀" to | T. >) will be emissive. The resulting EPR spectrum will be the net addition of these two transitions because they occur at the same magnetic field. As discussed above, the transition that arises from "T₀" will be more intense so the addition of transitions 1 and 3 produces a net emissive peak in the spectrum. The EPR spectrum shows an absorptive / emissive pattern with no net polarization 26,27 . There is no net polarization because the intensity of the low field absorptive peak exactly equals the

intensity of the high field emissive peak in the EPR spectrum. This result is typical for CIDEP electron spin polarization, as well as for CRPP that will be discussed below.

Figure 1.8b shows the energy level diagram and the corresponding EPR stick diagram for a doublet-doublet radical pair that exhibits Correlated Radical Pair Polarization (CRPP) 26,27 . The figure depicts a doublet-doublet radical pair that is formed from a singlet precursor and is weakly interacting during the EPR observation time. The S_0 and T_0 energy levels in the coupled radical pair basis set mix due to a difference in magnetic frequency of the two radicals in the pair by a mechanism that was discussed above for Figure 1.8a. The mixed energy levels are again represented by " S_0 " and " T_0 " in the figure. At early observation times when CRPP is present, " S_0 " has a greater proportion of the initial population than " T_0 ". Because the radical pair is formed from a singlet precursor, only those states that contain singlet character will be populated initially. | $T_1 >$ and | $T_2 >$ are pure triplet states so these states do not receive any of the initial population. " S_0 " contains more singlet character than " T_0 ", so " S_0 " will have a greater initial population.

In Figure 1.8a for pure CIDEP, the difference in energy between the " S_0 " and " T_0 " energy levels is equal to the difference in magnetic frequency of the two radicals of the radical pair as is shown in equation 1.2. When CRPP is present, the radicals of the pair are weakly interacting through the exchange interaction 2J. This interaction causes the singlet to be higher in energy than the triplet for a positive exchange interaction as is the case for the energy level diagram in Figure 1.8b^{26,27}. The difference in energy between

"S₀" and "T₀" is equal to the sum of the difference in magnetic frequency of the two radicals and the exchange interaction as is shown in equation 1.3.

$$\Delta \Omega = \lambda + 2J$$
 equation 1.3

λ is the difference in magnetic frequency of the two radical pair members as given by equation 1.2, and 2J is the exchange interaction between the two radical pair members. For pure CIDEP, transitions 1 and 3 occur at the same magnetic field, but this is no longer true for CRPP^{22,26,27}. The presence of the exchange interaction during the EPR observation time causes transitions 1 and 3, as well as transitions 2 and 4, to be split by the exchange interaction that is present. The difference in magnetic field between transitions 1 and 2, as well as transitions 3 and 4, is still the difference in magnetic frequency of the two radical pair members (same as for the CIDEP case in Figure 1.8a).

The intensity of all EPR transitions will be equal when CRPP is present as is shown in the EPR stick diagram in Figure 1.8b 22,26,27 . The intensity of an EPR transition is proportional to the product of the population difference of the two energy levels and the transition probability. The low field transition ("S₀" to | T. >) has a larger population difference than the transition from "T₀" to | T₊>. The transition probability for these transitions is proportional to the amount of triplet character in "S₀" and "T₀" because the transition is to the pure triplet. The low field transition has a lower transition probability than the "T₀" to | T₊ > transition because "S₀" contains less triplet character. The net result is that the two transitions will be equal in intensity. The transition that originates

from " S_0 " has a larger population difference but a smaller transition probability than the transition that originates from " T_0 ". These two effects are equal and opposite so the transitions are equal in intensity^{26,27}. The two high field transitions are also the same intensity because of an analogous argument.

Figure 1.8c shows an energy level diagram and EPR stick spectrum for a doubletdoublet radical pair that shows electron spin polarization through the "interacting" CIDEP-CRPP mechanism^{22,26,27}. In this figure, there is a positive exchange interaction so "S₀" lies higher in energy than "T₀". Initially "S₀" receives more population because the radical pair is formed from a singlet precursor. At later times, some of the initial population goes to the triplet as discussed above. The figure shows the case where the populations of the two mixed states have become accidentally degenerate²⁶. The transition probabilities have not changed from the pure CRPP case in Figure 1.8b, and the exchange interaction is still present during the EPR observation time. The result is an EPR spectrum whose transitions occur at the same magnetic field as the pure CRPP spectrum in Figure 1.8b. but the intensities of the transitions are no longer equal^{26,27}. The population difference is now equal for all transitions in the figure, so the transition probability is the only determinative factor for the intensity of the transition. Transitions that originate from "T₀" will be more intense than transitions originating from "S₀" because "T₀" contains more triplet character. The spectrum shows an E/A/E/A polarization pattern with net absorption for the first pair of exchange-split transitions and net emission for the second pair. This pattern is shown in the EPR stick diagram in the figure and is a consequence of "T₀" containing more triplet character than "S₀".

References

- 1. Wang, S.Y. Photochem. Photobiol. of Nucleic Acids 1976, Vols. I,II, Academic Press, N.Y.
- 2. Sancar, A.; Sancar, G.B.; Annu. Rev. Biochem. 1988, 57, 29.
- 3. Myles, G. and Sancar, A. Chem. Res. Tox. 1989, 2, 197.
- 4. Rupert, C.S. J. Gen. Physiol. 1962, 45, 703.
- 5. Rupert, C.S. J. Gen. Physiol. 1962, 45, 725.
- 6. Sancar, A. *Photolyase:* In *Advances in Electron Transfer Chemistry*; Mariano, P.E., Ed.; JAI Press: London, 1992; Vol. 2, pp. 215-272.
- 7. Sancar, A.; Sancar, G.B. J. Molec. Biol. 1984, 172, 223.
- 8. Eker, A.P.M.; Kooiman, P.; Hessels, J.K.C.; Yasui, A. J. Biol. Chem. 1990, 265, 8009.
- 9. Johnson, J.L.; Hamm-Alvarez, S.; Payne, G.; Sancar, G.B.; Rajagoplan, K.V.; Sancar, A. Proc. Natl. Acad. Sci. USA 1988, 85, 2946.
- 10. Eker, A.P.M.; Hessels, J.K.C.; van de Velde Biochemistry 1988, 27, 1758.
- 11. Eker, A.P.M.; Dekker, R.H.; Berends, W. Photochem. Photobiol. 1981, 33, 65.
- 12. Kiener, A.; Husain, I.; Sancar, A.; Walsh, C. J. Biol. Chem. 1989, 264, 13880.
- 13. Heelis, P.F.; Okamura, T. and Sancar, A. Biochemistry 1990, 29, 5694.
- 14. Kim, S.T.; Sancar, A.; Essenmacher, C.E. and Babcock, G.T. J. Am. Chem. Soc. 1992, 114, 4442.
- 15. Okamura, T.; Sancar, A.; Heelis, P.F.; Begley, T.P.; Hirata, Y. and Mataga, N. J. Am. Chem. Soc. 1991, 113, 3143.
- 16. Li, Y.F. and Sancar, A. Nucleic Acids Res. 1989, 18, 4885.
- 17. Payne, G.; Heelis, P.F.; Rohrs, B.R. and Sancar, A. Biochemistry 1987, 26, 7121.
- 18. Yeh, S.-R. and Falvey, D.E. J. Am. ('hem. Soc. 1991, 113, 8557.

- 19. Okamura, T.A.; Sancar, A.; Heelis, P.F.; Hirata, Y. and Mataga, N. J. Am. Chem. Soc. 1989, 111, 5967.
- 20. Li, Y.F.; Heelis, P.F. and Sancar, A. Biochemistry 1991, 30, 6322.
- 21. Park, H.W.; Kim, S.T.; Sancar, A. and Deisenhofer, J. Science 1995, 268, 1866.
- 22. Snyder, S.W. and Thurnauer, M.C. Electron Spin Polarization in Photosynthetic Reaction Centers: The Photosynthetic Reaction Center 1993, Vol.2 ed. Deisenhofer, J. and Norris, J.R. (Academic Press, SanDiego) p. 285.
- 23. Hoff, A.J. Q. Rev. Biophys. 1984, 17, 153.
- 24. Jenks, W.S. and Turro, N.J. Rev. Chem. Int. 1990, 13, 237.
- 25. Adrian, F.J. Rev. Chem. Int. 1986, 7, 173.
- 26. Norris, J.R.; Morris, A.L.; Thurnauer, M.C. and Tang, J. J. Chem. Phys. 1990, 92, 4239.
- 27. Snyder, S.W.; Morris, A.L.; Bondeson, S.R.; Norris, J.R. and Thurnauer, M.C. J. Am. Chem. Soc. 1993, 115, 3774.
- 28. Batchelor, S.N.; Heikkilä, H.; Kay, C.W.M.; McLauchlan, K.A. and Shkrob, I.A. *J. Chem. Phys.* 1992, 162, 29.

Chapter 2

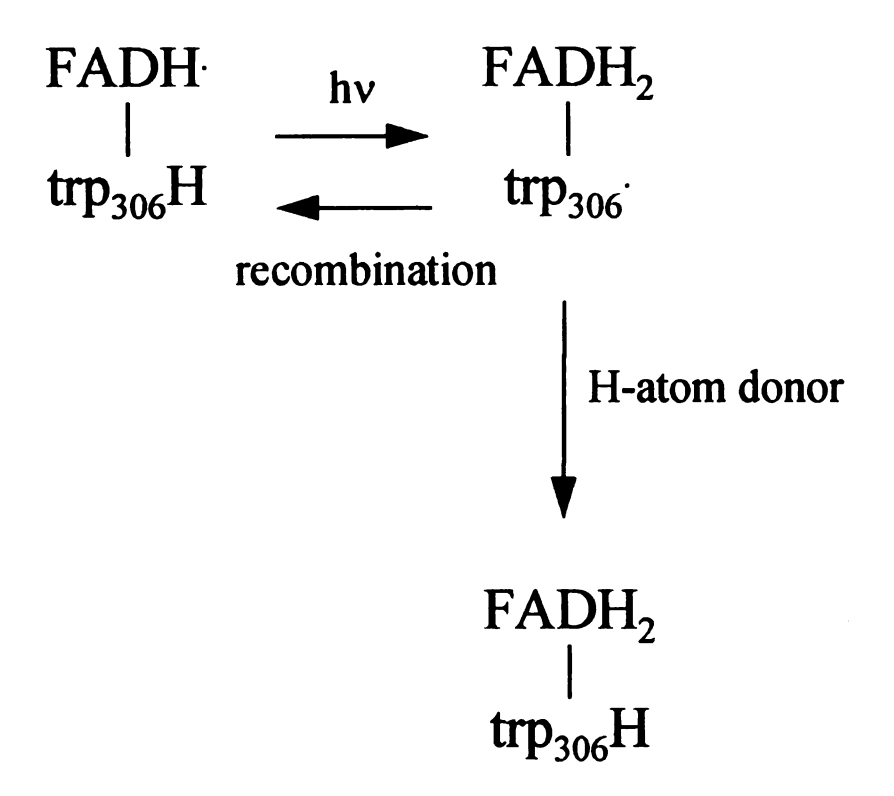
The Identification of a Transient Tryptophan Radical in the Photoreduction

Reaction of DNA Photolyase by Time-Resolved Electron Paramagnetic Resonance

Introduction

When DNA photolyase is isolated in vitro, one electron oxidation of the active form of the enzyme to the inactive FADH form occurs 1,2,3,4 (see Figure 1.5), as discussed in Chapter 1. This form of the enzyme is dark stable and catalytically inactive^{5,6}. Catalytic activity can be restored in the enzyme by irradiation of photolyase with visible light causing FADH to be photoreduced to the active form of the enzyme⁷. A proposed mechanism for photoreduction of photolyase to the active form of the enzyme is shown in Figure 2.1^{1,2}. Flash photolysis of the inactive enzyme causes hydrogen atom transfer from an amino acid donor to the flavin chromophore. Subsequent reduction of the amino acid donor results in reactivation of the enzyme^{1,2,7}. Optical studies of the photoreduction process in photolyase have suggested that tryptophan-306 is the internal amino acid donor^{7,8}. Each of the 15 tryptophan residues in the enzyme was individually replaced with phenylalanine, and the rate of photoreduction was monitored. In the eight mutants that were able to overproduce photolyase, all except the trp-306 to phe mutant were able to photoreduce FADH in spite of the mutation⁸. These results established that trp₃₀₆ is involved in photoreduction of photolyase⁸. In Chapter 1, a proposed mechanism for the excited states that form in the enzyme during photoreduction of the inactive enzyme was shown in Figure 1.6⁷. The mechanism proposes that photoexcitation of either FADH or

Figure 2.1. Proposed photoreduction mechanism in DNA photolyase.



Heelis, P.F.; Okamura, T. and Sancar, A. Biochemistry 1990, 29, 5694.

Figure 2.1

MTHF produces an excited doublet flavin state (2°FADH) and initiates the photoreduction reaction⁹. Within 100 ps, 2°FADH intersystem crosses to the quartet, 4°FADH^{7,9}. H-atom transfer from trp-306 to 4°FADH occurs in a microsecond to form the transient species FADH₂---2trp⁻⁷. In the presence of exogenous donors, trp is reduced to form the catalytically active enzyme. Without exogenous donors, H-atom recombination occurs to form the inactive, FADH-containing enzyme over several milliseconds⁷.

In this study, the identity of the amino acid donor is confirmed by time-resolved EPR as trp-306 using isotopic labeling and site directed mutagenesis^{10,11}. The time-resolved EPR spectrum has emissive and absorptive transitions suggesting that the transient FADH:---trp species is spin polarized due to interactions between these two members of the transient species¹⁰. Because of the similarity in polarization patterns between photolyase and the photosynthetic reaction center, a spin polarized mechanism analogous to the Correlated Radical Pair Mechanism (CRPP)^{12,13} is proposed.

Materials and Methods

Isolation of photolyase was carried out at the University of North Carolina in the laboratory of Professor Aziz Sancar and has been described previously^{14,15}. Isotopic labeling and site-directed mutagenesis were performed by Sancar as described elsewhere¹¹. Experiments were performed with samples that contained 0.1 mM enzyme, 20% glycerol, 50 mM potassium phosphate (pH 7.0), and 50 mM NaCl. 5 mM potassium ferricyanide was added to the sample to prevent reduction of the enzyme from FADH to FADH₂. The

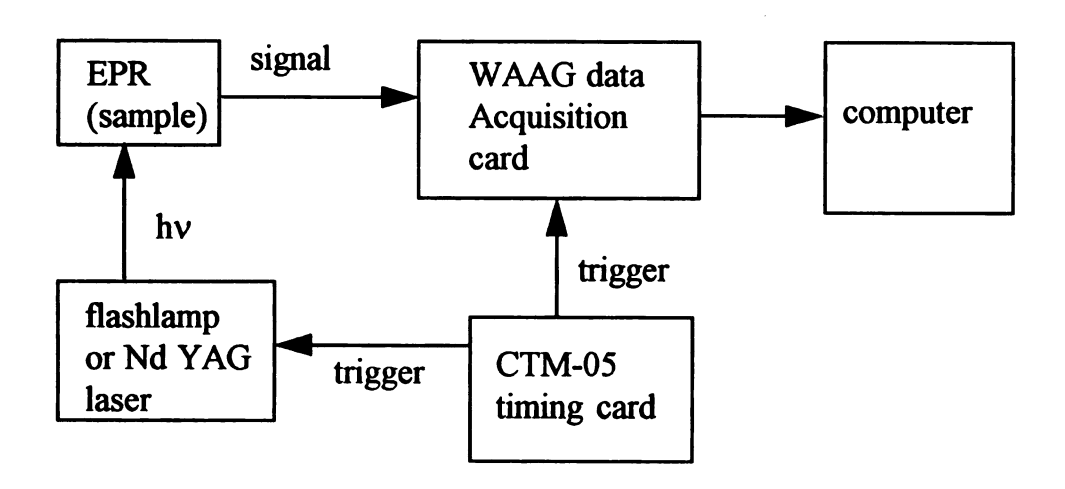
oxidation state of the flavin was monitored by taking the visible absorption spectrum of the sample with a Perkin Elmer Lamda 5 double beam UV/visible spectrophotometer. All experiments were performed at 277 K. EPR measurements were performed on a Bruker ER200D spectrometer with a TM011 cavity. The sample was held in the cavity with a 300 µl quartz flat cell (Wilmad, Buena, New Jersey). The microwave frequency was measured with a HP 5245 counter / 5255 frequency converter and the magnetic field was monitored with a Bruker ER035M NMR gaussmeter.

Photoexcitation of the sample was done with either a Xenon flashlamp or a Quanta-Ray DCR-11 pulsed Nd-YAG laser (Spectra-Physics, Mountain View, California). The flashlamp is critically damped with a pulse width of 17 µs and a lamp energy of 50 J¹⁶. The laser has a pulse width of 10 ns, a pulse energy of 20 mJ, and an excitation wavelength of 355 nm. Both excitation sources were used at a repetition rate of 1 Hz.

Kinetic traces were obtained as described previously¹⁷ and outlined in Figure 2.2. The signal output from the spectrometer was input into an 8-bit Markenrich waveform acquisition card (Markenrich Corporation, Duarte, California) that is capable of sampling from 50 ns to 0.5 ms. Multiple flashes were computer averaged to obtain the kinetic traces. The timing scheme used for kinetic traces is also shown in Figure 2.2. A MetraByte CTM-05 timing card (Metrabyte Corporation, Taunton, MA) that is software-controlled was used to control the timing sequence as shown in Figure 2.2b. The CTM-05 card provided a pulse at a 1 Hz repetition rate to the waveform acquisition card in order to trigger the collection of data. A software-controlled delay was set, and after the delay a

Figure 2.2. Block diagram and timing sequence for kinetic trace acquisition. a) shows the experimental setup for obtaining kinetic traces and b) shows the timing sequence that was used. The switching of the flashlamp and the WAAG board are done by a trigger pulse from the CTM-05 timing card.

a) Kinetic trace setup block diagram



b) Kinetic trace setup timing sequence

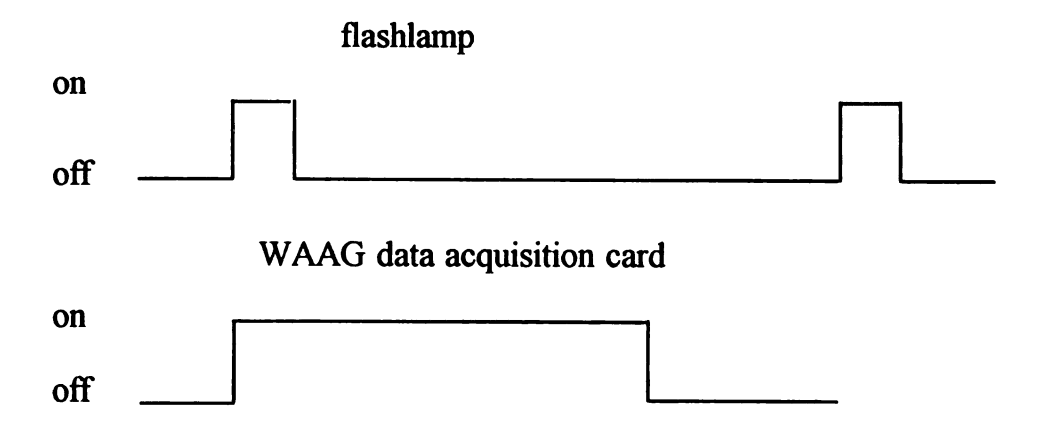


Figure 2.2

pulse was sent to trigger the excitation source. Data were stored for each flash and averaged to obtain the kinetic trace.

Time-resolved EPR spectra were recorded¹⁷ as shown in Figure 2.3a. The signal output from the spectrometer was input into a Stanford Research Systems SR250 gated integrator and boxcar averager (Palo Alto, California). The gated integrator electronically integrated the signal and sent the averaged signal to a PC to record the signal intensity at a particular magnetic field position. The field width of 100 G was swept slowly at a rate of 1000 s, and 1000 data points were collected during a sweep. With a 1 Hz excitation rate, the sample was excited at each data point collected.

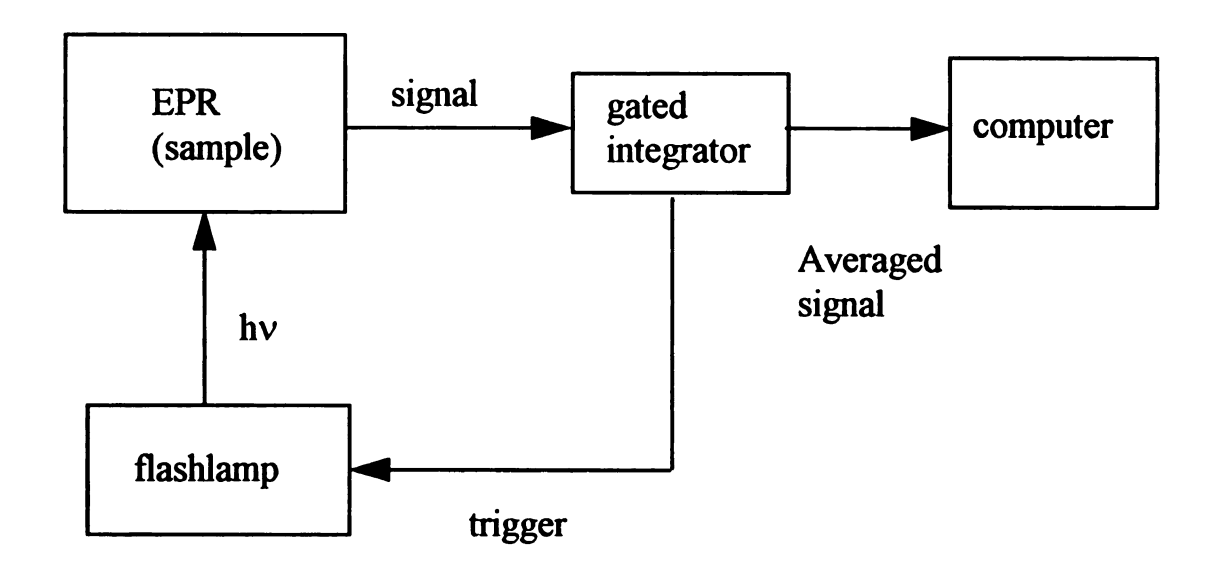
Timing of the instrument is outlined in Figure 2.3b. The gated integrator was triggered internally at 1 Hz. The trigger pulse was also output to the flashlamp to excite the sample at the same time the boxcar was triggered. A delay and aperture were set to capture a significant portion of the transient radical. The integrator conditions that were typically used were a trigger rate of 1 Hz, a delay of 4 μs, an aperture of 48 μs, and 3 averages per point. AC-coupling of greater than 10 Hz was used to discriminate against any stable signal that may be present. Typical EPR conditions were 2.8 G modulation amplitude, 6.3 mW microwave power, 9.22226 GHz microwave frequency, and a time constant of 35 μs.

Results

Figure 2.4 shows a dark stable CW EPR spectrum of inactive photolyase due to oxidation of the flavin chromophore to the semiquinone form, FADH (see Figure 1.5).

Figure 2.3. Block diagram and the timing sequence for the gated integrator setup. a) shows a block diagram of the gated integrator and b) shows the timing sequence that was used.

a) Block diagram gated integrator setup



b) Timing sequence

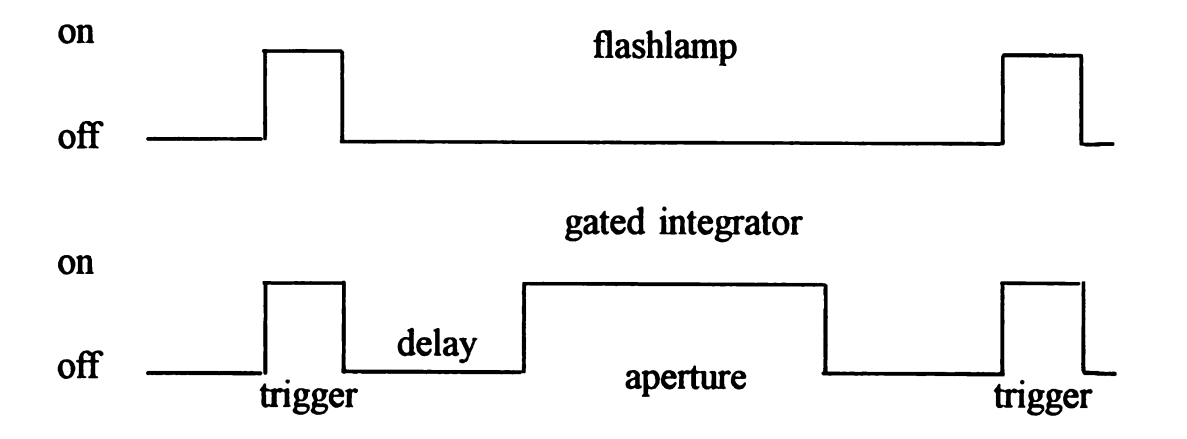


Figure 2.3

Figure 2.4. Dark stable flavin radical EPR spectrum in DNA photolyase. Experimental conditions were: 6.3 mW microwave power, 9.22226 Ghz microwave frequency, 35 µs time constant, 3290 G centerfield, 100 G sweep, 2.8 G modulation amplitude.

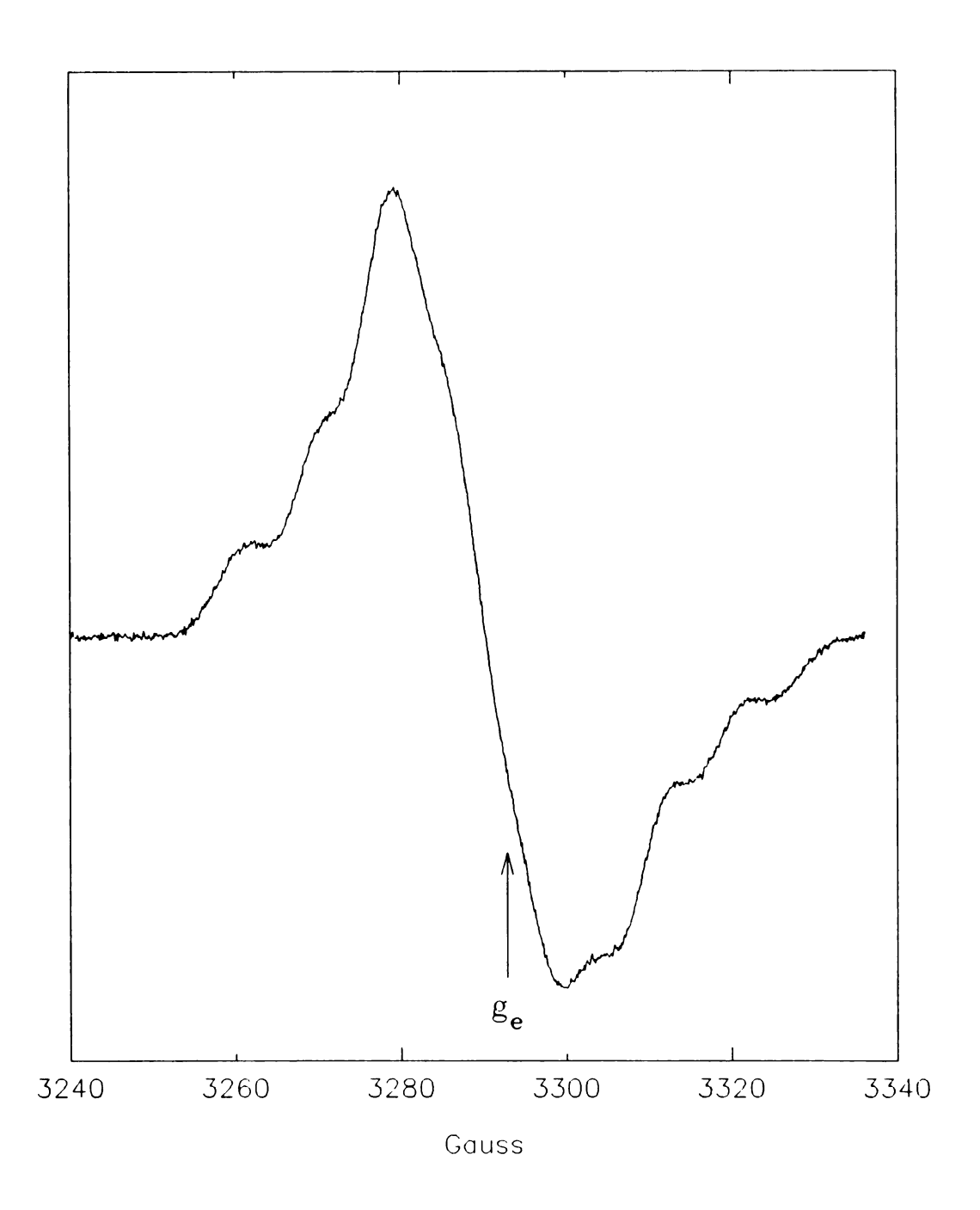


Figure 2.4

The spectrum has no well-resolved hyperfine couplings and an apparent g-value of 2.0039. The absence of resolved hyperfine couplings and the apparent g-value of the dark stable spectrum in Figure 2.4 are in agreement with previous reports of flavin doublet radicals that occur in proteins. Flash photolysis of the inactive enzyme whose EPR spectrum is shown in Figure 2.4 produced an intense EPR transient signal in the g=2 region. The kinetic trace of this signal is shown in Figure 2.5. Figure 2.5a was obtained by exciting the sample with a Xenon flashlamp, and Figure 2.5b with a Nd-YAG laser. The kinetic trace of this signal shows that the rise and fall of the light-induced radical occurs with a half time of approximately 35 us. The observed half time for radical formation and decay is most likely the instrument response time due to the use of 100 kHz modulation and does not represent the true kinetics for the transient radical. Artifacts due to the longer pulse width of the Xenon flashlamp (17µs) are not present as a comparison of Figure 2.5a to 2.5b shows. When the excitation pulse was shortened to 10 ns as in Figure 2.5b, the kinetics of the transient radical were essentially the same as for a 17 us pulse width. These results suggest that the transient radical EPR signal is unaffected by the method of excitation that is used.

Figure 2.6 shows the microwave power dependence for the transient radical's EPR signal. The signal intensity initially increases linearly with an increase in the square root of the microwave power. The maximum signal intensity occurs at a microwave power of 6.3 mW. All further experiments were performed at this microwave power in order to obtain the maximum signal to noise ratio. At higher microwave powers the signal intensity decreases. Later in this chapter and in chapter 4 evidence will be presented that shows

Figure 2.5. Kinetic traces of the transient radical at 3290 G. The trace in a) was taken with the flashlamp as the excitation source and is 600 averages. The trace in b) was taken with the YAG laser and is 1000 averages. Experimental conditions were: 6.3 mW microwave power, 9.22226 Ghz microwave frequency, 35 µs time constant, 3290 G microwave field, and 2.8 G modulation amplitude.

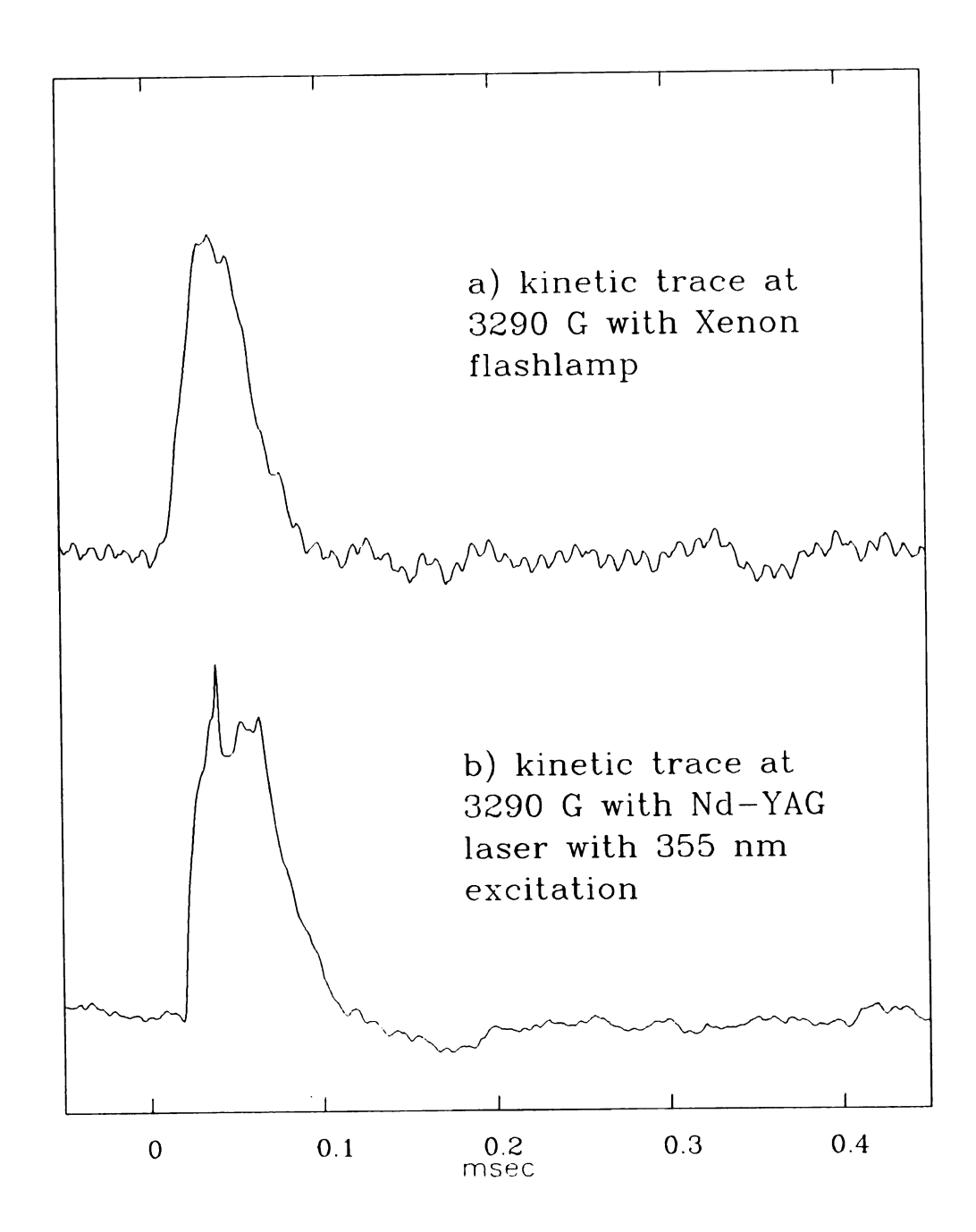


Figure 2.5

Figure 2.6. Power dependence of the transient EPR signal in DNA photolyase. Experimental conditions were: 9.22226 Ghz microwave frequency, 35 µs time constant, 2.8 G modulation amplitude. Photolyase samples were excited with the flashlamp.

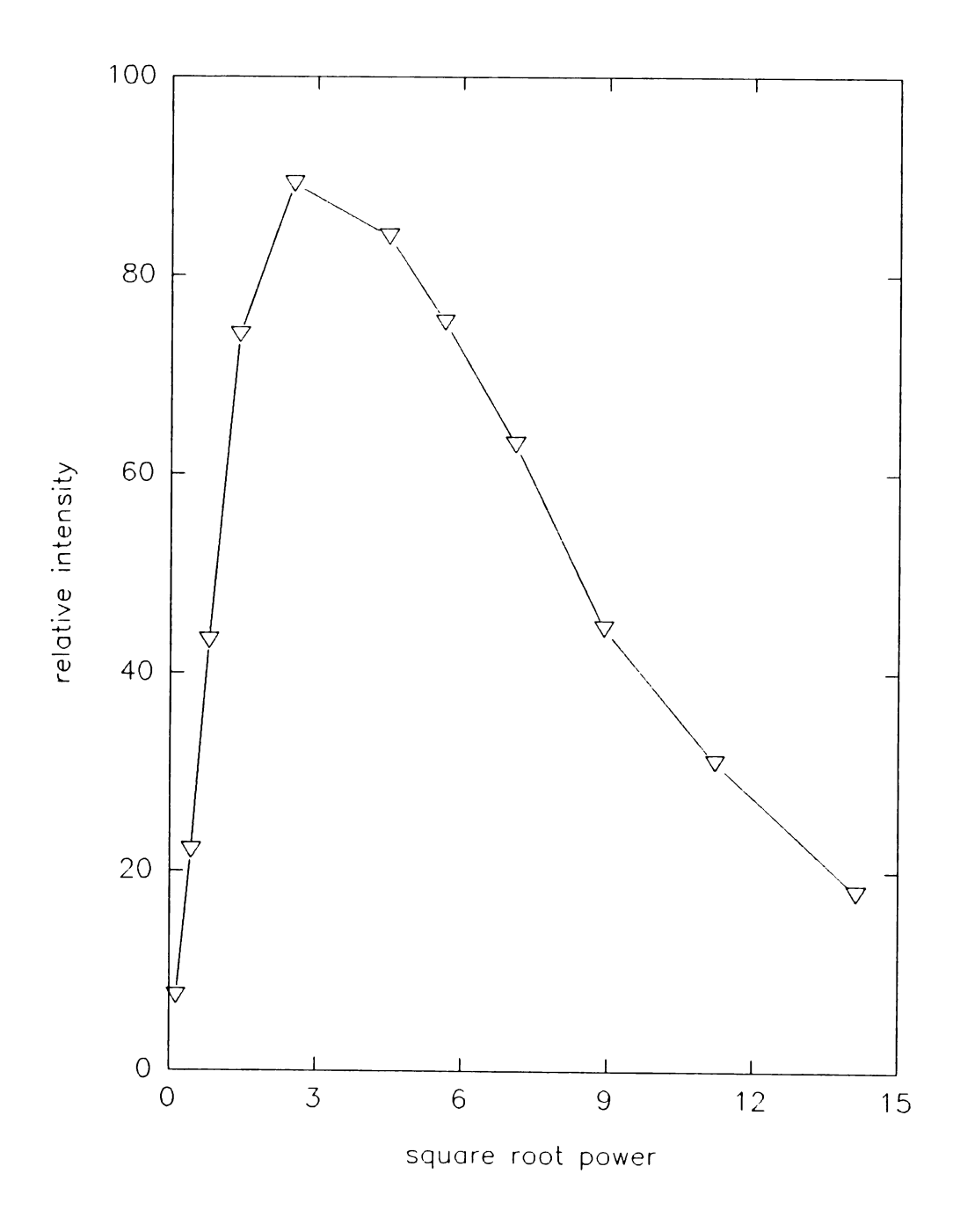


Figure 2.6

that the transient EPR signal in photolyase is spin polarized due to magnetic interactions among two radicals in a radical pair. Other spin polarized radical pairs have been shown to exhibit Torrey oscillations at high microwave powers¹⁸. Torrey oscillations arise from a electron spin phase shift of a radical pair from a singlet to a triplet. This spin phase shift changes the phase of spin polarization and results in a change of phase of the EPR signal as well. Signal damping for each phase shift and a constant frequency are characteristics of Torrey oscillations. In photolyase, these phase shifts at high microwave powers due to Torrey oscillations are not present. Their absence is probably attributable to our detection scheme by field modulated EPR, which limits our time resolution to 35 µs.

Figure 2.7 shows a light saturation curve for the transient radical when the flashlamp is used as the excitation source. The curve shows that at full lamp intensity the signal intensity is beginning to plateau to a maximum value suggesting that the sample is light saturated at the typical lamp energies that were used. The transient EPR signal is linearly dependent upon the light intensity that was used (see Figure 2.7). This linear dependence suggests that the process that is observed upon photoexcitation of the inactive enzyme is a one photon reaction.

Using gated integration techniques, a spectrum was obtained for the transient radical and is shown in Figure 2.8a. The spectrum is an average of five individual scans taken over a 100 G scan range. The spectrum has three major transitions in a 1:2:1 intensity ratio and each is split by 15 G (solid arrows). Superimposed on these larger splittings are smaller ones (less than 5 G) as shown by the dashed arrows in Figure 2.8a. The apparent g-value for the transient radical in Figure 2.8a is 2.0028 and is typical for an

Figure 2.7. Light saturation plot for the transient radical in DNA photolyase. Experimental conditions were: 6.3 mW microwave power, 9.22226 Ghz microwave frequency, 35 µs time constant, 3290 G magnetic field, and 2.8 G modulation amplitude. Light intensity was measured by exciting the sample with the flashlamp and placing neutral density filters in front of the cavity.

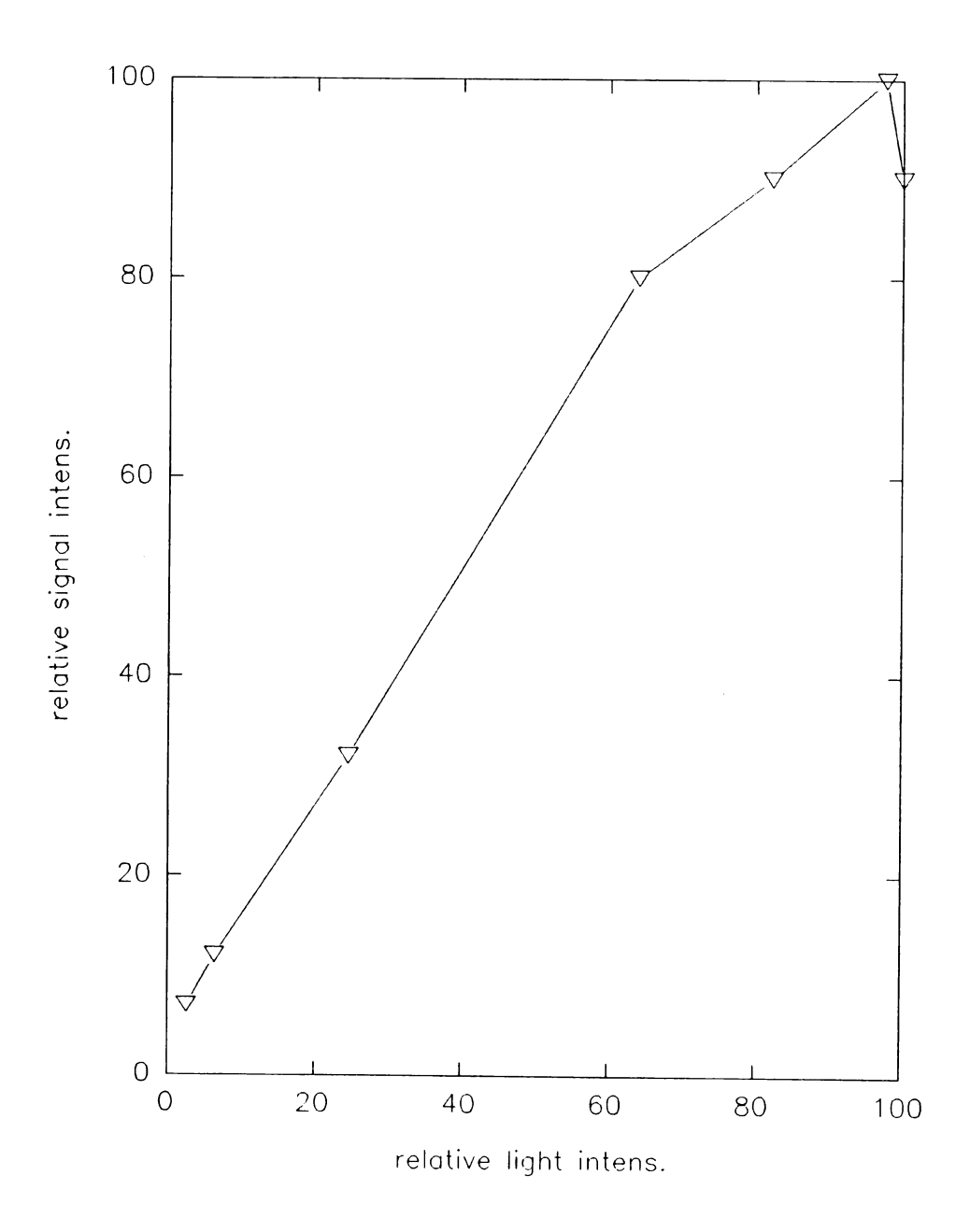


Figure 2.7

Figure 2.8. Transient EPR spectra in DNA photolyase. a) is a wild type sample and b) contains tryptophan that is deuterated at the positions indicated by the asterisks in the inset. a) is the average of 5 scans and b) is the average of 20 scans. Experimental conditions were: 6.3 mW microwave power, 9.22226 Ghz microwave frequency, 35 µs time constant, 3290 G centerfield, 100 G sweep, 2.8 G modulation amplitude, and 1000 second scans. Boxcar conditions were: 3 averages per point, 1 Hz flash repetition rate, 4 µs delay, 48 µs aperture, trigger rate of 1 Hz, and AC-coupling of greater than 10 Hz.

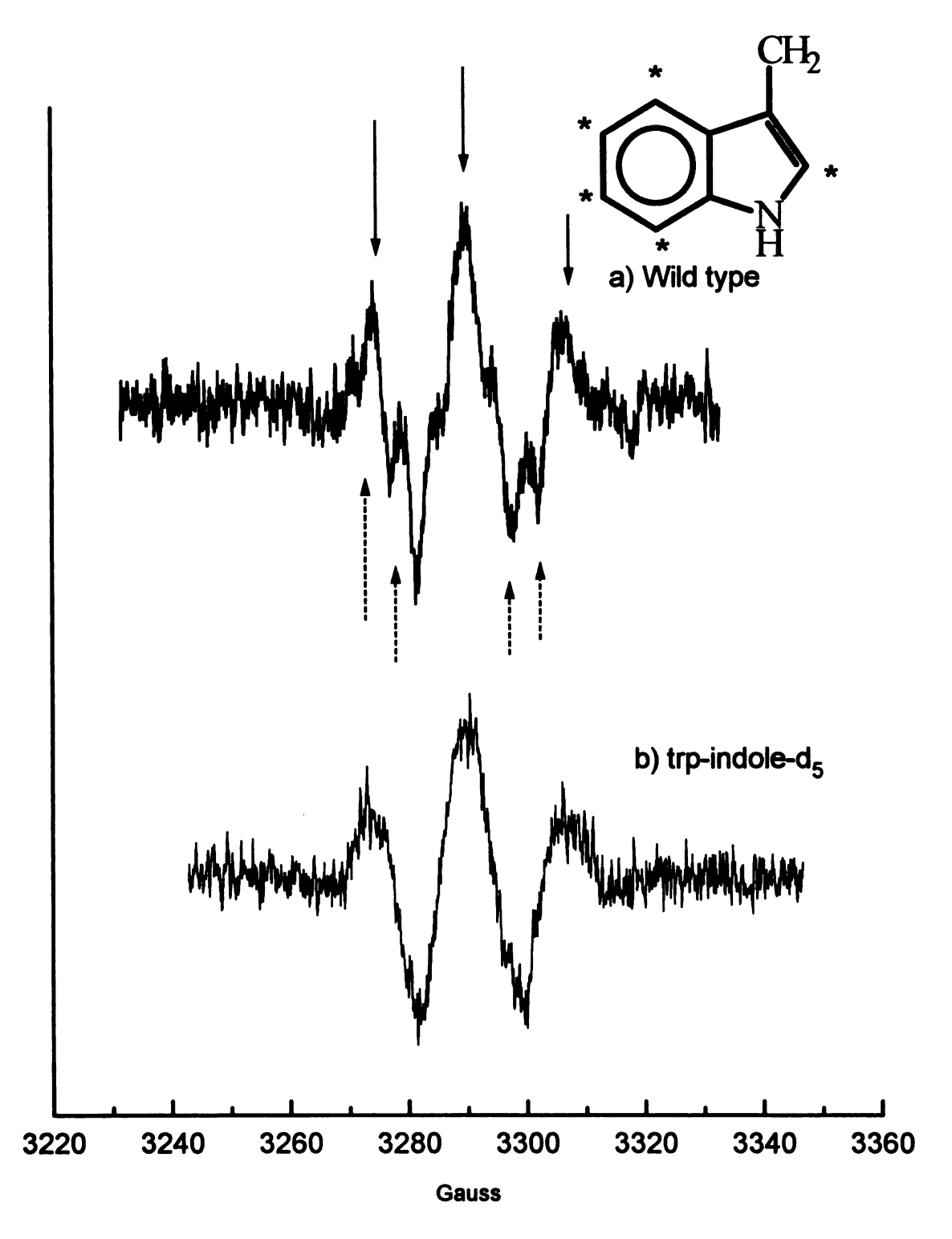


Figure 2.8

organic radical. Figure 2.8b shows a transient spectrum for a sample that was isotopically labeled with deuterium on tryptophan molecules in the protein at the positions that are indicated with asterisks on the tryptophan structure in the inset to the figure. Isotopic labeling of the sample was performed in the laboratory of Dr. Aziz Sancar at the University of North Carolina School of Medicine in Chapel Hill, North Carolina and has been described elsewhere ^{14,15}. The spectrum has the same apparent g-value and shows the same 1:2:1 intensity ratio with a hyperfine splitting of 15 G as the wild type sample in Figure 2.8a. The smaller couplings that are present in the wild type sample (dashed arrows in Figure 2.8a) are not resolved in the deuterated sample in Figure 2.8b.

Discussion

The isolated, inactive form of DNA photolyase contains a flavin semiquinone radical (FADH)^{5,19} as seen in Figure 1.6 and Figure 2.1. The dark CW EPR spectrum in Figure 2.4 confirms this assignment¹⁰. The spectrum has a g-value (2.0039) that is consistent with other reported flavin radicals. Optical studies have suggested that the inactive enzyme can be photoreduced to the active form (see Figure 2.1) by H-atom transfer from a tryptophan side chain to FADH^{-7,19,20}. The products of the photoreduction reaction are a neutral tryptophan doublet radical and a fully reduced triplet flavin (FADH₂)^{7,10,11}. In the presence of exogenous donors, the tryptophan radical is reduced to form the active enzyme^{7,21}. Without donors, the transient tryptophan radical accepts an H-atom from FADH₂ to form the inactive enzyme in a recombination reaction.

Photoexcitation of the inactive enzyme produces an intense transient signal in the g=2 region of the EPR spectrum¹⁰. The kinetic trace of the transient radical is shown in Figure 2.5. The decay kinetics of the radical show a decay phase with a half time of 35 µs. The rise of the transient and the fast decay are not true half times, but rather the response time of the instrument. The kinetic trace in Figure 2.5 was taken at a magnetic field of 3290 G. Kinetic traces at other field positions also show the same kinetics and ratios of the fast to slow phase.

Gated integration techniques were used to obtain the EPR spectrum of the transient radical (see Figure 2.8a) that forms following photoexcitation of the enzyme. The EPR spectrum shows three major couplings in a 1:2:1 ratio. This pattern is consistent with coupling to two equivalent nuclei, most likely the two β -methylene protons in tryptophan (see Chapter 3).

To confirm that tryptophan is the transient amino acid radical that is involved in the photoreduction reaction, a sample with tryptophan that is deuterated on the indole ring was prepared. The inset to Figure 2.8 shows the tryptophan structure and the asterisks denote the positions where deuterium replaced hydrogen. The deuterated sample (Figure 2.8b) has a transient EPR spectrum that has the same three major couplings as the wild type sample, but the smaller couplings are no longer resolved. This result confirms tryptophan involvement in the photoreduction reaction. Deuteration of the sample changes hyperfine couplings throughout the transient EPR spectrum, as can be seen by comparing Figure 2.8a with 2.8b. Because the entire spectrum is changed, the transient spectrum probably arises from only the tryptophan radical, with no contribution from

flavin. If a flavin radical were also observed, some portions of the transient spectrum would be unaffected by tryptophan deuteration.

Figure 2.9 shows the integrated transient absorption spectrum of the wild type and deuterated samples whose first-derivative spectra are shown in Figure 2.8. A radical whose spin energy levels are populated according to a Boltzman distribution shows all absorptive transitions. Figure 2.8 shows that, for both the wild type and deuterated samples, some of the transitions are emissive in the transient EPR spectrum. Emissive transitions are characteristic of an EPR spectrum that is electron spin polarized due to interactions between two members of a radical pair^{22,23}. It was shown above that the transient, spin polarized EPR signal probably arises from a tryptophan radical. The model in Figure 1.6 proposes that the transient radical that is formed will be trp and a FADH₂ species. In order for spin polarization to occur a radical pair must form. In the photolyase photoreduction reaction, the most logical choice for the other radical pair member is a triplet flavin radical because of spin conservation requirements.

The model in Figure 1.6 proposes the following scheme for photoreduction in photolyase⁷. After the enzyme is photoexcited, an excited doublet flavin radical ^{2*}FADH intersystem crosses to the quartet. The quartet flavin ^{4*}FADH accepts an H-atom from trp-306 to form the transient radical whose EPR spectrum is shown in Figure 2.8. The transient species that forms following hydrogen atom transfer is trp--FADH₂. The spin polarized character of the transient EPR spectrum in Figure 2.8 suggests that the proposed mechanism in Figure 1.6 must be modified to include the formation of a radical pair which is necessary for spin polarization. The transient species that forms following hydrogen

Figure 2.9. Integrated transient spectra for a) wild type and b) deuterated photolyase samples.

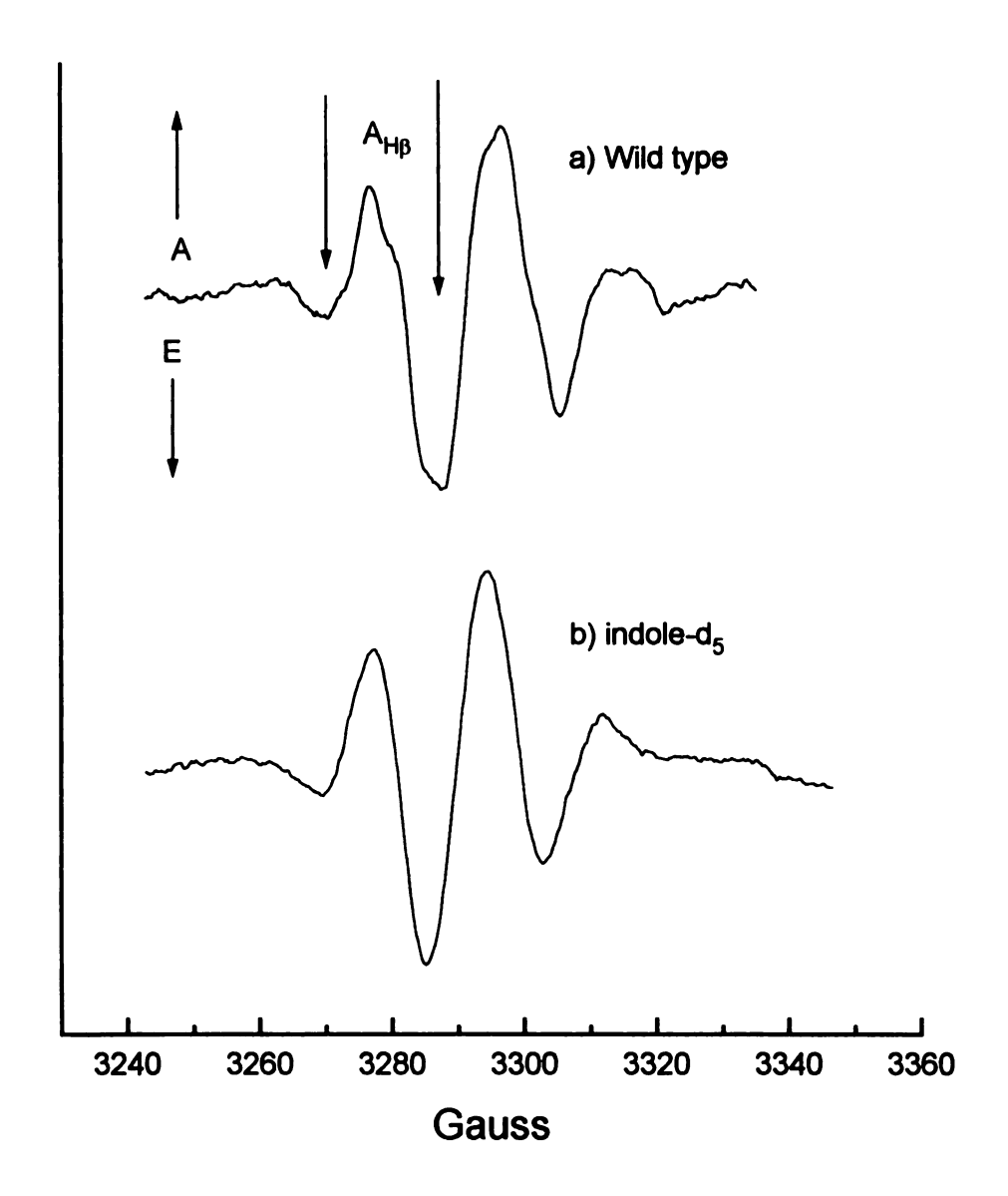


Figure 2.9

atom transfer from trp-306 to ^{4*}FADH is expected to obey spin conservation. Before hydrogen atom transfer, the overall spin of the two species is a quartet. If spin conservation is preserved, the quartet character must be preserved after H-atom transfer. In order to attain an overall quartet character for the radical pair, the flavin species must be a triplet because of the doublet character of trp-306. Figure 2.10 shows the new reaction mechanism for photoreduction in photolyase that includes an explanation for the spin polarized state in photolyase¹⁰. Photoexcitation of FADH produces an excited doublet flavin species ^{2*}FADH. Within 100 ps intersystem crossing to the quartet occurs and forms ⁴*FADH. Hydrogen atom transfer from ⁴*FADH produces the transient ³ FADH₂--trp species that is the state that produces the spin polarized EPR spectrum that is shown in Figure 2.9. Intersystem crossing of ³*FADH₂ to the ground state (FADH₂) followed by H-atom transfer from an external donor produces the active (FADH₂containing) enzyme. In the absence of external hydrogen atom donors the transient FADH₂--trp species recombines in several milliseconds to reform the inactive FADHcontaining enzyme.

Triplet-doublet radical pair polarization in solution reactions has been reported and is explained by the Radical Triplet Pair Polarization (RTPM)^{24,25,26}. RTPM predicts a polarization pattern that is half in emission and half in absorption with a superimposed net polarization. The polarization pattern in Figure 2.9 is alternating in emission and absorption with no net polarization. The absence of net polarization rules out RTPM as a possible explanation of spin polarization that occurs during photoreduction of photolyase.

Figure 2.10. Proposed reaction mechanism for photolyase that is derived from the experimental results reported here.

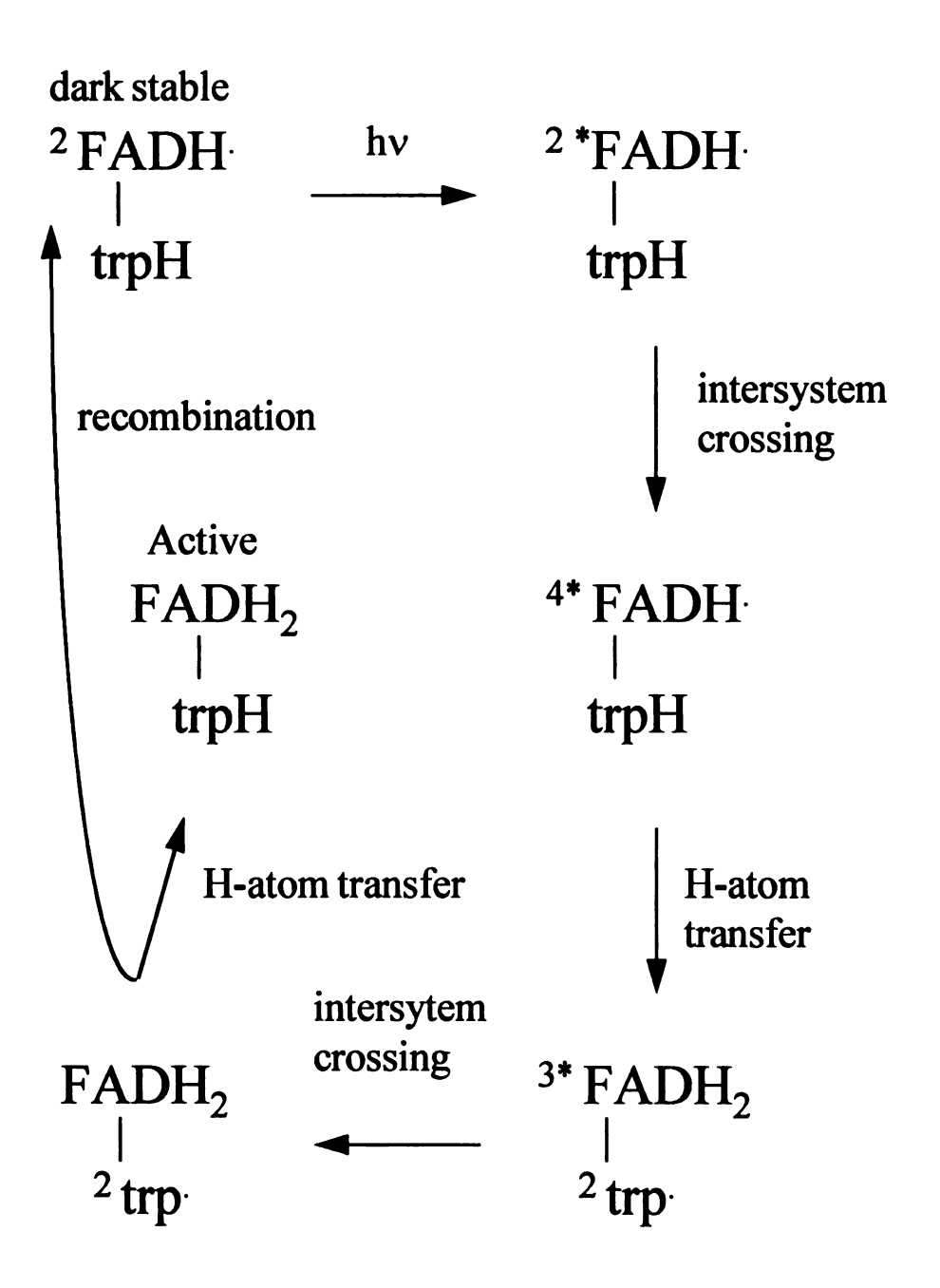


Figure 2.10

The alternating polarization pattern in Figure 2.9 is similar to the Correlated Radical Pair Polarization (CRPP) that is observed for doublet-doublet radical pairs in photosynthetic reaction centers^{12,13}. The alternating pattern is proposed to arise from a splitting of a transition into an emissive-absorptive doublet by the exchange energy between the two radical pair members during the observation time by EPR. Non-zero exchange interactions during EPR observation times have only been observed when the two radical pair members are protein bound such as in photolyase and photosynthetic reaction centers. Therefore, spin polarization in photolyase is proposed to arise from an analogous polarization mechanism to CRPP that is extended to the triplet-doublet case. The manifestations of this model and mechanism will be discussed in more detail in chapters 3 and 4.

References

- 1. Sancar, A. *Photolyase:* In *Advances in Electron Transfer Chemistry*; Mariano, P.E., Ed.; JAI Press: London, 1992; Vol. 2, pp. 215-272.
- 2. Kim. S.T.; Malhotra, K.; Sancar, A. In *Biological Responses to Ultraviolet Radiation*; Urbach, F., Ed.; Valdenmar: Overland Park, KS, 1992.
- 3. Okamura, T.; Sancar, A.; Heelis, P.F.; Begley, T.P.; Hirata, Y.; Mataga, N. J. Am. Chem. Soc. 1991, 113, 3143.
- 4. Yeh, S.-R. and Falvey, D.E. J. Am. Chem. Soc. 1991, 113, 8557.
- 5. Payne, G.; Heelis, P.F.; Rohrs, B.R.; Sancar, A. Biochemistry 1987, 26, 7121.
- 6. Li, Y.F. and Sancar, A. Nucleic Acids Res. 1991, 18, 4885.
- 7. Heelis, P.F.; Okamura, T.; Sancar, A. Biochemistry 1990, 29, 5694.
- 8. Li, Y.F.; Heelis, P.F.; Sancar, A. Biochemistry 1991, 30, 6322.
- 9. Okamura, T.A.; Sancar, A.; Heelis, P.F.; Hirata, Y.; Mataga, N. J. Am. Chem. Soc. 1989, 111, 5967.
- 10. Essenmacher, C.; Kim, S.-T.; Atamian, M.; Babcock, G.T.; Sancar, A. J. Am. Chem. Soc. 1993, 115, 1602.
- 11. Kim, S.-T.; Sancar, A.; Essenmacher, C.; Babcock, G.T. *Proc. Natl. Acad. Sci. USA* 1993, 90, 8023.
- 12. Norris, J.R.; Morris, A.; Thurnauer, M.C.; Tang, J. J. Chem. Phys. 1990, 92, 4239.
- 13. Bittl, R.; Schulten, K.; Turro, N.J. J. Chem. Phys. 1990, 93, 8260.
- 14. Sancar, A.; Sancar, G.B. J. Mol. Biol. 1984, 172, 223.
- 15. Sancar, G.B.; Smith, F.W.; Sancar, A. Nucleic Acids Res. 1983, 11, 677.
- 16. Yerkes, C. Ph.D. dissertation 1982, Michigan State University, East Lansing, MI.
- 17. Hoganson, C.W.; Babcock, G.T. Biochemistry 1988, 27, 5848.

18 (

19. **I**

20. 1

21

22. .

24]

23.

25.]

26.]

- 18. Gierer, M.; van der Est, A.; Stehlik, D. Chem. Phys. Letts. 1991, 186, 238.
- 19. Eker, A.M.P.; Kooiman, P.; Hessels, J.K.C.; Yasui, A. J. Biol. Chem. 1990, 265, 8009.
- 20. Heelis, P.F.; Payne, G.; Sancar, A. Biochemistry 1987, 26, 4634.
- 21. Malhotra, K.; Kim, S.-T.; Walsh, C.T.; Sancar, A. J. Biol. Chem. 1992, 267, 15406.
- 22. Jenks, W.S.; Turro, N.J. Rev. Chem. Int. 1990, 13, 237.
- 23. Adrian, F.J. Rev. Chem. Int. 1986, 7, 173.
- 24. Blatter, C.; Jent, F.; Paul, H. Chem. Phys. Lett. 1990, 166, 375.
- 25. Kawai, A.; Okutsu, T.; Obi, K. J. Phys. Chem. 1991, 95, 9130.
- 26. Kawai, A.; Obi, K. J. Phys. Chem. 1992, 96, 52.

Chapter 3

The trp-306 radical in photolyase is a cation radical suggesting that photoreduction occurs through electron transfer rather than hydrogen atom transfer

Introduction

A proposed model for photoreduction of photolyase that includes an explanation of the spin polarized character of the tryptophan radical is shown in Figure 2.10¹. In this model, photoexcitation of FADH produces an excited doublet state², ^{2*}FADH. Intersystem crossing to the quartet occurs within 100 ps² and is followed by hydrogen atom transfer³ from an amino acid side chain donor that has been identified by time-resolved EPR¹ and optical studies as tryptophan-306⁴. The transient radical pair that forms contains a doublet tryptophan radical (trp') and triplet flavin (^{3*}FADH₂)¹. The excited triplet flavin intersystem crosses to the ground electronic state and is followed by reduction of trp-306 by an exogenous donor to form the active (FADH₂ containing) enzyme². In the absence of exogenous donors, FADH₂ recombines with trp to form the inactive FADH form of the enzyme².

The proposed active form of the enzyme (see Figure 1.3) contains a reduced flavin adenine dinucleotide in its neutral dihydro form (FADH₂)^{2,5}. Hartman and Rose studied flavin model compounds and concluded that the anionic, singly protonated form is eight times more active in dimer repair process than the doubly protonated neutral form⁶. These results suggest that the active form of photolyase may contain FADH rather than FADH₂ and that photoreduction in the enzyme occurs by an electron rather than hydrogen atom

transfer reaction mechanism⁷. Figure 3.1 shows possible reaction mechanisms for hydrogen atom and electron transfer in photolyase. Figure 3.1a shows the previously proposed hydrogen atom transfer reaction mechanism^{2.5}. Photoexcitation of the inactive enzyme followed by hydrogen atom transfer from trp-306 to FADH produces a neutral tryptophan radical and FADH₂. Exogenous donors reduce trpH to form the active enzyme that contains FADH₂. An alternate reaction mechanism for photoreduction in photolyase that involves electron transfer instead of hydrogen atom transfer is shown in Figure 3.1b⁷. After photoexcitation of the enzyme, electron transfer from trp-306 to FADH produces a tryptophan cation radical and the catalytically active FADH⁷ Reduction of trpH⁺ by exogenous donors produces the active enzyme that contains FADH.

Huckel-McLauchlin spin density calculations have been carried out for the cationic and neutral forms of the trp radical⁸ and the results are shown in Figure 3.2. The tryptophan cation radical has large spin density at the C(2) α -proton and at the C(3) β -methylene carbon positions, while the neutral tryptophan radical has significant spin density at the N(1) nitrogen and C(3) β -methylene carbon positions. Isotopic labeling of tryptophan should allow an identification of the ionic character of the trp radical that occurs during photoreduction of the enzyme.

In the work presented in this chapter, we show that photoreduction in photolyase occurs through an electron transfer mechanism as shown in Figure 3.1b, rather than by the hydrogen atom transfer mechanism that is shown in Figure 3.1a. The implication of the

Figure 3.1. Possible photoreduction mechanisms in photolyase.

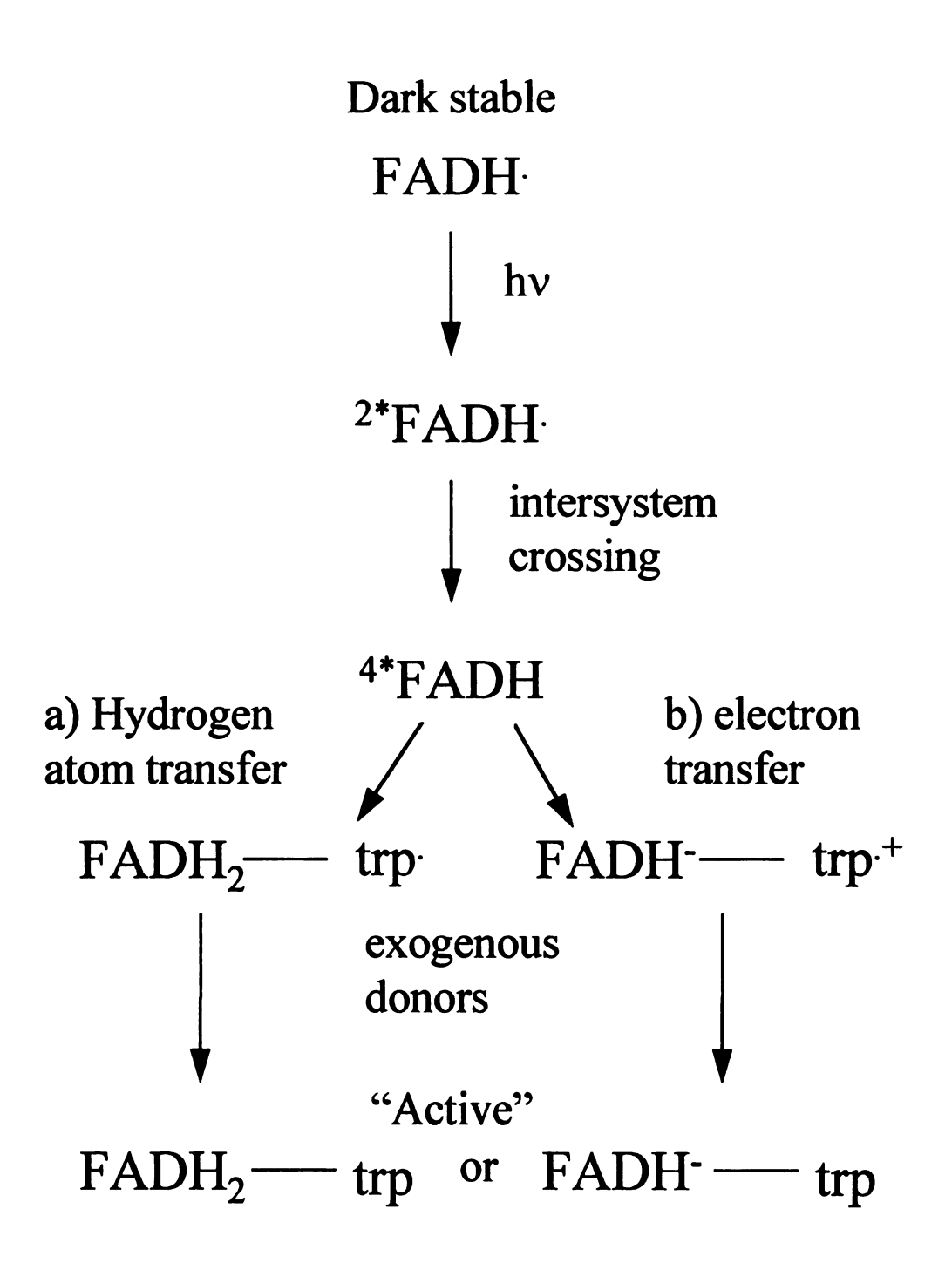
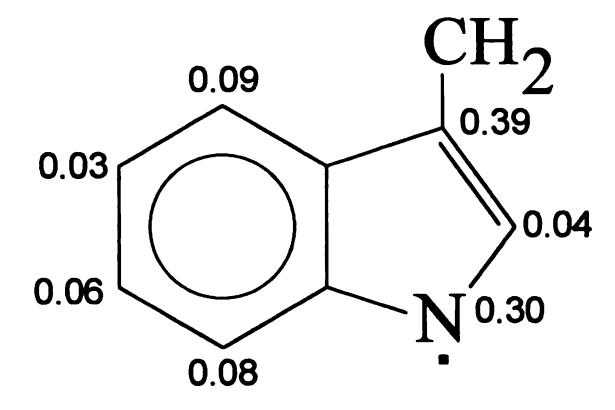


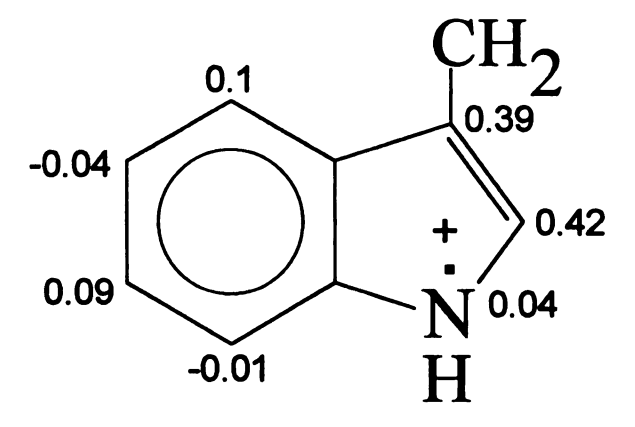
Figure 3.1

Figure 3.2. Calculated electron spin densities for the cation and neutral tryptophan radicals.

a) neutral trp radical



b) cation trp radical



Hoffman, B.M.; Roberts, J.E.; Kang, C.H.; Margoliash, E. *J. Biol. Chem.* 1981, 256, 6556.

Figure 3.2

results presented here is that the active form of the enzyme contains a flavin in its fully reduced anionic form (FADH) instead of the previously proposed FADH₂ species.

Materials and Methods

The enzyme was prepared in the laboratory of Professor Aziz Sancar at the University of North Carolina and, the preparation of the enzyme has been described elsewhere. Incorporation of isotopic labels into the enzyme and preparation of site directed mutants were carried out as described previously. 5 mM potassium ferricyanide was added to the sample to prevent the reduction of the enzyme from the FADH form to FADH2 during the course of the experiment. Typical enzyme concentrations were 0.1 mM. The reaction buffer contained 50 mM potassium phosphate buffer pH=7.0, 50 mM NaCl, and 20% glycerol.

Photoexcitation of the sample was carried out with a Xenon flashlamp that was critically damped with a pulse width of 17 μ s, a lamp energy of 50 J, and a repetition rate of 1 Hz. It was determined that all flashes were light saturating (see Figure 2.7).

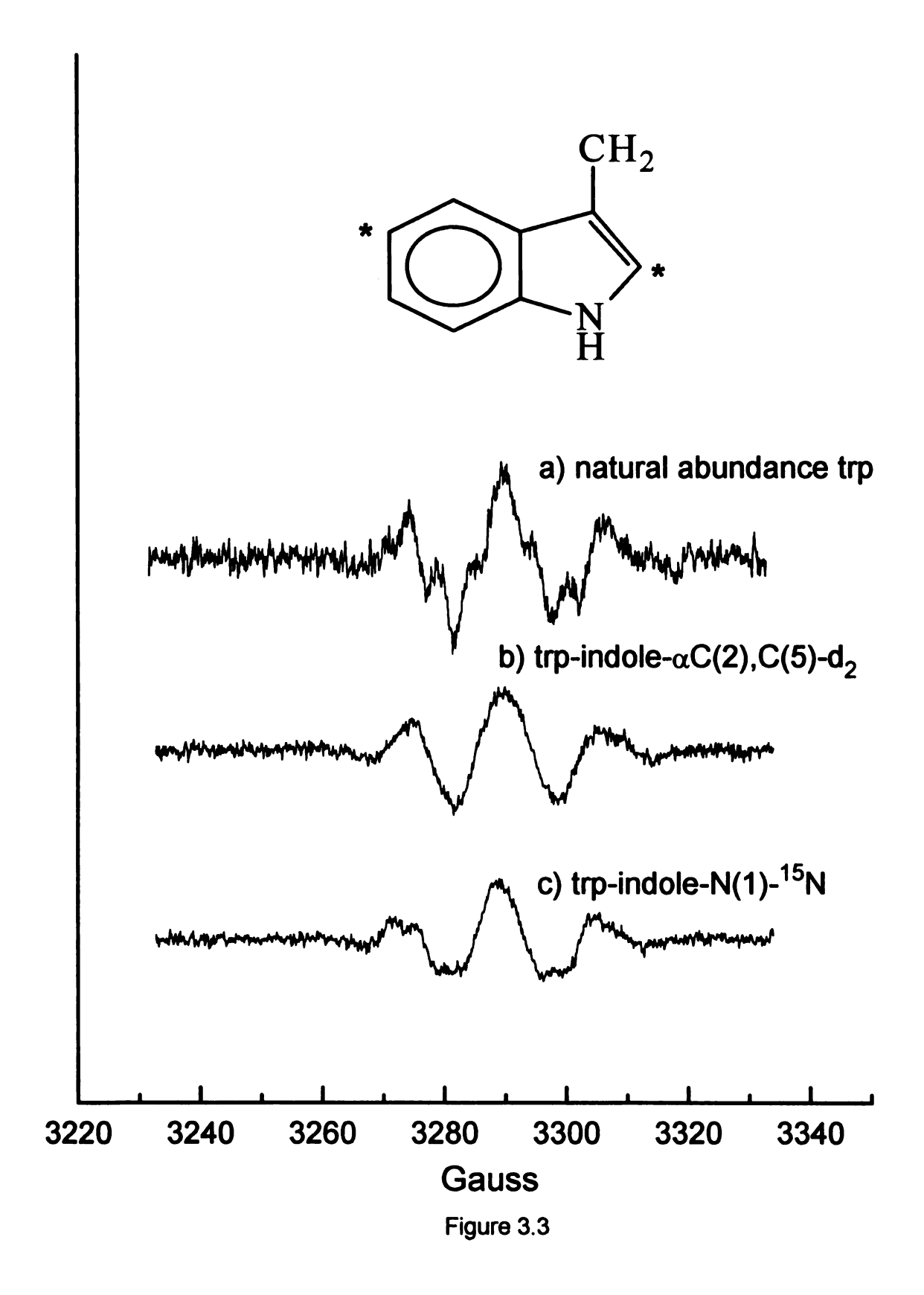
CW EPR measurements were carried out at 273 K on a Bruker ER200D spectrometer that is fitted with a Varian TM011 mode cavity. The magnetic field was measured with a Bruker ER035M NMR gaussmeter and the microwave frequency was monitored with a Hewlett Packard HP 5245 counter \ 5255 frequency converter. A microwave frequency of 9.22 GHz, a microwave power of 6.3 mW, a time constant of 35 µs, and a modulation amplitude of 2.8 G was used to perform the experiments.

Time-resolved EPR measurements were obtained by the experimental setup described in Chapter 2¹⁰. The field scan range was 100 G and a sweep time of 1000 s was used. Conditions for the gated integrator were as follows: trigger rate of 1 Hz, 3 averages per point, a 4 µs delay, and a 48µs aperture. AC-coupling of greater than 10 Hz was used to discriminate electronically against any stable signals that may be present.

Results

Figure 3.3b is a time-resolved EPR spectrum of the transient tryptophan radical that forms during photoreduction of a photolyase sample that contains deuterium labeled tryptophan at the positions indicated by the asterisks on the tryptophan structure in the inset of the figure. The spectrum has the same apparent g-value (2.0028) as the wild type sample whose transient spectrum is shown in Figure 3.3a. The transient spectrum in Figure 3.3b has three large hyperfine couplings (~15 G) that are present in a 1:2:1 ratio and an absorption spectrum that has an alternating emission and absorption pattern (data not shown) that is similar to the absorption spectrum for the wild type sample that is shown in Figure 2.9. The smaller hyperfine couplings of less than 5 G, which are present in the wild type transient spectrum that is shown in Figure 3.3a, are not resolved in the isotopically labeled sample whose transient spectrum is shown in Figure 3.3b. The dark stable flavin spectrum of this isotopically labeled sample shows no apparent differences from the wild type sample whose dark CW EPR spectrum is shown in Figure 2.4. Figure 3.3c shows a transient spectrum of the tryptophan radical in a photolyase sample that contains tryptophan that is isotopically labeled with ¹⁵N. The transient spectrum has the

Figure 3.3. Isotopically labeled samples of DNA photolyase. Isotopic labeling of the samples is described in Kim, S.T.; Sancar, A.; Essenmacher, C. and Babcock, G.T. *Proc. Natl. Acad. Sci. USA* 1993, 90, 8023. Experimental conditions were: 6.3 mW microwave power, 9.22226 GHz microwave frequency, 1000 sec scan, 40 scans, 2.8 G modulation amplitude, 35 µs time constant, 3220-3350 G microwave field, 3 averages, 1 Hz repetition rate, 4 µs delay, 48 µs aperture, and AC-coupling of greater than 10 Hz.



same apparent g-value as a wild type sample, and the dark stable CW EPR spectrum of the flavin semiquinone radical shows no visible change from the wild type sample spectrum in Figure 3.3a. The transient spectrum shows the same 15 G hyperfine coupling and alternating emission and absorption pattern as the wild type sample. The smaller couplings in the wild type sample have changed due to the isotopic substitution with ¹⁵N in this sample and suggest that some of the smaller couplings arise from unpaired spin density at the nitrogen in the tryptophan structure.

Figure 3.4 shows transient spectra for various site-directed mutant samples. Figure 3.4b and 3.4c show transient spectra for W306Y and W306F mutants, respectively. Neither mutant is able to form a transient radical as can be seen by comparing Figures 3.4b and 3.4c to the wild type sample in Figure 3.4a. Figure 3.4d and 3.4e show transient spectra for W157F and W418F mutant samples. These mutant samples have transient spectra that are virtually identical to the wild type sample in Figure 3.4a. Protein conformational changes due to a mutation at a site that is not involved in photoreduction can be ruled out as the reason for the absence of transient EPR spectra in the W306Y and W306F mutants because the W157F and W418F mutants still show a transient spectrum. All mutants have a dark stable flavin spectrum that is indistinguishable from the wild type sample. Therefore, it can be concluded that the reason for the absence of a transient EPR signal in the W306F and W306Y mutants is that trp-306 is the radical that is observed in the EPR spectrum and that phe and tyr are not able to be oxidized by the flavin doublet radical, apparently due to a difference in redox potentials of these amino acids.

Figure 3.4. Tryptophan mutants of DNA photolyase. Samples preparation is described in Kim, S.T.; Sancar, A.; Essenmacher, C. and Babcock, G.T. *Proc. Natl. Acad. Sci. USA* **1993**, *90*, 8023. Experimental conditions were: 6.3 mW microwave power, 9.22226 GHz microwave frequency, 1000 sec scan, 40 scans, 2.8 G modulation amplitude, 35 μs time constant, 3220-3350 G microwave field, 3 averages, 1 Hz repetition rate, 4 μs delay, 48 μs aperture, and AC-coupling of greater than 10 Hz.

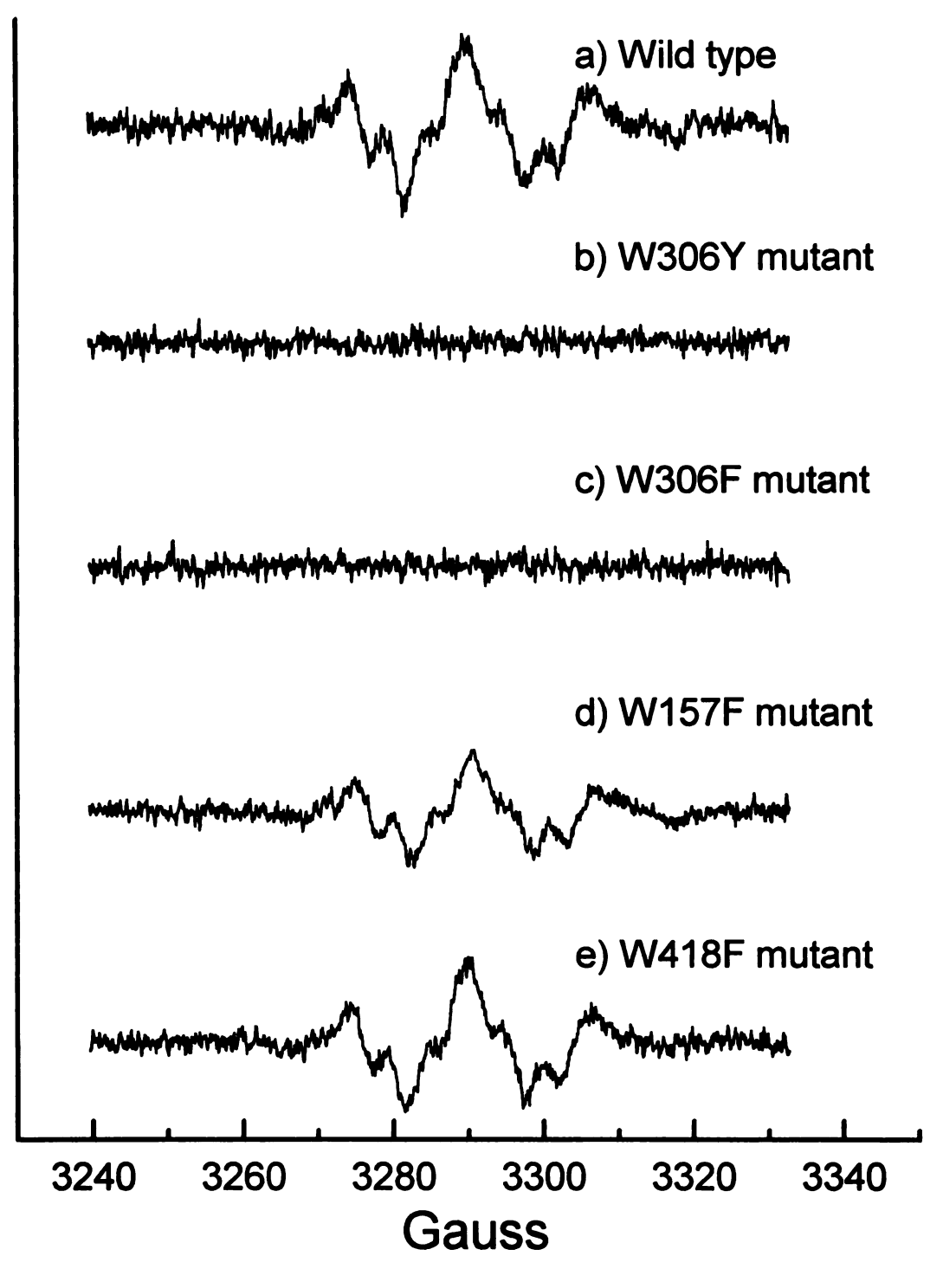


Figure 3.4

Discussion

The mechanism for photoreduction in photolyase that is shown in Figure 2.10 predicts that the transient radical that forms during the reaction is a neutral tryptophan doublet radical that is formed by hydrogen atom transfer from trp-306 to FADH. The ionic character of the tryptophan radical in photolyase has been determined by optical spectroscopy^{1,4}, but this technique cannot unambiguously distinguish between a cation and neutral radical in photolyase samples. Figure 3.1 shows two possible reaction schemes for photoreduction in photolyase. Figure 3.1a shows hydrogen atom transfer from trp-306 to FADH which produces a neutral tryptophan radical and FADH₂¹. Figure 3.1b shows an electron transfer mechanism from trp-306 to FADH to produce a transient cation tryptophan radical and FADH-7. A comparison of the time-resolved EPR spectra of isotopically labeled samples with the transient EPR spectrum of the wild type sample in Figure 3.3a should determine the mechanism of photoreduction in photolyase. If hydrogen atom transfer is the mechanism for photoreduction, a neutral tryptophan radical is predicted. If electron transfer occurs in photoreduction, a cation tryptophan radical should be present.

Huckel-McLaughlin spin density calculations have been performed for the cation and neutral tryptophan radicals⁸ and are shown in Figure 3.2. Spin density calculations have been used previously and the results have been shown to be quite reliable when they are used in a qualitative manner^{11,12,13,14}. The cation and neutral forms of the tryptophan radical show significant differences in spin density distributions, and these differences

allow a determination of the ionic character of the transient radical that forms during photoreduction by isotopically labeling photolyase samples. The cation radical has large spin density at the C(2) and C(3) carbons while all the other positions do not show any significant spin density. The neutral tryptophan radical shows significant spin density at the C(3) carbon and N(1) nitrogen positions. The hyperfine coupling in an EPR spectrum is directly proportional to the spin density at that position for nitrogen atoms. Coupling due to α -protons (protons that are bonded to a carbon in the aromatic ring) is given by the McConnell relation 15,16 that is shown in equation 3.1.

$$A_{\alpha} = Q\rho$$
 equation 3.1

 ρ is the spin density at the adjacent carbon, Q is the McConnell constant and is -25 G for α -protons, and A_{α} is the experimentally observed hyperfine coupling constant. Coupling due to β -methylene protons (protons that are bound to a methyl carbon that is bonded to a ring carbon) is given by equation 3.2.

$$A_{\beta} = 58 \rho \cos^2 \theta$$
 equation 3.2

 ρ is the spin density at the ring carbon, A_{β} is the observed hyperfine coupling in Gauss, and θ is the dihedral angle between a plane that contains the ring carbon, the methyl carbon, and a perpendicular to the ring plane and a plane that contains the ring carbon, the methyl carbon, and the β -methylene proton as illustrated in Figure 3.5. Figure 3.6 shows

Figure 3.5. Angles used for calculation of hyperfine coupling constants for β -methylene protons of tryptophan.

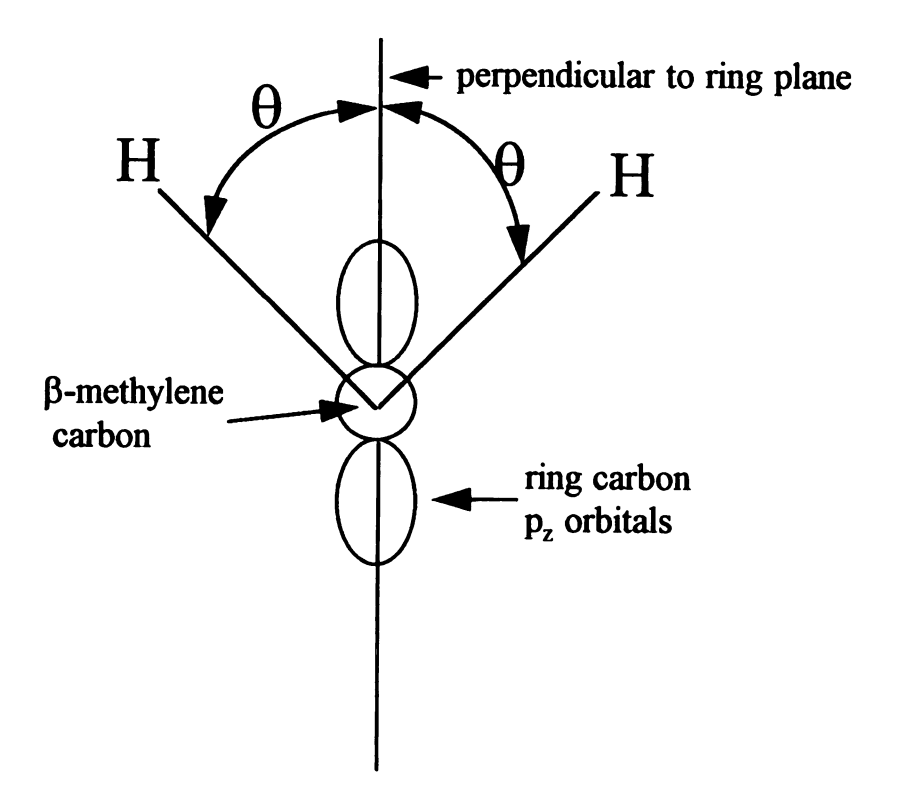


Figure 3.5

Figure 3.6. Tryptophan numbering scheme.

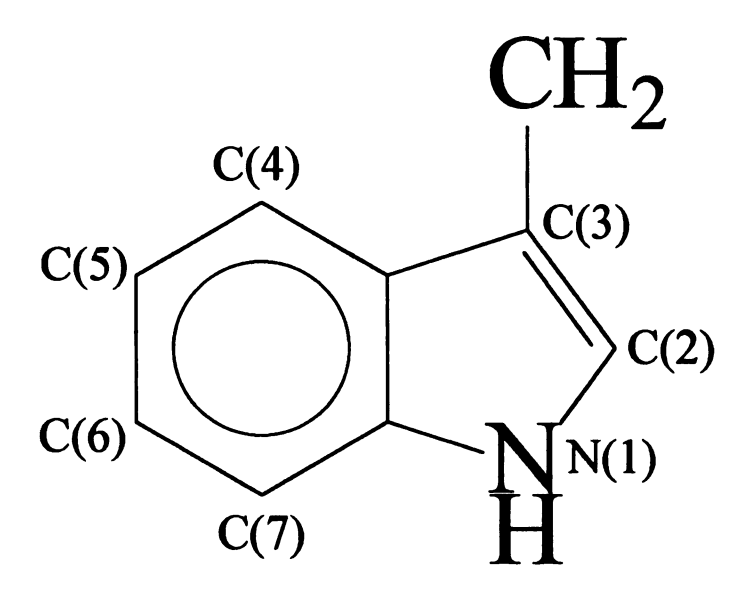


Figure 3.6

the numbering scheme for tryptophan. Both the neutral and cation tryptophan radicals have significant spin density at the C(3) β -methylene carbon and, as a result, deuteration of the β -methylene protons will not help in the determination of the ionic character of the transient radical. Specific deuteration of the C(2) α -proton will distinguish between the cation and neutral tryptophan radicals. Specific deuteration at the C(2) position is not expected to alter the spin density distribution of the transient radical. Deuterium has a Q constant (see equation 3.1) that is one-sixth that of hydrogen. Therefore, if the transient radical is a cation, implying an electron transfer mechanism, hyperfine couplings that are due to this proton should be six times smaller when deuterium has replaced hydrogen and significant changes to the experimental spectrum are expected. If the transient radical is a neutral tryptophan radical (hydrogen atom transfer), the transient spectrum should remain largely unchanged because the spin density at C(2) is insignificant.

Figure 2.8b shows a transient EPR spectrum for a sample that was specifically deuterated at the α -ring proton positions that are indicated by the asterisks on the tryptophan structure in the inset to the figure. The larger hyperfine couplings (~15 G) that are present in a 1:2:1 ratio in the wild type sample (solid arrows) in Figure 2.8a are also observed in the deuterated sample in Figure 2.8b. The smaller hyperfine couplings (dashed arrows in Figure 2.8a) that are present in the wild type sample are not resolved in the isotopically labeled sample in Figure 2.8b. The McConnell constant, Q in equation 3.1, is approximately -4 G for an α -deuteron, one-sixth the value of Q for an α -proton. The difference in energy in magnetic field units between the dashed arrows in Figure 2.8a is approximately 5 G. Upon isotopic substitution with deuterium, the smaller hyperfine

couplings (~5 G) that are present in the wild type sample are no longer resolved in the deuterated sample. Therefore, the smaller hyperfine couplings (dashed arrows in Figure 2.8a) can be attributed to hyperfine coupling to one or more α -protons that were replaced with deuterium in the isotopic labeling experiment. The hyperfine coupling of an α -deuteron in the sample whose spectrum is shown in Figure 2.8b will be less than 1 G (calculated with Q = -4 G in equation 3.1). A hyperfine coupling of this magnitude (< 1 G) is not expected to be resolved because the linewidth of the EPR transitions in photolyase are at least 3 G. Therefore, the assignment of the smaller hyperfine couplings to one or more α -protons is consistent with the experimental observation that replacement of α -protons with deuterium results in the loss of resolution of the smaller hyperfine couplings in the transient spectrum in photolyase.

A hyperfine coupling due to an α -proton on the tryptophan ring suggests that the transient EPR spectrum in Figure 2.8a arises from a cation rather than a neutral tryptophan radical. The calculated spin density distribution for the neutral tryptophan radical that is shown in Figure 3.2 shows that no significant spin density exists at any of the α -proton positions. The absence of spin density at these positions rules out a neutral tryptophan radical as a possible source of the transient EPR spectrum in Figure 2.8a. The spin density distribution for the cation tryptophan radical is also shown in Figure 3.2 and shows that a spin density of 0.42 is estimated at the C(2) α -proton position. Hyperfine coupling due to the α -proton at the C(2) position on the tryptophan cation radical is calculated using equation 3.1 to be 10 G. the calculated hyperfine coupling value due to the C(2) α -proton is in agreement with the experimentally observed value of 5 G when

consideration is given to the qualitativeness of spin density calculations 11,12,13,14 . The results of the spin density and hyperfine coupling calculations support cation tryptophan radical formation during photoreduction of photolyase and also suggest that the 5 G hyperfine coupling that is present in the wild type EPR transient spectrum in Figure 2.8a arises from coupling to the C(2) α -proton.

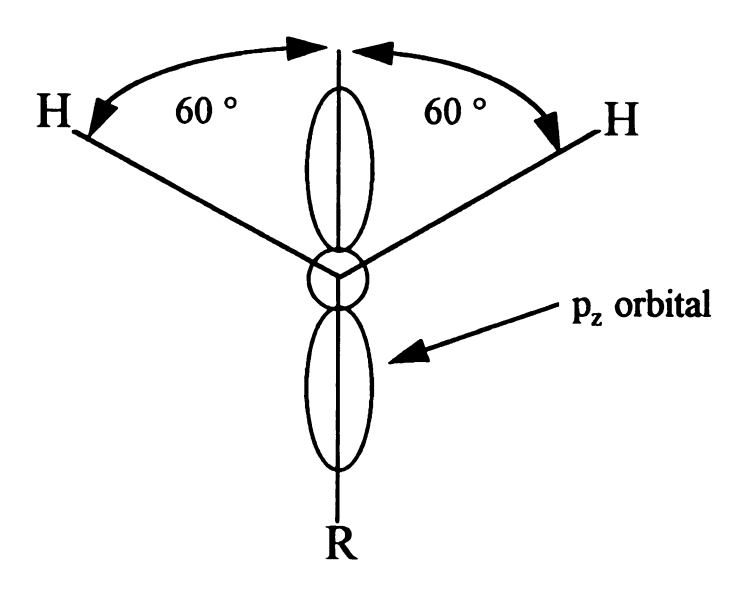
In order to test further the ionic nature of the transient tryptophan radical that is observed during photoreduction of the inactive enzyme, a sample that contained tryptophan that was isotopically labeled with deuterium at the positions indicated by the asterisks on the tryptophan structure in the inset to Figure 3.3 was prepared. The sample contains deuterium at the C(2) and C(5) positions. The transient EPR spectrum for this isotopically labeled sample is shown in Figure 3.3b. The transient spectrum has an apparent g-value of 2.0028 and a dark stable CW EPR spectrum that is indistinguishable from a wild type sample. The transient spectrum in Figure 3.3b has the same hyperfine couplings as the transient spectrum in Figure 2.8b that originated from a sample where all five α-protons were replaced with deuterium. The large 15 G hyperfine coupling is present in this sample, but the smaller 5 G hyperfine coupling (dashed arrows in Figure 2.8a) that is present in the wild type sample is not resolved when the C(2) and C(5) α protons are replaced with deuterium. Since only the C(2) and C(5) α-protons are replaced with deuterium in the sample whose transient spectrum is shown in Figure 3.3b, the smaller 5 G hyperfine coupling that is present in wild type samples must arise from coupling to one or both of the α -protons at these positions. Figure 3.2 shows that neither the neutral or cation tryptophan radical has significant spin density at the C(5) position;

therefore, the 5 G hyperfine coupling in the wild type transient spectrum most likely arises from coupling to an α -proton at the C(2) position. Hyperfine coupling that arises from a C(2) α -proton is consistent with tryptophan cation radical formation during photoreduction of the inactive enzyme.

If the transient radical that forms during photoreduction of inactive photolyase is a tryptophan cation radical as is predicted by the transient spectra of the photolyase samples that were isotopically labeled with deuterium (see Figure 3.3a and Figure 3.3b), the large 15 G hyperfine coupling that is present in the wild type transient spectrum in Figure 3.3a will arise from coupling to the two β-methylene protons at the C(3) carbon. hyperfine coupling pattern for the wild type transient spectrum show three transitions that are split by 15 G and are in a 1:2:1 ratio suggesting that these large hyperfine couplings arise from two equivalent nuclei. If the 15 G hyperfine coupling in the wild type spectrum are due to coupling to the two β -methylene protons at the C(3) carbon, the coupling will be proportional to the dihedral angle between a normal to the tryptophan ring plane and the β-methylene proton (see equation 3.2 and Figure 3.5). In order to observe identical hyperfine couplings for the two β -methylene protons the dihedral angle, θ in equation 3.2, must be equal for the two protons. The geometry of the four substituents to the βmethylene carbon is expected to be tetrahedral, and two possible spatial arrangements of the ligands exist and are shown in Figure 3.5. Figure 3.7a shows a low energy configuration where the two protons form a 60° angle with the dihedral plane and the peptide linkage, denoted by R in the figure, lies axial to the tryptophan ring plane. The geometry for the β-methylene carbon ligands that is shown in Figure 3.7a predicts a spin

Figure 3.7. Possible geometries for tryptophan β -methylene protons.

a) Low Energy conformation



b) High Energy conformation

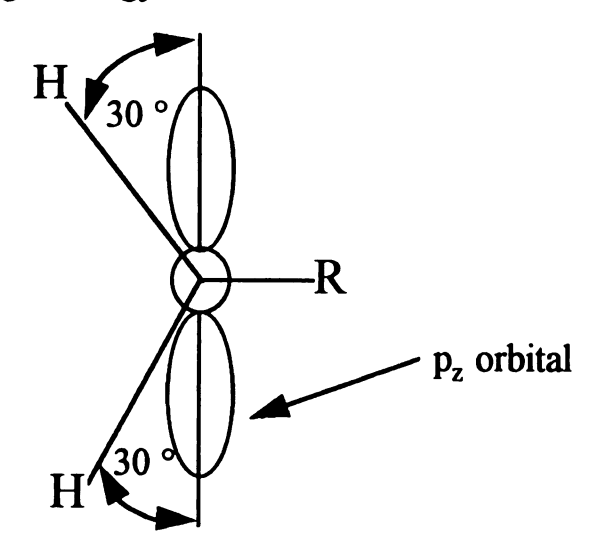


Figure 3.7

density of one at the C(3) carbon (see equation 3.2) when a hyperfine coupling of 15 G is observed experimentally. The spin density distribution that is shown in Figure 3.2 for the cation radical predicts a spin density of 0.39 at the C(3) carbon and suggests that the geometry of the ligands must be different than the one that is shown in Figure 3.7a. Figure 3.7b shows a high energy geometry of the ligands where the two β-methylene protons lie on the same side of the p_z orbital and form a 30° angle with the dihedral plane. In this geometry the peptide linkage lies equatorial to the tryptophan ring plane. The geometry in Figure 3.7b predicts a spin density of 0.34 at the C(3) carbon and is in much better agreement with the experimentally observed hyperfine coupling of 15 G in the wild type transient spectrum.

Another possibility for the three transitions that are split by 15 G in the wild type spectrum in Figure 3.3a is that the three transitions are in a 1:1:1 ratio that arises from the N(1) nitrogen with a nuclear spin of one. The neutral tryptophan radical has sufficient spin density at N(1) to produce a hyperfine coupling of 15 G but the cation does not (see Figure 3.2). Isotopic substitution of ¹⁴N with ¹⁵N in tryptophan should show the origin of the large 15 G coupling. If the transient radical in photolyase is a cation, as the deuterated samples (Figure 2.8b and 3.3b) predict, the three line pattern and its coupling should not significantly change when isotopic substitution of ¹⁴N with ¹⁵N is performed. If the transient radical is a neutral tryptophan, the three line pattern should collapse to a two line pattern with different couplings because of the difference in nuclear spin of these two isotopes (nuclear spin = 1/2 for ¹⁵N).

The transient EPR spectrum⁷ in Figure 3.3c arises from a sample in which ¹⁴N tryptophan is replaced by ¹⁵N. The major three line pattern is still present in a 1:2:1 ratio as in the wild type sample in Figure 3.3a. The smaller couplings (5 G) in the wild type sample are affected by this isotopic substitution which suggests that the hyperfine coupling due to nitrogen is less than 5 G. The small hyperfine coupling due to nitrogen gives further support for the transient radical being a cation and for the large 15 G coupling being due to the two β-methylene protons that are in the high energy configuration that is shown in Figure 3.7b.

The isotopic substitution experiments presented here, in addition to the spin density distribution calculations in Figure 3.2, have shown that there is a large spin density at C(2) and C(3) and a much smaller density at the N(1) nitrogen. The results show that the transient radical that forms during photoreduction of inactive photolyase is most likely a tryptophan cation radical. The results also show that the geometry of the ligands to the β-methylene carbon is probably the high energy configuration that is shown in Figure 3.7b where the peptide linkage is equatorial to the tryptophan ring plane base upon equation 3.2 and a 15 G hyperfine coupling that is observed experimentally.

Optical studies have suggested that tryptophan-306 is the internal H-atom donor to FADH during photoreduction of the enzyme¹⁷. Site-directed mutagenesis was used to confirm this assignment^{2,7}. Figure 3.4 shows various photolyase mutant samples. Figure 3.4b and 3.4c show the W306Y and W306F mutant transient spectra. Neither mutant exhibits any transient radical formation, but both samples still show a dark stable flavin EPR spectrum that is indistinguishable from the wild type sample (Figure 2.4). The

absence of a transient photo-induced EPR signal in these mutants confirms the assignment of trp-306 as the internal H-atom donor in photolyase. The transient EPR signals in Figure 3.4d and 3.4e arise from the W157F and W418F mutants. Both mutants show a dark stable flavin and transient spectra that are indistinguishable from the wild type sample as can be seen by comparing Figure 3.4d and 3.4e to Figure 3.4a. This result shows that any long range effects due to a mutation at a site that is different from the site of photoreduction does not affect the ability of the enzyme to photoactivate.

The assignment of trp₃₀₆ as the internal amino acid donor during photoreduction of inactive photolyase agrees well with the recently reported crystal structure for the enzyme¹⁸. The structure shows that trp₃₀₆ is located 13 Å away from the flavin chromophore, and this residue is located near the surface of the protein¹⁸. During photoreduction of inactive photolyase, the tryptophan residue reduces FADH³. An exogenous donor subsequently reduces tryptophan to reactivate the enzyme³. In order for tryptophan reduction by an exogenous donor to occur, the residue must be accessible to the solvent. The location of trp₃₀₆ near the protein surface makes it an ideal candidate as the internal amino acid donor during photoreduction of inactive photolyase because exogenous donors will have access to the site.

The mechanism for photoreduction that is shown in Figure 2.10 does not account for the experimental observations here. In order for a tryptophan cation radical to form, electron transfer from trp₃₀₆ to FADH must occur not H-atom transfer as previously suggested. Figure 3.1b outlines a possible mechanism for electron transfer in photolyase. Following photoexcitation of the enzyme, an excited flavin doublet state forms ^{2*}FADH.

Intersystem crossing to the quartet followed by electron transfer produces the transient radical pair which is a trp.⁺ and FADH.

The results presented here also suggest that the active form of the enzyme contains FADH and not FADH₂ as shown in Figure 2.10. Hydrogen transfer to FADH could occur at later times to produce FADH₂, but this is not expected. Hartman and Rose have studied dimer repair with flavin model compounds⁶. Their results show that the anionic singly protonated flavin is eight times more efficient at dimer repair than the neutral doubly protonated flavin. Furthermore, the fully reduced form of photolyase has an optical spectrum¹⁹ that closely resembles the spectrum of the anionic, singly protonated form of flavin mononucleotide (FMNH) rather than the doubly protonated form FMNH₂²⁰. Therefore, FADH is much more likely candidate for the active form of the enzyme considering model compound work and the presence of FADH after electron transfer in the photoreduction process in photolyase.

Figure 3.8 shows a proposed mechanism for photoreduction that takes into account the experimental observations presented here. Photoexcitation of the dark stable FADH species produces an excited doublet, ²*FADH. In 100 ps, the flavin intersystem crosses to the quartet, ⁴*FADH. Within 1 µs electron transfer from trp₃₀₆ produces a trpH⁺---³*FADH radical pair. Intersystem crossing to the ground state by the flavin produces FADH. Without exogenous donors, the radical pair recombines over several milliseconds. In the presence of external donors trpH⁺ is reduced to form the active enzyme that contains FADH

Figure 3.8. Proposed mechanism for photoreduction in photolyase based on the experimental results presented in this chapter.

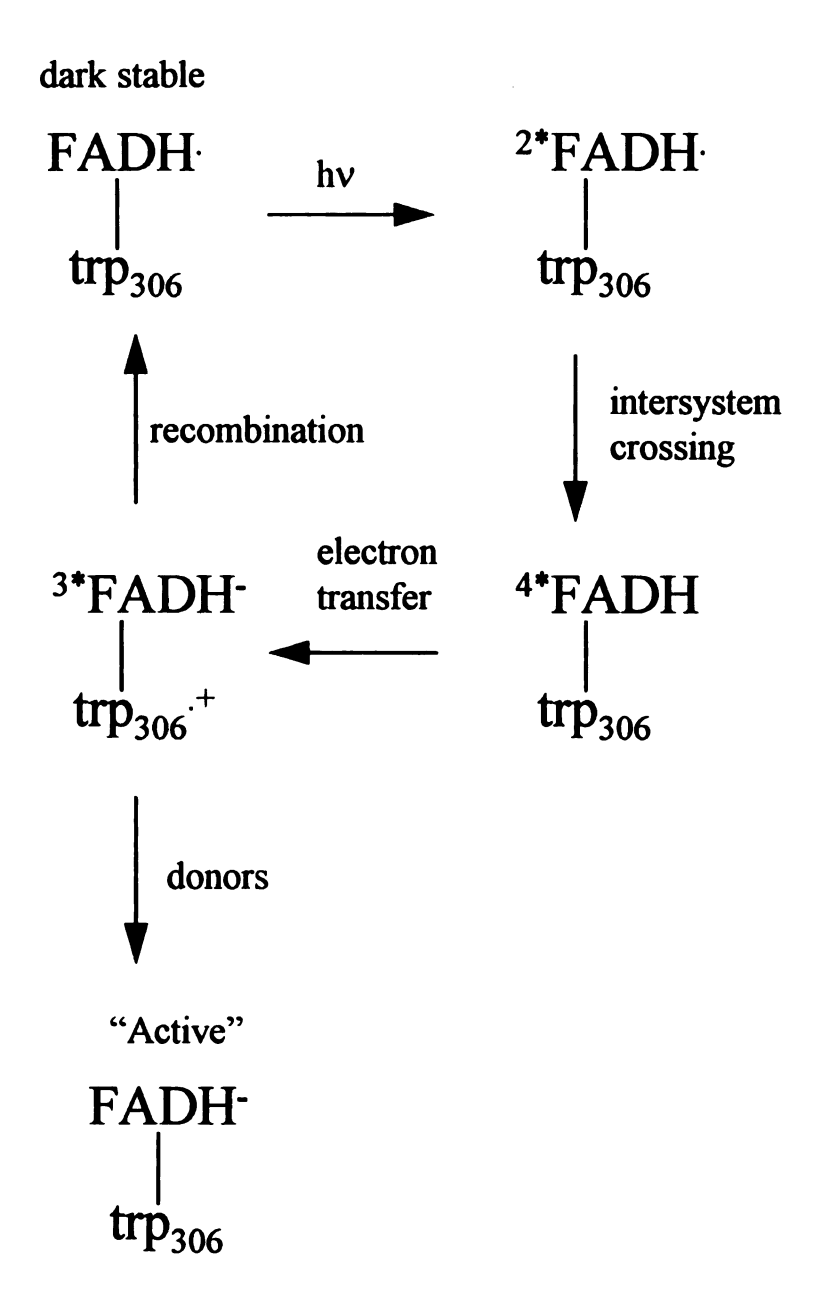


Figure 3.8

This study has shown by isotopic labeling that photoreduction in photolyase occurs by an electron transfer rather than H-atom transfer mechanism. These results also imply that the active form of the enzyme is FADH and not FADH₂ as previously proposed.

References

- 1. Essenmacher, C.; Kim, S.T.; Atamian, M.; Babcock, G.T.; Sancar, A. J. Am. Chem. Soc. 1993, 115, 1602.
- 2. Okamura, T.A.; Sancar, A.; Heelis, P.F.; Hirata, Y.; Mataga, N. J. Am. Chem. Soc. 1989, 111, 5967.
- 3. Heelis, P.F.; Okamura, T.; Sancar, A. Biochemistry 1990, 29, 5694.
- 4. Li, Y.F.; Heelis, P.F.; Sancar, A. Biochemistry 1991, 30, 6329.
- 5. Kim, S.T.; Sancar, A.; Essenmacher, C.; Babcock, G.T. J. Am. Chem. Soc. 1992, 114, 4442.
- 6. Hartman, R.F.; Rose, S.D. J. Am. Chem. Soc. 1992, 114, 3559.
- 7. Kim, S.T.; Sancar, A.; Essenmacher, C.; Babcock, G.T. *Proc. Natl. Acad. Sci. USA* 1993, 90, 8023.
- 8. Hoffman, B.M.; Roberts, J.E.; Kang, C.H.; Margoliash, E. J. Biol. Chem. 1981, 256, 6556.
- 9. Sancar, G.B.; Smith, F.W.; Reid, R.; Payne, G.; Levy, M.; Sancar, A. J. Biol. Chem. 1987, 262, 478.
- 10. Hoganson, C.W.; Babcock, G.T. *Biochemistry* 1988, 27, 5848.
- 11. McLachlan, A.A.D. Mol. Phys. 1960, 3, 233.
- 12. Streitweiser, A., Jr. *Molecular Orbital Theory for Organic Chemists* 1961 (Wiley, New York).
- 13. Tople, J.A.; Beveridge, D.L.; Dobosh, P.A. J. Chem. Phys. 1967, 47, 2026.
- 14. Tople, J.A.; Beveridge, D.L.; Dobosh, P.A. J. Am. Chem. Soc. 1968, 90, 4201.
- 15. McConnell, H.M. J. Chem. Phys. 1956, 24, 764.
- 16. McConnell, H.M.; Chesnut, D.B. Chem. Phys. Letts. 1958, 28, 107.
- 17. Payne, G.; Heelis, P.F.; Rohrs, B.R.; Sancar, A. Biochemistry 1987, 26, 7121.

- 18. Park, H.W.; Kim, S.T.; Sancar, A. and Deisenhofer, J. Science 1995, 268, 1866.
- 19. Heelis, P.F.; Payne, G.; Sancar, A. Biochemistry 1987, 26, 4634.
- 20. Ghisla, S.; Massey, V.; Lhoste, J.-M.; Mayhew, S.G. Biochemistry 1974, 13, 589.

Chapter 4

The Photoreduction Mechanism in DNA Photolyase: Correlated Triplet-Doublet

Radical Pair Polarization Arising From Differences in Hyperfine Frequencies

Introduction

A current model for the photoreduction / photoactivation process that incorporates the results in Chapters 2 and 3 is shown in Figure 3.8. Briefly, the model suggests that the photoreduction reaction is initiated by photoexcitation of the FADH chromophore and leads to an electronically excited doublet state (2*FADH)². Intersystem crossing to the quartet (4*FADH) is postulated to occur within 100 ps³ and is followed by electron transfer from a nearby amino acid residue in 1 µs. Flash photolysis and time-resolved EPR studies with site-directed mutants and isotopically labeled samples have identified this residue as tryptophan-306 in its cationic form^{1,4,5}. In the absence of exogenous donors, the transient species that forms following electron transfer (FADH—²trp₃₀₆) recombines over 7 ms⁶ to produce the catalytically inactive FADH form of the enzyme. One electron reduction of the tryptophan cation radical when exogenous donors are present gives rise to the active FADH form of the enzyme^{1,3}. In an earlier version of the photoreduction / photoactivation process, electron transfer from the excited doublet state flavin was postulated.

We showed previously that the transient species that forms following electron transfer from trp₃₀₆ in the photoreduction reaction is spin polarized due to magnetic interactions between a triplet flavin anion and doublet tryptophan cation radical pair⁵.

Other triplet-doublet radical pair polarizations have been reported and the resulting polarization patterns have been explained by the Radical Triplet Pair Mechanism (RTPM)^{7,8}. Hyperfine dependent polarization in combination with a net intensity for the spectrum are characteristic for this type of spin polarization^{8,9}, but photolyase does not exhibit any net polarization⁵ and, as we concluded previously, this indicates that RTPM cannot explain the spin polarization that is observed in the photolyase system. The timeresolved EPR spectrum of the transient species shows a polarization pattern that is alternating in emissive and absorptive transitions and is similar to Correlated Radical Pair Polarization (CRPP) observed in doublet-doublet radical pairs in photosynthetic reaction centers^{10,11}. Because of the similarity in polarization patterns, we propose an analogous polarization mechanism for triplet-doublet radical pairs called Correlated Triplet-Doublet Radical Pair Polarization (CTDRPP)⁵. We present here a description of CTDRPP and show the interactions that are responsible for this type spin polarization in triplet-doublet radical pair systems. Interpretation of the data we have obtained for photolyase within this model allows us to modify the reaction mechanism in Figure 3.8 so that electron transfer proceeds directly from the flavin excited doublet state.

Materials and Methods

Preparation of DNA photolyase has been described previously^{12,13}. To prevent reduction of FADH to FADH₂ during the course of the experiment 5mM potassium ferricyanide was added to the sample. Typical enzyme concentrations were 0.1-0.2 mM.

Flash photolysis of the enzyme was performed with a Xenon flashlamp with a 17 µs pulse width and a lamp energy of 50 J. It was determined that all flashes were near saturating.

Time-resolved EPR measurements were made by using a Bruker ER200D spectrometer at a temperature of 277 K. A 300 μl flat cell (Wilmad, Buena, New Jersey) was used to hold the sample and was placed in a Varian TM011 mode cavity that was modified to be compatible with the Bruker spectrometer¹⁴. The microwave frequency was measured with a Hewlett-Packard 5245 frequency counter / 5255 frequency converter and the magnetic field was monitored with a Bruker ER035M NMR gaussmeter. All experiments were performed at a microwave frequency of 9.22 GHz, a modulation amplitude of 2.8 G, a time constant of 35 μs, and a microwave power of 6.3 mW, unless otherwise noted.

Detection of the rise and decay kinetics of the transient radical following flash photolysis of the flavin radical-containing enzyme has been described previously 15. Transient spectra were recorded with an IBM data acquisition card that is interfaced to a personal computer. A Stanford Research Systems SR250 gated integrator and boxcar averager (Palo Alto, California) was used to electronically integrate the transient signal and to trigger the Xenon flashlamp. A 4µs delay and 48 µs aperture were used to integrate the transient signal and obtain the amplitude of the signal as a function of the magnetic field. The field was stepped slowly at a rate of 0.1 Gauss/sec and the flashlamp was pulsed at 1 Hz to obtain the amplitude of the transient at 1000 equally spaced magnetic field positions.

Results

Photoexcitation of the dark stable FADH species produces an intense transient EPR signal in the g=2 region that we previously assigned to the tryptophan-306 cation radical⁵. The kinetic trace of the transient radical was shown in Fig. 2.5. The transient radical shows a half time of 35 µs. The 35 µs component is not a true kinetic half time of the transient radical but is instead the response time of the instrument because of the use of 100 kHz magnetic field modulation. The decay kinetics of the transient radical are the same regardless of the magnetic field position (data not shown), suggesting that the transient radical arises from only the trp radical of the radical pair. This conclusion is in agreement with previous observations that show that specific deuteration of tryptophan changes hyperfine couplings throughout the transient EPR spectrum⁵.

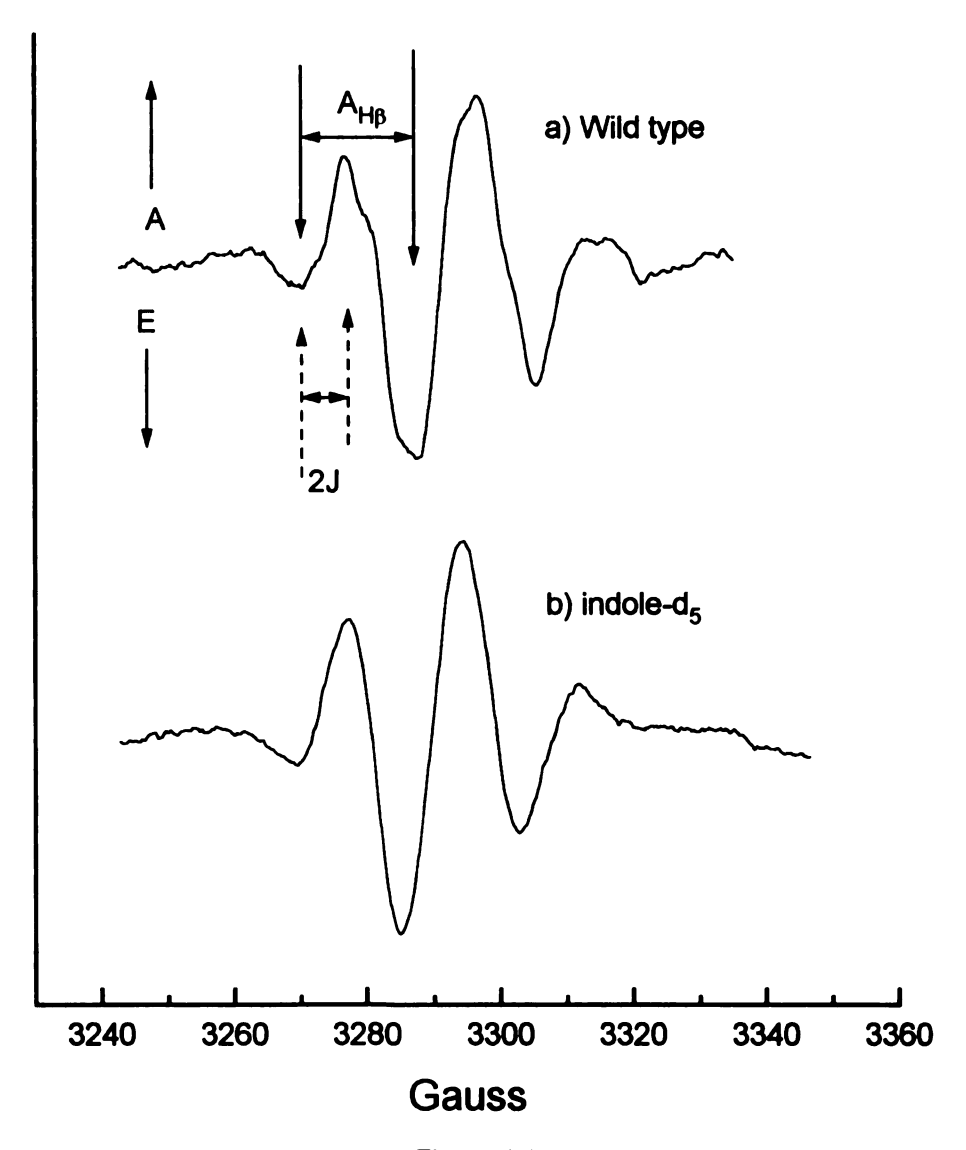
The transient, first derivative EPR spectrum for the radical whose kinetic trace is shown in Figure 2.5 is shown in Fig. 2.8a. Three major peaks are present (solid arrows in Fig. 2.8a) in a 1:2:1 ratio and are split by 15 G. We have previously shown that these transitions arise from coupling to two β -methylene protons on the transient tryptophan cation radical^{1,5}. The fact that the two β -CH₂ protons have identical hyperfine couplings to within our detection limits indicates that their dihedral angles with respect to the C(3) p_Z orbital that carries the unpaired spin density are equal and have values of 30° (see Chapter 3). Smaller splittings (< 5 G) superimposed on the major hyperfine couplings originate from couplings to an α -proton at the C(2) position of the tryptophan ring and to nitrogen at the N(1) position^{1,5}. Figure 2.8b shows a spectrum that originates from an

enzyme sample in which tryptophan was specifically deuterated at the α -ring positions. The loss of hyperfine structure confirms the tryptophan origin of the radical and allows us to assign couplings to the α -protons of the ring in the radical.

The integrated, absorption spectra of the two transient first-derivative spectra in Fig. 2.8 are shown in Figure 4.1. Figure 4.1a is the transient spectrum for the wild type sample, while Figure 4.1b is the corresponding spectrum for the tryptophan ring deuterated sample. Six major transitions can be identified in each spectrum and they alternate between emission and absorption. The major 15 G splitting that we observe in the transient, first-derivative in Fig. 2.8 and assign as the -CH₂ hyperfine coupling A_{Hp} is also present in the absorption spectra in Figure 4.1, and is observed as the splitting between each absorptive-emissive pair of transitions (shown as solid arrows in Figure 4.1a). Each of these pairs is further split into an emissive and absorptive component (dashed arrows in Figure 4.1a) that are separated by approximately 7.5 G. This splitting is identified as the exchange coupling, J, below. The smaller couplings (< 5 G) that are observed in Figure 2.8a are also present in Figure 4.1a as shoulders to the six major transitions.

Discussion

Electron spin polarization arises from the magnetic interaction between two members of a radical pair and the spin polarized spectrum shows emissive and absorptive transitions that are enhanced in intensity due to a non-Boltzman population difference Figure 4.1. Transient absorption spectra for a)wild type and b) deuterated photolyase samples. The spectra were obtained by numerically integrating the transient first-derivative EPR spectra in Figure 2.8a and Figure 2.8b.



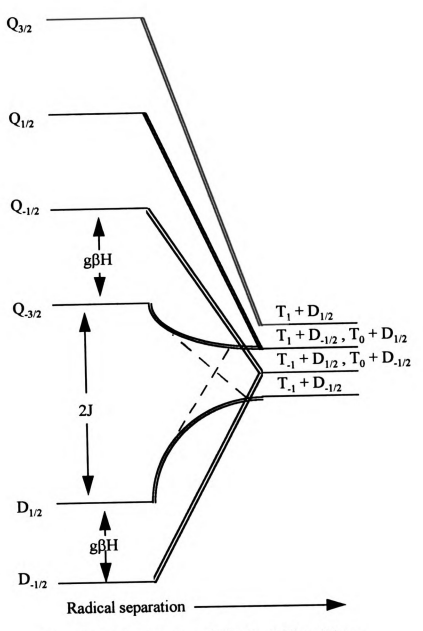
olyase first-

Figure 4.1

between the magnetic energy levels^{16,17}. We have shown that the transient tryptophan radical in Figure 2.8 is spin polarized; the most obvious manifestation of the nonthermalized character of the transient radical is the presence of emissive transitions in the time-resolved spectrum⁵. The absorption spectrum of the transient radical that is shown in Figure 4.1a clearly shows the emissive character of certain transitions and supports the spin polarization mechanism that has been proposed⁵. The isolated, inactive enzyme contains a doublet flavin radical. FADH: that abstracts an electron from trp-306 when the enzyme is photoexcited^{1,18}. The transient, spin polarized EPR signal in Figure 2.5 that arises from photoexcitation of the inactive enzyme has been shown to originate from only a doublet tryptophan-306 cation radical⁵. In order for spin polarization to occur in photolyase, a radical pair must form following photoexcitation of the enzyme. A likely candidate for the other radical pair member is a triplet FADH species because spin conservation is expected following electron transfer. Any other choice for the other radical pair member will not allow electron spin conservation or spin polarization to occur. Therefore, we have proposed that the second member of the radical pair in photolyase is a triplet FADH species that is not detectable by room temperature EPR^{1,5}. Consistent with this interpretation is the fact that previous studies of triplet flavin radicals have shown that their detection by EPR at room temperature is difficult¹⁹. The identification of excited flavin intermediates in the photoreduction reaction of the inactive enzyme by optical spectroscopy gives further support for triplet flavin radical formation in inactive photolyase during photoreduction 1,3,18,20.

The energy level diagram for the coupled basis set of a triplet-doublet radical pair and the individual magnetic states that lead to these energy levels are shown in Figure 4.2.

Figure 4.2. Magnetic states of triplet-doublet radical pair and the energy levels and state mixing in the coupled basis set that are formed from interactions within the radical pair.



nd state

Kawai, A.; Okutsu, T. and Obi, K. J. Phys. Chem. 1991, 95, 9130.

Figure 4.2

Figure 4.2 shows the magnetic substates of the triplet and doublet radicals that lead to the coupled basis energy levels. The T_{+1} and $D_{1/2}$ form the quartet state with an electron spin S_z of 3/2 ($Q_{3/2}$) while the T_{-1} and $D_{-1/2}$ levels form the $Q_{-3/2}$ state in the coupled basis set of the triplet-doublet radical pair. The $Q_{1/2}$, $Q_{-1/2}$, $D_{+1/2}$, and $D_{-1/2}$ states in the coupled basis set are formed by the magnetic states of the triplet and doublet radicals as is shown in Figure 4.2. Figure 4.2 also shows the energy level diagram for a coupled triplet-doublet radical pair. The four quartet states are separated by the Zeeman energy, $g\beta H$, where g is the electronic g value, g is the Bohr magnetron, and g is the magnetic field. The doublet states are also separated by the Zeeman energy, and the difference in energy between the doublet and the quartet (difference between $D_{1/2}$ and $Q_{1/2}$) is the exchange interaction energy 2J between the doublet and triplet radicals of the radical pair.

Net polarization in triplet-doublet radical pairs. Triplet-doublet radical pairs in non-biological solution systems show electron spin polarization that is explained by the Radical Triplet Pair Mechanism (RTPM)^{7,8,9}. The spin-polarized EPR spectrum of a triplet-doublet radical pair that exhibits RTPM shows a polarization pattern that is dependent upon the nuclear spin quantum and a superimposed net absorptive or emissive component^{8,9}. Net emissive polarization arises from state mixing between the -3/2 quartet (Q_{-3/2}) and the 1/2 doublet (D_{1/2}) states in the coupled basis set of the triplet-doublet radical pair, while net absorptive polarization arises from state mixing between the Q_{3/2} and D_{-1/2} states (see Figure 4.2). State mixing occurs because of a perturbation from the zero field splitting energy that is shown in equation 4.1⁸.

$$H_{r6} = D(S_{41}^2 - 1/3S_T^2) + E(S_{42}^2 - S_{43}^2)$$
 (equation 4.1)

D and E are the zero field splitting parameters, and S is the electron spin operator. The subscript T denotes the total spin and ϕ is the zero field axis system. The mixed state that forms as a result of state mixing is shown in equation 4.2

$$Q_{3/2} = |Q_{3/2}\rangle + \lambda |D_{1/2}\rangle$$
 (equation 4.2)

where " $Q_{-3/2}$ " is a linear combination of the $Q_{-3/2}$ and $D_{1/2}$ states and λ is given by equation 4.3

$$\lambda = (\langle Q_{-3/2} | H_{zfs} | D_{1/2} \rangle) / (E_Q - E_D)$$
 (equation 4.3)

where H_{zfi} is given by equation 4.1 and E_Q - E_D is the energy difference between the $Q_{\cdot 3/2}$ and $D_{1/2}$ states. For experiments performed at X-band frequencies, the energy difference between $Q_{\cdot 3/2}$ and $D_{1/2}$ is greater than 6000 G. In order for any significant state mixing between the $Q_{\cdot 3/2}$ and $D_{1/2}$ states to occur, λ must be significant. The zero field splitting energy is typically 600 G while the difference in Zeeman energy between the $Q_{\cdot 3/2}$ and $D_{1/2}$ states is on the order of 6000 G. These values give a value for λ of 0.1. When the two radicals of the radical pair diffuse to a region of high exchange energy, the energy difference between the two states, E_Q - E_D , is reduced to a value that is much closer to the zero field splitting energy H_{zfi} which allows significant state mixing in equation 4.2 to

occur. Figure 4.2 shows that, in the region of high exchange energy, the $Q_{.3/2}$ state is converted to $D_{1/2}$ and $D_{1/2}$ is converted to the $Q_{.3/2}$ state. When the two radicals of the pair separate to a region of zero exchange, only the quartet states are able to cross back to separated triplet and doublet radicals^{8,9}. The doublet states cannot cross back to the region of separated radicals and result in triplet quenching. Triplet quenching produces separated doublet radicals with enhanced α spin resulting in net emissive polarization in the time-resolved EPR spectrum^{8,9}. For absorptive polarization, the states involved are $Q_{3/2}$ and $D_{-1/2}$ states; the arguments then run parallel to those above for emissive polarization^{8,9}.

Hyperfine dependent component of RTPM. Hyperfine dependent spin polarization in RTPM arises from state mixing between the $Q_{1/2}$ and $D_{1/2}$ states and the $Q_{-1/2}$ and $D_{-1/2}$ states in the coupled basis set of the radical pair⁸ (see Figure 4.3). Mixing between these states is induced by the perturbation shown in equation 4.4 and arises from the different precessional frequencies of each member of the radical pair.

$$\omega = \Delta g + \Sigma_i A_i m_{si} - \Sigma_i A_i m_{si}$$
 (equation 4.4)

 ω is the sum of the difference in g-values (in frequency units) of the two radicals and the sum of the differences in hyperfine frequencies where A is the hyperfine coupling constant and m_S is the nuclear spin quantum number. Equation 4.5 shows the mixing for the eigenfunction that is represented by " $Q_{1/2}$ " in Figure 4.3.

$$"O_{10}" = |O_{10}| + \lambda |D_{10}|$$
 (equation 4.5)

where λ is shown in equation 4.6

$$\lambda = (\langle Q_{1/2} | \omega | D_{1/2} \rangle) / (E_O - E_D)$$
 (equation 4.6)

where ω is given by equation 4.4 and the denominator to equation 4.6 is the difference in energy between the doublet and the quartet. The other mixed states in Figure 4.3 are formed by analogous equations to equation 4.5 with ω (see equation 4.4) being the perturbation that causes the state mixing. The result is a spin-polarized, transient spectrum that is half emissive and half absorptive, similar to the Radical Pair Mechanism for doublet-doublet radical pairs 16,17 .

RTPM does not explain polarization patterns in photolyase. Spin polarization in photolyase cannot be explained by RTPM because this mechanism does not predict the polarization pattern that is observed in photolyase⁵. The polarization pattern in Figure 4.1a alternates between emissive and absorptive transitions and is inconsistent with RTPM where a transient spectrum that is half in emission and half in absorption is predicted for the hyperfine dependent component. The absence of net polarization in Figure 4.1a also precludes RTPM as a possible mechanism for spin polarization in photolyase and differences between non-biological and protein samples contributes to the absence⁵. Net emissive polarization, as discussed above, results from state mixing between the $Q_{-3/2}$ and $D_{1/2}$ states^{8,9}. Because the difference in energy between these states at X-band is large, a

Figure 4.3. Triplet-doublet state mixing from precessional frequency differences in the radical pair in the absence of an exchange interaction.

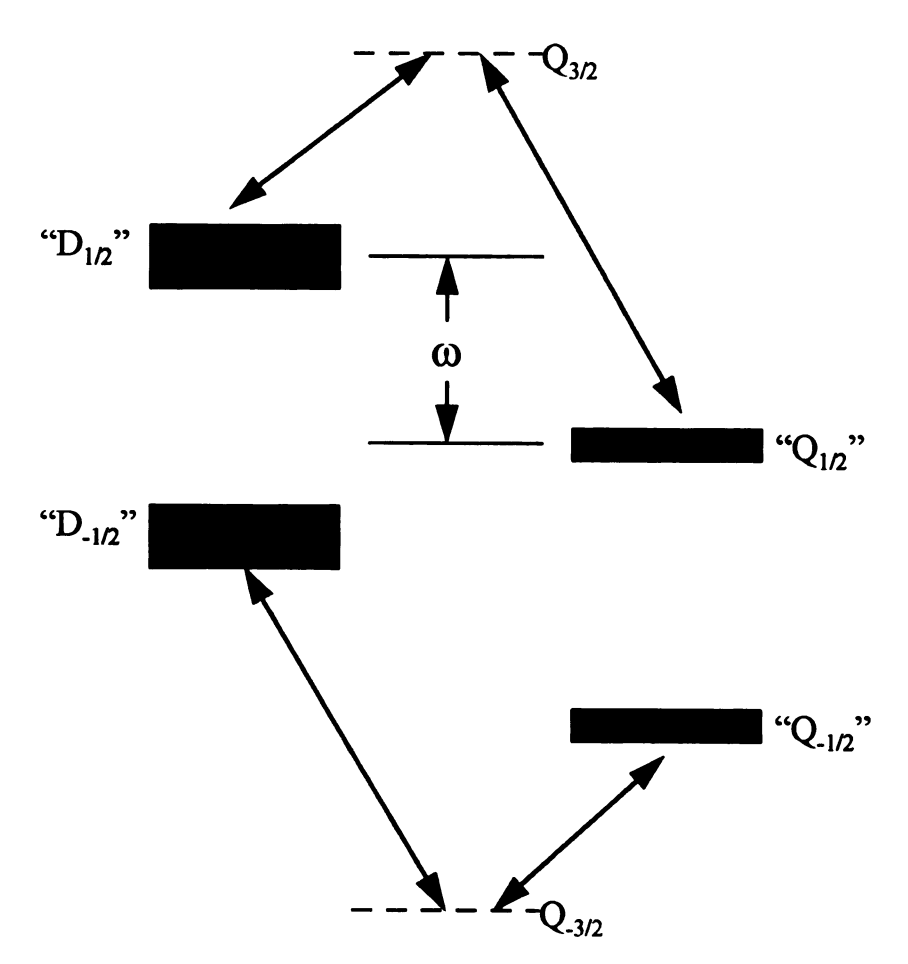


Figure 4.3

in the

large exchange interaction is necessary to mix these states effectively. Previous triplet-doublet radical pair polarizations occurred in solution reactions where diffusion of each radical pair member to a region of high exchange energy is possible^{8,9}. In photolyase, the radical pair is protein bound, thus preventing any diffusion from occurring. Without diffusion, the radical pair remains at a fixed separation throughout the reaction⁵. The high exchange energy that is needed for effective state mixing is not attainable with protein bound radical pairs, and this results in no net polarization in photolyase.

Correlated Radical Pair Polarization. Doublet-doublet radical pairs that are transiently present in the photosynthetic reaction centers show an alternating emissive and absorptive polarization pattern that is similar to the pattern in Figure 4.1a^{10,11}. Electron spin polarization in reaction centers is explained by the Correlated Radical Pair Polarization (CRPP) mechanism^{10,11}. CRPP predicts four transitions that are alternating in emission and absorption for a doublet-doublet radical pair when there are no resolved hyperfine couplings. Figure 1.8b shows the energy levels for the coupled basis set of the doubletdoublet radical pair. State mixing between the singlet and zero triplet energy levels produces the eigenfunctions "S₀" and "T₀" in the figure by the perturbation ω ($\Delta\Omega$ in Figure 1.8b) that is shown in equation 4.4. In order for CRPP to occur in a doubletdoublet radical pair, the two radicals must have a non-zero exchange interaction energy during the observation time by EPR¹⁰. Figure 1.8b illustrates pure CRPP for a doubletdoublet radical pair when no hyperfine coupling is observed. In the figure a positive exchange interaction (singlet is higher in energy than the triplet) and a singlet precursor are assumed. Initially when the precursor state is a singlet only the "S₀" and "T₀" energy

levels are populated because these eigenfunctions are the only ones that have any singlet character. The "S₀" energy level receives more of the initial population because it has more singlet character than the "T₀" energy level. The four transitions that arise from a CRPP mechanism with a singlet precursor and a positive exchange interaction are shown at the bottom of Figure 1.8b. The transition that occurs at the lowest magnetic field is the $S_0 \rightarrow T$, transition and, as the figure illustrates, this transition will be in emission. The other three transitions arise from the energy levels that are depicted in the figure. The result is a spin polarized EPR spectrum with equally intense lines and an E/A/E/A pattern (E denotes emission and A absorption). The two low field transitions $(S_0 \rightarrow T$, and $T_0 \rightarrow T_+)$ arise from one radical of the radical pair and the difference in energy between these two anti-phase transitions is the exchange interaction between the two members of the radical pair. The two high field transitions $(T_0 \rightarrow T_-)$ and $S_0 \rightarrow T_+)$ also form an anti-phase E/A pattern with the difference in energy being the exchange interaction between the two radical pair members. These two transitions arise from the other member of the radical pair. The difference in energy between each of these anti-phase doublet E/A pairs is the difference in precessional frequencies of the two radicals in the radical pair and is given by ω ($\Delta\Omega$ in the figure) in equation 4.4^{10,11}. If the sign of the exchange interaction or the precursor state is changed an opposite phase A/E/A/E pattern is predicted by CRPP¹⁰.

The equality in the intensity of the EPR transitions for pure CRPP as shown in Figure 1.8b arises from spin conservation of the radical pair 10 . For a singlet precursor, the amount of singlet character in "S₀" and "T₀" determines how much of the initial population each eigenfunction will receive. The T₊ and T₋ energy levels do not receive any of the

initial population because these energy levels do not contain any singlet character. The intensity of an EPR transition is proportional to the product of the population difference between the two energy levels involved in the transition and the transition probability for a transition to occur. The transition probability for a transition is proportional to the amount of triplet character that is contained in each eigenfunction because the transitions that are observed in CRPP are to the pure triplet state eigenfunctions T_+ and T_- . For the "S₀" eigenfunction, the population difference is greater than "T₀" but the transition probability is smaller. The opposite is true for "T₀" eigenfunction. The net result is that all of the transitions are equal in intensity for a spin polarized CRPP spectrum^{10,11}.

Figure 1.8c shows a CIDEP-CRPP spectrum that is observed when the radical pair has had time to evolve away from its initial population distribution 10,11 . At later times, the population distribution amongst the "S₀" and "T₀" energy levels is no longer determined by the precursor state of the radical pair. Figure 1.8c shows the case when the populations are accidentally equal, but numerous other distributions are also possible. The equality in populations of "S₀" and "T₀" makes the population differences with the pure triplet state eigenfunctions equal. This redistribution in population does not affect the transition probabilities to the pure triplet states and the intensity of each transition reflects this fact. The two low field transitions (S₀ \rightarrow T. and T₀ \rightarrow T₊) are still split by the exchange interaction energy, but the resulting emissive and absorptive transitions are no longer equal in intensity. The S₀ \rightarrow T. transition has a lower transition probability than the T₀ \rightarrow T₊ transition and the result is an E/A pattern that shows net absorption. The two high field transitions (T₀ \rightarrow T. and S₀ \rightarrow T₊) show an E/A pattern with net emission. The overall

spectrum still shows no net polarization because the amount of net absorption that is observed for the low field radical is exactly offset by the amount of net emission that occurs for the high field radical. In the absence of an exchange interaction during the observation time by EPR, the polarization pattern in Figure 1.8c would show an A/E pattern which is formed by net absorption in the two low field transitions and net emission in the two high field transitions^{10,11}.

The spin polarized spectra in Figure 1.8b and Figure 1.8c are observed because of state mixing between the S₀ and T₀ eigenfunctions due to a difference in the g-values of the two radicals of the radical pair¹⁰. Equation 4.4 shows that state mixing can occur because of a difference in the g-values and/or a difference in hyperfine coupling frequencies of the two radicals of the radical pair. When state mixing occurs primarily because of a difference in the g-values of the two radicals of the radical pair, net effect spin polarization occurs 16,17. If state mixing occurs because of a difference in hyperfine coupling frequencies of the two radicals, multiplet effect spin polarization results 16,17. Figure 4.4 illustrates net and multiplet effect spin polarization in the presence and absence of the exchange interaction during the observation time by EPR for doublet-doublet radical pairs with a singlet precursor. Figure 4.4a shows net effect spin polarization when the exchange interaction was positive but is zero at the observation time by EPR. An A/E pattern results with absorption arising from one radical and emission from the other¹⁰. When a positive exchange interaction is present during the observation time by EPR, afour line E/A/E/A pattern is seen as is shown in Figure 4.4b¹⁰. The two low field transitions show net absorption while the two high field transitions show net emission¹⁰. Figure 4.4c

Figure 4.4. EPR stick diagrams for net and multiplet effect electron spin polarization in the presence and absence of an exchange interaction.

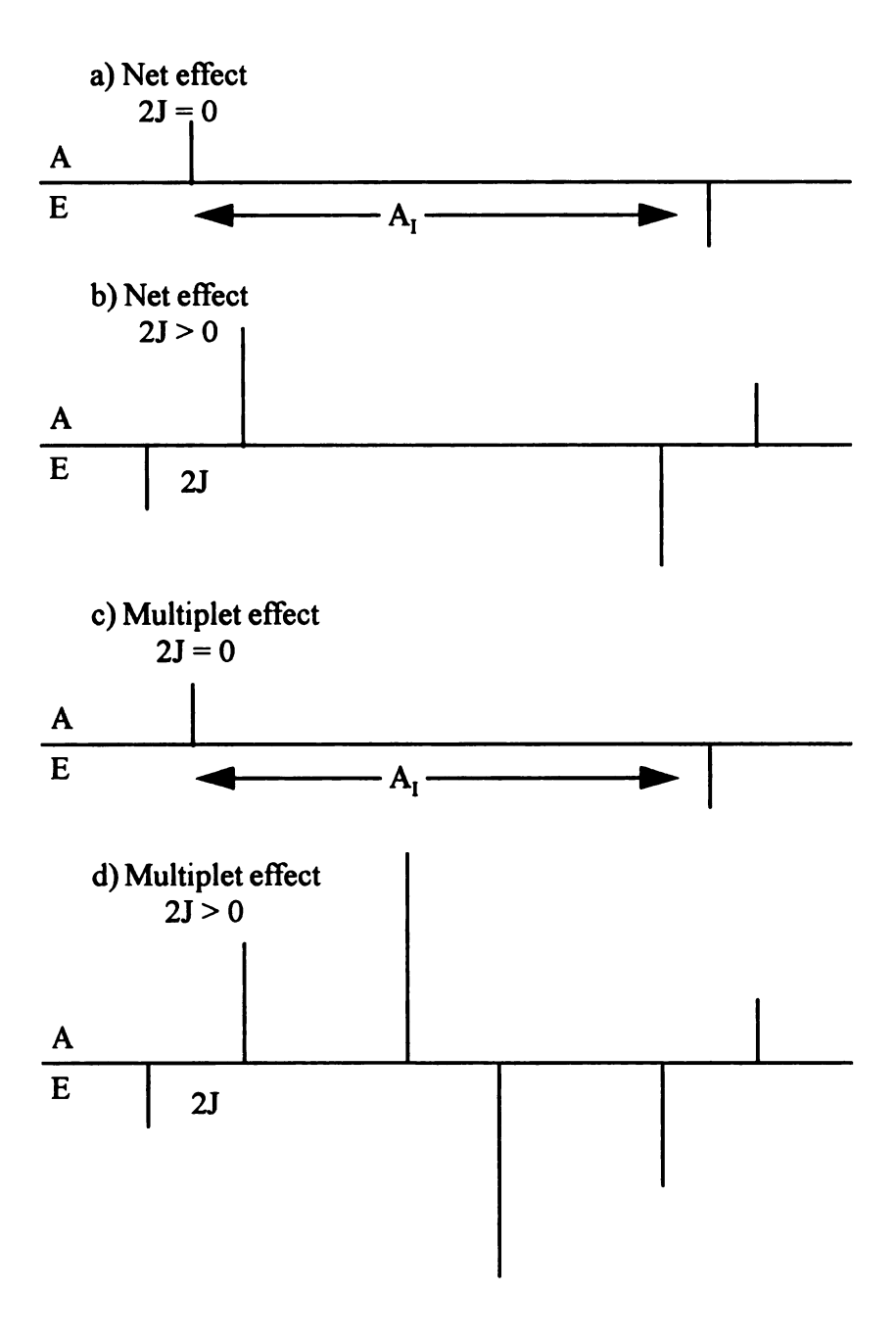


Figure 4.4

shows a spin polarized spectrum that arises from multiplet effect spin polarization from one radical that has hyperfine coupling to an I=1 nucleus. The spectrum shows an A/E pattern that arises from coupling to the $m_I=1$ nucleus of the radical. The low field absorptive transition arises from the $m_I=1$ transition, while the high field emissive transition arises from the $m_I=-1$ transition. The $m_I=0$ transition is not spin polarized and, consequently, this transition cannot be observed in the spin polarized EPR spectrum^{16,17}. Figure 4.4d shows multiplet spin polarization when an exchange interaction is present during the observation time by EPR. The low field E/A pair arises from the $m_I=1$ transition which has been split by the exchange interaction. This exchange split pair shows net absorption analogous to the $m_I=1$ transition in Figure 4.4c when the exchange interaction is zero. The center E/A pair arises from the $m_I=0$ transition and shows no net polarization, and the high field E/A pair arises from the $m_I=-1$ transition and shows net emission. The entire spectrum shows no net polarization as is required in a CRPP spectrum^{10,11}.

A mechanism analogous to CRPP occurs in photolyase. The polarization pattern for photolyase that is shown in Figure 4.1 is an alternating emissive and absorptive pattern that is similar to patterns that have been observed in photosynthetic reaction centers^{10,11}. The similarity in polarization patterns of photolyase and reaction centers suggests that spin polarization in photolyase occurs by an analogous mechanism to CRPP, but in a triplet-doublet manifold⁵. Figure 4.5 shows the energy level diagram and transitions for the coupled basis set of the radical pair for a triplet-doublet system that exhibits Correlated Triplet-Doublet Radical Pair Polarization (CTDRPP). The spin polarized stick spectrum that is shown at the bottom of the figure is shown for both radicals that show a positive

Figure 4.5. Triplet-doublet state mixing from precessional frequency differences in the radical pair in the presence of an exchange interaction with a doublet precursor.

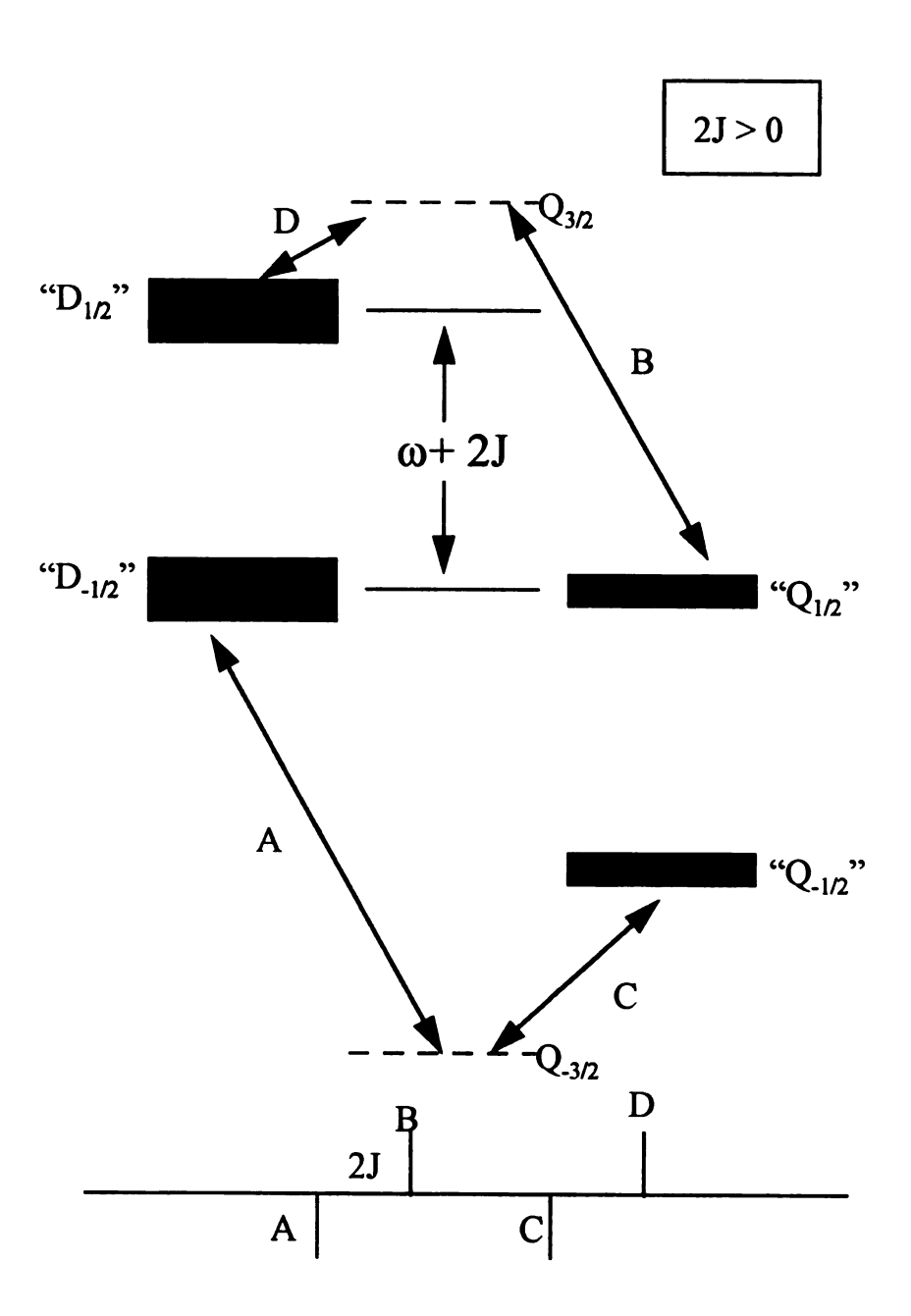


Figure 4.5

n the

exchange interaction, have no observable hyperfine coupling, and originate from a doublet precursor. State mixing between the $D_{1/2}$ and $Q_{1/2}$ unmixed energy levels produce the "D_{1/2}" and "Q_{1/2}" levels in the coupled basis set by the perturbation that is shown in The mixed eigenfunctions, " $D_{1/2}$ " and " $Q_{1/2}$ ", are formed by linear combinations of the unmixed energy levels as shown in equations 4.5 and 4.6. The "D_{-1/2}" and " $Q_{-1/2}$ " mixed eigenfunctions are formed by an analogous mechanism to the " $Q_{1/2}$ " and " D_{12} " state mixing that is described above. Initially, with a doublet precursor only the energy levels that contain doublet character are populated. Therefore, only the mixed eigenfunctions receive any of the initial population as illustrated in Figure 4.5. population will be larger for the "D_{1/2}" and "D_{-1/2}" energy levels because they contain more doublet character than the "Q_{1/2}" and "Q_{-1/2}" eigenfunctions. The four transitions that arise from the energy level diagram in Figure 4.5 are shown at the bottom of the figure. The two transitions labeled A and B arise from one member of the radical pair and form an E/A exchange split doublet. In the absence of an exchange interaction, transitions A ("D_{-1/2}" \rightarrow Q_{-3/2}) and B ("Q_{1/2}" \rightarrow Q_{3/2}) would be equal in energy. When the exchange interaction is present A and B are split by the exchange interaction as illustrated in Figure 4.5. The transitions that are labeled C and D also form an E/A pair that is formed by a splitting from the exchange interaction of the radical pair, and these two transitions arise form the other radical pair member. The difference in energy between each exchange split pair is given in equation 4.4 as the difference in precessional frequencies of the two radical pair members. The resulting spin polarized spectrum is one that shows four transitions that are equal in intensity and has an E/A/E/A pattern. At later times the precursor state no longer determines the population distribution of the radical pair, and each transition in the exchange split doublet will no longer be equal in intensity. Figure 4.6 shows that at later times the radical pair has more quartet character, but the transition probabilities to the pure quartet states do not change. Transition A is lower in intensity than transition B and this exchange split pair shows net absorption. Net emission is observed for the other exchange split pair that includes transitions C and D. The resulting spin polarized spectrum still shows no net polarization because the amount of net absorption that is observed for transitions A and B is balanced by the amount of net emission for transitions C and D.

The polarization pattern in Figure 4.1a shows six transitions that are in an E/A/E/A/E/A pattern with no net polarization⁵. The polarization patterns in Figures 4.5 and 4.6 for CTDRPP predict four transitions when a net effect (difference in g-values dominate equation 4.4) is observed. Therefore, the polarization pattern in photolyase cannot arise from net effect CTDRPP. The transient spectrum in Figure 4.1a has been shown to originate from a tryptophan cation radical (see Chapter 2) because the triplet flavin radical is undetectable at room temperature in our experiments⁵. If the transient absorption spectrum in Figure 4.1a originates from net effect spin polarization as outlined in Figure 4.3b, the transient spectrum would show net polarization. Figure 4.3b shows that one radical of the radical pair is in absorption, while the other is in emission when net effect spin polarization is observed. In photolyase, the triplet flavin radical ³FADH is undetectable and only a doublet TrpH⁺ is observed⁵. The absence of net polarization in photolyase rules out net effect CTDRPP as a mechanism because only half of the spectrum

Figure 4.6. Triplet-doublet state mixing in the presence of an exchange interaction with a doublet precursor at later reaction times.

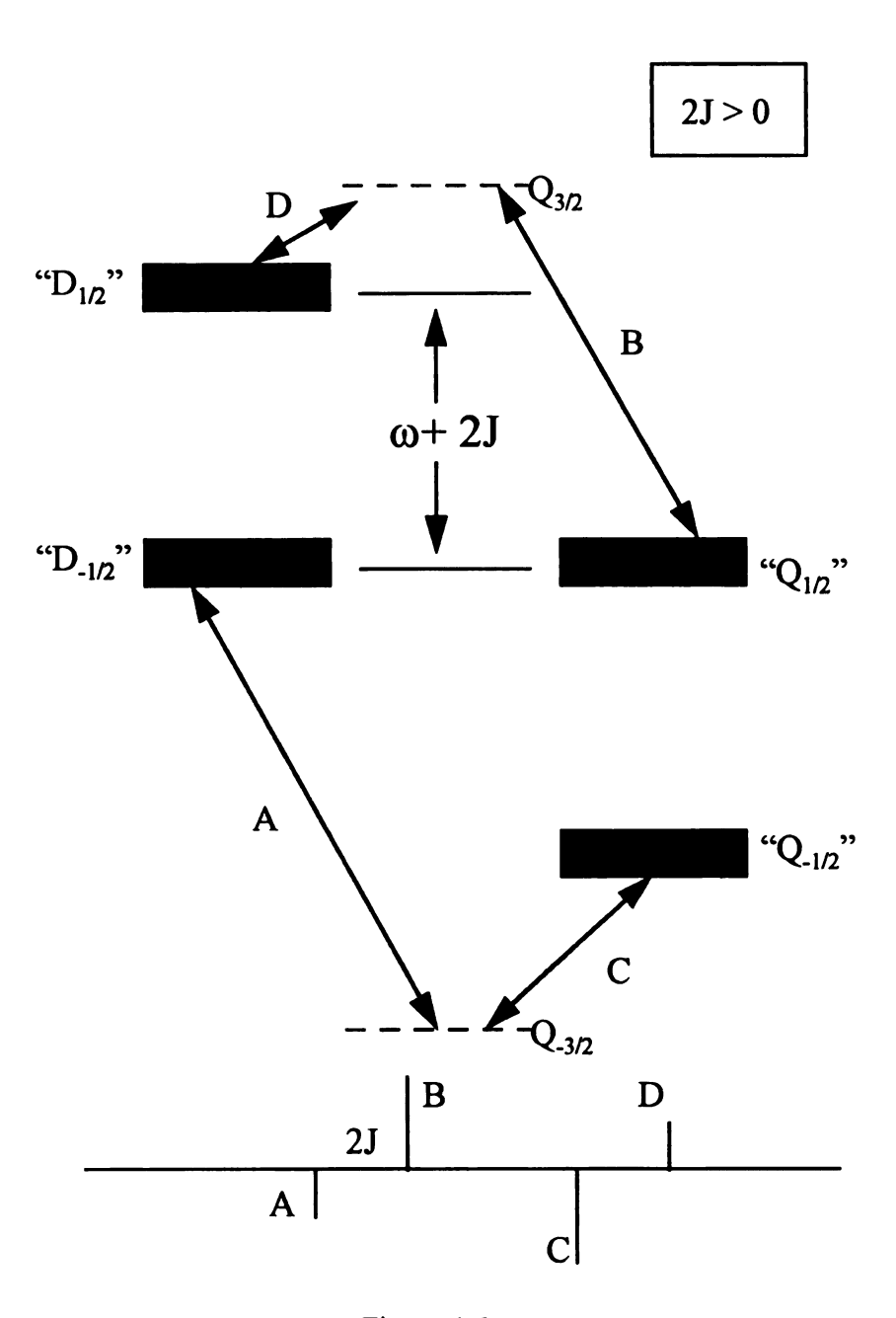


Figure 4.6

on with a

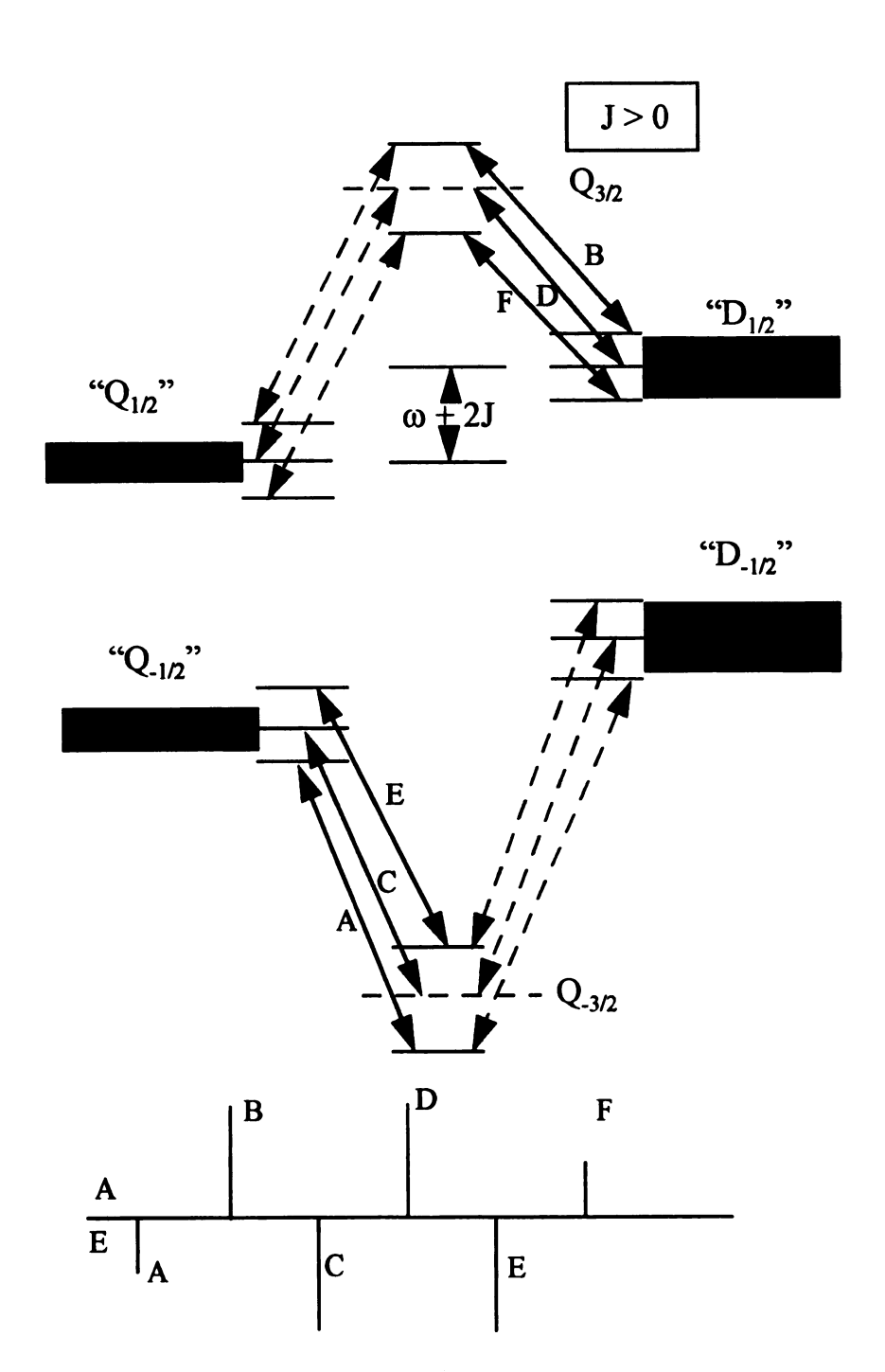
(the emissive or absorptive half) would be seen. Other evidence that supports multiplet rather than net effect spin polarization in photolyase are the g-values of the triplet flavin and doublet tryptophan radicals. The apparent g-value for the transient tryptophan radical is 2.0028. Triplet flavin radicals are expected to have a g-value of 2.0039¹⁹. State mixing between the "Q_{1/2}" and "D_{1/2}" energy levels by the perturbation in equation 4.4 is required in order to observe CTDRPP. The difference in energy between each exchange split doublet is equal to the perturbation ω in equation 4.4 (see Figure 1.8b for analogy to CRPP). The difference between each doublet in photolyase (denoted A_{Hβ} in the figure) in Figure 4.1a is 15 G. In order for net effect CTDRPP to occur in photolyase, the difference in g-values of the two radical pair members must be 15 G. In photolyase the difference in g-values between trpH⁺ and ^{3*}FADH is only 2 G. Therefore, spin polarization in photolyase must arise from multiplet rather than net effect CTDRPP.

The polarization pattern in Figure 4.1a is E/A/E/A/E/A with no net polarization. It has been shown previously that this pattern arises from two equivalent nuclei that are the β-methylene protons on the tryptophan cation radical (see chapter 3). Figure 4.7 shows an energy level diagram for a spin polarized mechanism that explains the polarization pattern in photolyase. The figure shows the pure quartet energy levels, Q_{3/2} and Q_{-3/2}, are initially unpopulated when the precursor state is a doublet. The four mixed states; "Q_{1/2}", "D_{1/2}", "Q_{-1/2}" and "D_{-1/2}", are formed by the perturbation in equation 4.4, and the linear combination of pure states that the mixed states are composed of is shown in equations 4.5 and 4.6. The mixed states are the only eigenfunctions that receive any of the initial population because they are the only states that have any doublet character. Each of the

six zeeman energy levels in Figure 4.7 are further split into three sublevels that arise from hyperfine coupling to the two β-methylene protons on the tryptophan cation radical. The triplet-doublet radical pair whose energy level diagram is shown in Figure 4.7 also has a positive exchange interaction (doublet lies higher in energy than the quartet). The six solid arrows in the figure show the six transitions that arise in photolyase. The bottom of the figure shows the stick diagram EPR spectrum for the transitions in the energy level diagram. Transitions A and B arise from the $m_I = 1$ transition and are split into an E/A pair that are separated in energy by the exchange interaction between the two members of the triplet-doublet radical pair. The absorptive transition is higher in intensity because of a rephasing of the radical pair from pure doublet to a state with partial quartet character. Transitions C and D arise from the $m_I = 0$ transition, are equal in intensity, and also are split by the exchange interaction of the radical pair. Transitions E and F arise from the mi = -1 transition and show net emission. The total spin polarized spectrum shows no net polarization as required by CTDRPP and CRPP rules. The six transitions that are denoted by the dashed arrows are not observed because these transitions arise from the triplet member of the radical pair which is not observable by EPR at room temperature in photolyase.

The diagram in Figure 4.7 predicts that the splitting between the transitions in the first E/A pair in the transient spectrum in Figure 4.1a (denoted as 2J in the figure) is the exchange interaction between the doublet tryptophan and triplet flavin radicals in photolyase. This suggests that the exchange interaction in photolyase is 7-8 G. As discussed above, the state mixing between the quartet and doublet eigenfunctions is

Figure 4.7. Hyperfine state mixing in a triplet-doublet radical pair with a doublet precursor.



ouble

Figure 4.7

induced by the perturbation in equation 4.4. The mixing in photolyase is primarily due to a difference in hyperfine coupling frequencies (multiplet effect) of the radical pair members rather than a difference in g-values (net effect). Multiplet effect CRPP has yet to be reported, but these effects are common in other spin polarization mechanisms such as RTPM and RPM. The perturbation in equation 4.4 is approximately equal to the difference in energy between the exchange split doublets (A_{Hβ} in Figure 4.1a) and is approximately 15 G in photolyase. The results here are the first reported case of a CRPP-type polarization in a triplet-doublet system and the first time that CRPP-type polarization is driven by hyperfine frequency differences rather than a difference in g-values.

Differences from CRPP in Photolyase. Even though spin polarization in photolyase and the photosynthetic reaction centers is very similar, there are some differences. Deuteration of reaction centers increases the amount of spin polarization^{11,21}, while deuteration in photolyase causes a loss in polarization by a factor of 2-3⁵. An explanation of this seemingly contradictory result lies in the method of deuteration that was used. Reaction center deuteration consisted of incubating the sample in D₂O and causes a large number of protons to be exchanged with deuterium¹¹. Linewidth broadening in reaction center EPR signals has been proposed to arise primarily from unresolved hyperfine coupling to protons¹¹. Deuterium has an intrinsic hyperfine coupling that is smaller than hydrogen, and as a result the linewidth will be smaller in samples that have the exchangeable protons replaced by deuterium. Considerable overlap occurs between the absorptive and emissive component of the exchange-split pair. A smaller linewidth will enhance the intensity of each transition in the exchange-split pair because

less overlap occurs¹¹. In photolyase, specific deuteration of the α-ring protons on the tryptophan ring was performed^{1,5}. As a result, fewer protons are replaced by deuteriums than in the reaction center case. Deuteration of tryptophan will reduce the difference in hyperfine frequencies between the two members of the radical pair. The main factor in producing spin polarization in photolyase is this difference in hyperfine frequencies. Deuteration of tryptophan reduces the difference in hyperfine frequencies of the two radical pair members, therefore, less spin polarization will result. In reaction centers, spin polarization mainly occurs through g-value differences of the two radicals, so linewidth reduction effects dominate¹¹. In photolyase, deuteration affects the difference in hyperfine coupling more strongly than linewidth considerations. The effect of deuteration in photolyase is that less state mixing occurs as seen in equation 4.4. Because less state mixing occurs, the polarization in photolyase will decrease as well.

Determination of the Precursor State in Photolyase. The energy level diagram in Figure 4.7 correctly predicts the polarization pattern for photolyase that is shown in Figure 4.1a and suggests that this diagram is an accurate representation of the energy levels of the triplet-doublet radical pair in photolyase. The diagram in Figure 4.7 is for a triplet-doublet radical pair that shows hyperfine coupling to two equivalent nuclei with a nuclear spin of 1/2, has a positive exchange interaction, originates from a doublet precursor, and mixes quartet and doublet states of the triplet-doublet radical pair through a difference in hyperfine coupling frequencies of the two radical pair members. An alternate energy level diagram which is shown in Figure 4.8 can also account for the polarization pattern for photolyase that is shown in Figure 4.1a. Figure 4.8 is an energy level diagram for a triplet-doublet radical pair that shows hyperfine coupling to two

Figure 4.8. Triplet-doublet state mixing with a quartet precursor in the presence of an exchange interaction.

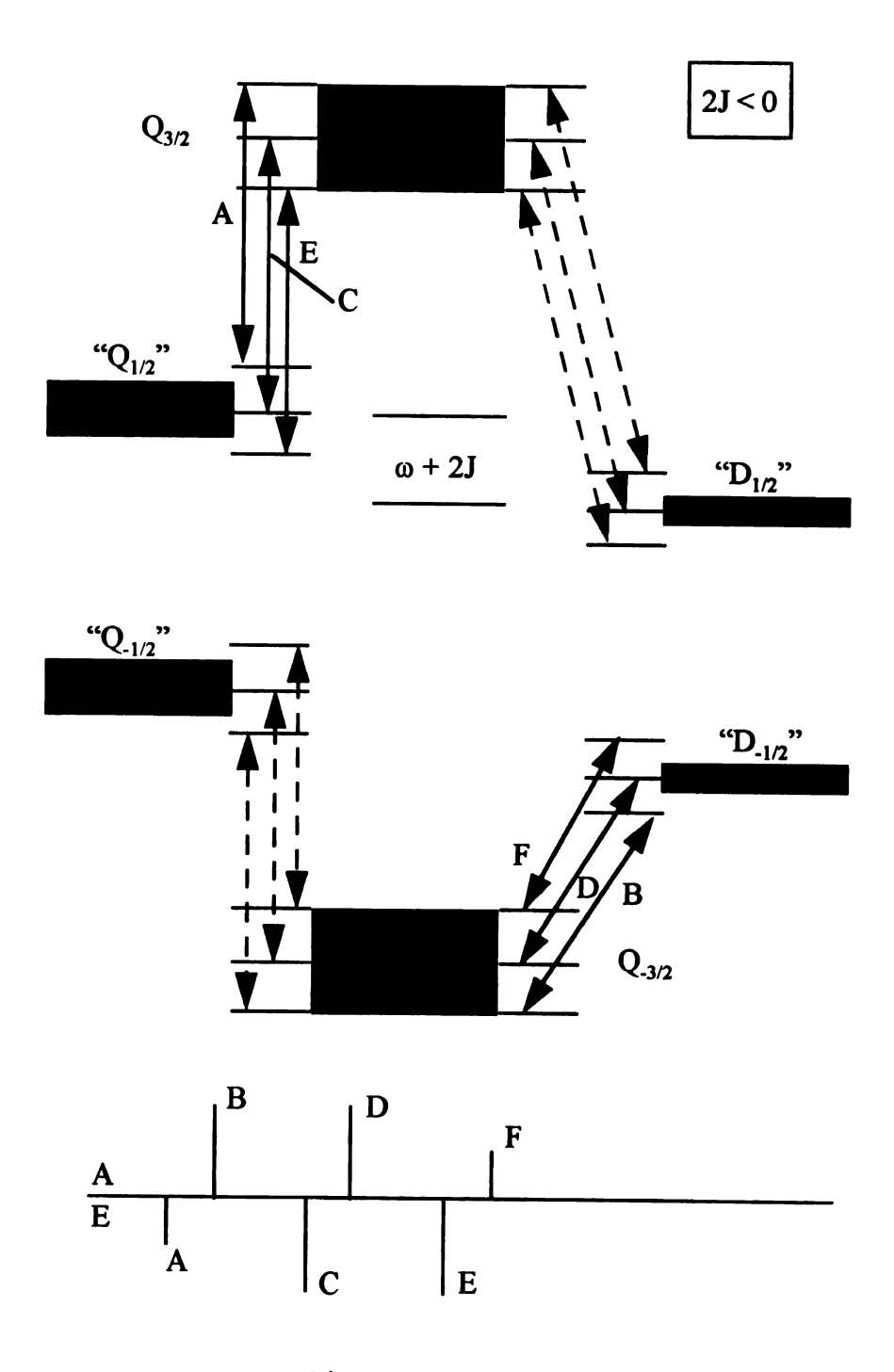


Figure 4.8

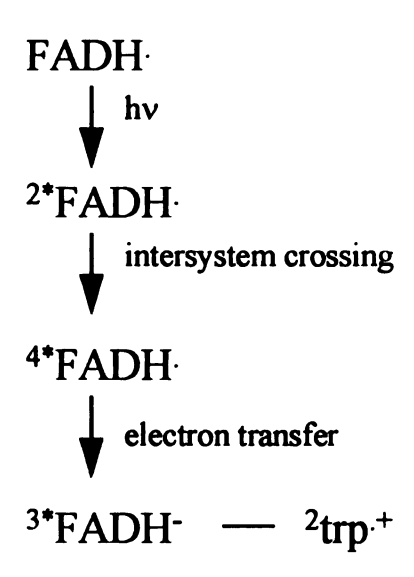
equivalent spin = 1/2 nuclei and mixes states through a difference in hyperfine coupling frequencies of the two radical pair members (see equation 4.4). The polarization pattern that is predicted from the energy level diagram in Figure 4.8 is shown at the bottom of the figure as an E/A/E/A/E/A pattern, and this pattern is the same as the one predicted by the energy level diagram in Figure 4.7. The difference between Figure 4.7 and Figure 4.8 is the sign of the exchange interaction and the precursor state of the triplet-doublet radical pair. Figure 4.8 shows the energy levels for a triplet-doublet radical pair that has a negative exchange interaction (doublet lies lower in energy than the quartet) and originates from a quartet precursor. Even though the sign of the exchange interaction and the precursor state are different for Figures 4.7 and 4.8, both figures correctly predict the polarization pattern that occurs in photolyase following flash photolysis of the inactive enzyme.

Figure 4.9a shows a possible mechanism for the formation of a triplet-doublet radical pair during photoreduction of inactive photolyase when the radical pair forms from a quartet precursor. Flash photolysis of the inactive enzyme (FADH containing) produces an excited doublet state, ^{2*}FADH. Intersystem crossing to the quartet occurs to produce ^{4*}FADH. Electron transfer from an amino acid side chain that has been identified previously as tryptophan-306 forms a triplet flavin anion radical ^{3*}FADH and a doublet cation radical trp.⁺. The triplet-doublet radical pair that forms produces a spin polarization pattern by the mechanism that is discussed above and shown in Figure 4.8.

An alternate mechanism for spin polarization in photolyase is shown in Figure 4.9b. The mechanism in Figure 4.9b is triplet-doublet radical pair formation that arises from a doublet precursor. Flash photolysis of inactive photolyase produces an excited

Figure 4.9. Reaction mechanisms for spin polarization in inactive photolyase.

a) Quartet precursor triplet-doublet radical pair



b) Doublet precursor triplet-doublet radical pair

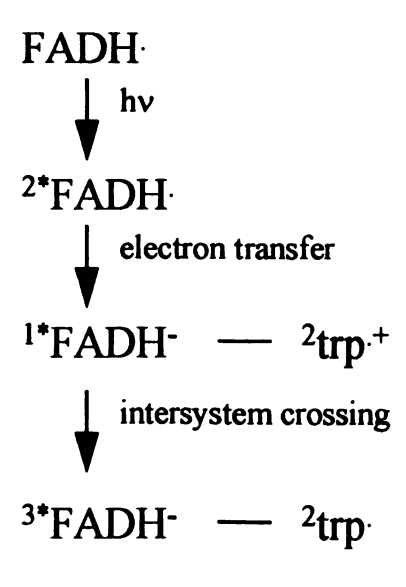


Figure 4.9

doublet state ²*FADH. Electron transfer from trp-306 to ²*FADH produces an excited singlet anion radical ¹*FADH and trp.⁺. The excited singlet ¹*FADH intersystem crosses to the triplet ³*FADH and spin polarization results from the triplet-doublet radical pair as shown in Figure 4.7.

The two mechanisms for spin polarization in photolyase that are shown in Figure 4.9 show triplet-doublet radical pair formation, but the precursor state for the spin polarized state is different in each case. Quartet precursor spin polarization as shown in Figure 4.9a arises from the excited flavin quartet precursor state ⁴FADH and suggests that the exchange interaction between the two radical pair members must be negative in order to observe an E/A/E/A polarization pattern (see Figure 4.8). Doublet precursor spin polarization, as shown in Figure 4.9b, arises from a singlet-triplet radical pair precursor state 1°FADH -- trp.+ and suggests that the exchange interaction between the doublet and triplet radicals must be positive in order to observe the polarization pattern that is seen experimentally in photolyase (see Figure 4.7). The difference between Figure 4.9a and Figure 4.9b is the sequence in which intersystem crossing of the flavin mojety occurs in relation to electron transfer from trp-306. For a quartet precursor, intersystem crossing must precede electron transfer, while the reverse must be true in order to observe doublet precursor spin polarization. At the present time insufficient experimental evidence exists to distinguish between these two mechanisms, but the arguments that follow suggest a reasonable choice and allow us to postulate a mechanism for photoreduction in photolyase.

Comparison of electron transfer rates with the photosynthetic reaction center. A comparison of the electron transfer rates of photolyase and the bacterial reaction center provide evidence for the doublet precursor mechanism in Figure 4.9b rather than the quartet precursor one in Figure 4.9a. Optical data have been interpreted to indicate that the excited flavin doublet state, with a lifetime of 100ps, intersystem crosses to the quartet, and electron transfer follows in a microsecond. The polarization pattern of the transient radical in photolyase that is shown in Figure 4.1a suggests that the rate of electron transfer must be 100 ps rather than the optical data prediction of a microsecond. Transient spin polarized spectra in the bacterial reaction center, which exhibit CRPP, set the value of the exchange interaction between the bacterial pheophytin and the chlorophyll dimer to 7.5 G^{11,22}. This value is similar to the exchange interaction in photolyase which we estimate to be 7-8 G. Because the exchange interaction is similar in these two proteins we expect that the rates of electron transfer will also be similar. The rate of electron transfer, as given by Marcus theory²³, is shown in equation 4.7.

$$k_{et} = 2\pi/h V_R^2 FC$$
 (equation 4.7)

 k_{et} is the rate of electron transfer, V_R^2 is the electronic coupling, and FC is the Franck-Condon factor. The similarity in the exchange interaction of both proteins suggests that the electronic coupling between the donor and acceptor is also very similar because both the exchange interaction and the electronic coupling are dependent upon the distance that separates the donor and acceptor. The FC term in equation 4.7 could differ between the

two proteins, because this term depends on the difference in free energy of the reactants and the reorganization energy of the reaction. Moser et. al. have shown that the FC term in equation 4.7 can modulate the rate, but not to any great extent. These authors suggest²⁴ that even though the rate can theoretically change by 5 orders of magnitude with a change in FC, such large rate changes are not observed experimentally. The electron transfer rate in nature is modulated instead by varying the distance between the two reactants, which results in a change in the electronic coupling of the two reactants. We cannot calculate the rate of electron transfer in photolyase because we do not know the free energy change or reorganization energy of the reaction. The findings of Moser et. al.²⁴ indicate that the electron transfer rate in photolyase should be similar to the rate between BPh and BChl in reaction centers because similar exchange interactions in each system implies that the distance between the donor and acceptor is also similar. The rate of electron transfer in bacterial reaction centers has been reported to be 3 ps^{25,26}. In photolyase, the spin polarization data in Figure 4.1a imply that the rate should be on a ps time scale owing to the similarity in exchange interactions, while the optical data suggests a rate of 1µs². The similarity in exchange interactions insinuate that the rate of electron transfer in photolyase should be much faster than the optical data prediction. If the rate of electron transfer in photolyase were a microsecond as the optical data suggest, the rate of electron transfer with similar distances would have to decrease FC in photolyase by more than 5 orders of magnitude. This result is contrary to what has been observed previously for electron transfer reactions²⁴. If the rate were on a ps time scale for photolyase, the FC term would not have to decrease the rate by such a large factor. Therefore, an electron

transfer rate on a ps time scale is much more likely in photolyase. A ps time scale electron transfer rate also implies that electron transfer must precede intersystem crossing in photolyase. Optical studies of photolyase show two species with lifetimes of 100 ps and 1 µs². We have shown above that the species with a 100 ps lifetime must decay as a result of electron transfer from trp-306 to FADH. The slower decaying species has to arise from intersystem crossing of ¹°FADH to ³°FADH if the 100 ps species arises from electron transfer. The mechanism in Figure 4.9b for doublet precursor spin polarization shows that electron transfer precedes intersystem crossing of the flavin radical and is in agreement with the electron transfer rate in photolyase being on a picosecond time scale. The mechanism in Figure 4.9a for quartet precursor spin polarization cannot account for a rate of electron transfer that is faster than the rate of intersystem crossing, and the discussion above implies that the correct mechanism for photoreduction in photolyase is the one in Figure 4.9b where the triplet-doublet radical pair is formed from a doublet precursor.

Calculated energies of doublet and quartet. Further evidence that supports the mechanism given in Figure 4.9b is the relative energies of the quartet and doublet states. Theoretical calculations²⁷ have shown that a quartet state should be higher in energy than a doublet. If the flavin excited quartet state ^{4*}FADH is higher in energy than the excited doublet flavin state, intersystem crossing to the quartet as shown in Figure 4.9a is not expected. This gives strong support for the mechanism in Figure 4.9b where intersystem crossing from the excited flavin singlet to the triplet occurs rather than intersystem crossing from an excited doublet to the quartet as proposed in Figure 4.9a.

Other evidence that supports the formation of a triplet-doublet radical pair in photolyase that arises from a doublet precursor is the sign of the exchange interaction that is necessary in order to observe an E/A/E/A/E/A pattern as in Figure 4.1a for photolyase. Figure 4.8 shows that, when the triplet-doublet radical pair originates from a quartet precursor, a negative exchange interaction (doublet lies lower in energy than the quartet) is necessary in order to observe a polarization pattern that is similar to the one that is observed in photolyase. Figure 4.7 shows a polarization pattern that arises from a tripletdoublet radical pair that originates from a doublet precursor and implies that a positive exchange interaction (doublet lies higher in energy than the quartet) is needed to observe this pattern. Neutral radical pairs in solution reactions are expected to have a negative exchange interaction in accordance with Hund's rule⁹. Adrian has shown that it is theoretically possible to have a positive exchange interaction in cases where the two radical pair members are ionic¹⁷. This result has been proved experimentally by work in which the authors showed that all ionic radical pairs that were used had a positive exchange interaction²⁸. The photosynthetic reaction center, which also has an ionic radical pair, has been shown to have a positive exchange interaction¹¹. These results suggest that the exchange interaction in photolyase is most likely positive because the radical pair members are ionic (see Chapter 3). A positive exchange interaction implies that the triplet-doublet radical pair in photolyase must arise from a doublet precursor as shown in Figure 4.9b because Figure 4.7 shows that a positive exchange interaction requires a doublet precursor in order to show a polarization pattern that is in agreement with the pattern that is observed in photolyase.

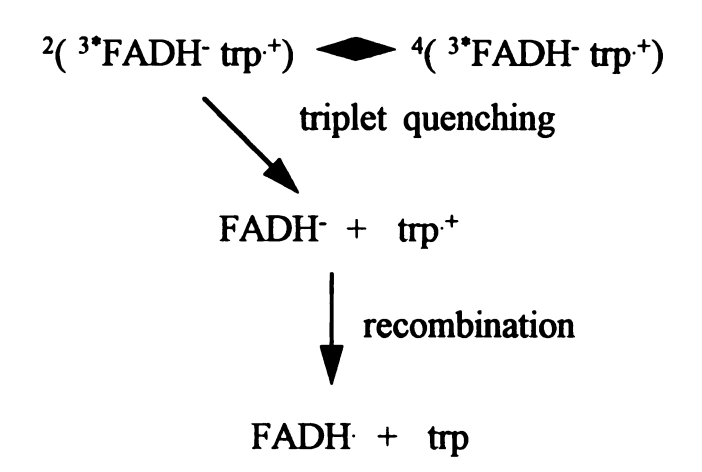
Rationalization of data with previous optical studies. The mechanism for spin polarization in photolyase shown in Figure 4.9b is inconsistent with the mechanism that was proposed previously from optical data¹⁸ (Figure 3.8). This implies that electron transfer from tryptophan to the excited flavin occurs when the flavin is in an excited doublet rather than an excited quartet state (compare Figure 3.8 with Figure 4.9b). The optical data used to assign electron transfer to the excited quartet state has a low signal to noise ratio and makes differentiation of the two mechanisms difficult¹⁷. Furthermore, detection of a tryptophan radical was not searched for optically until 4µs after the excitation of the enzyme¹⁸ owing to experimental limitations. Both mechanisms (Figure 3.8 and Figure 4.9b) predict that the transient tryptophan radical will be present at this time and the two mechanisms cannot be distinguished based on this data.

Explanation of kinetics in photolyase. The kinetic trace for the transient tryptophan radical in photolyase that is shown in Figure 2.5 reflects the mechanism that was discussed above. The instrument-limited rise of the transient radical corresponds to the quenching of ^{1*}FADH and the appearance of doublet precursor polarization. Figure 4.7 shows the relative populations of each state following singlet quenching. The only states with any initial population will be the states that have doublet character. These states are the D_{1/2} and D_{-1/2} states and also the Q_{1/2} and Q_{-1/2} states due to state mixing as in equation 4.4. The decay of the transient radical could be due to either recombination of the radical pair or quenching of ^{3*}FADH to the ground singlet state as shown in Figure 4.10. Figure 4.10a shows triplet quenching of the triplet-doublet radical pair preceding recombination. The excited triplet flavin can only be quenched through the doublet states²⁹ of the radical pair, resulting in an excess of quartet character, which manifests itself as quartet precursor spin

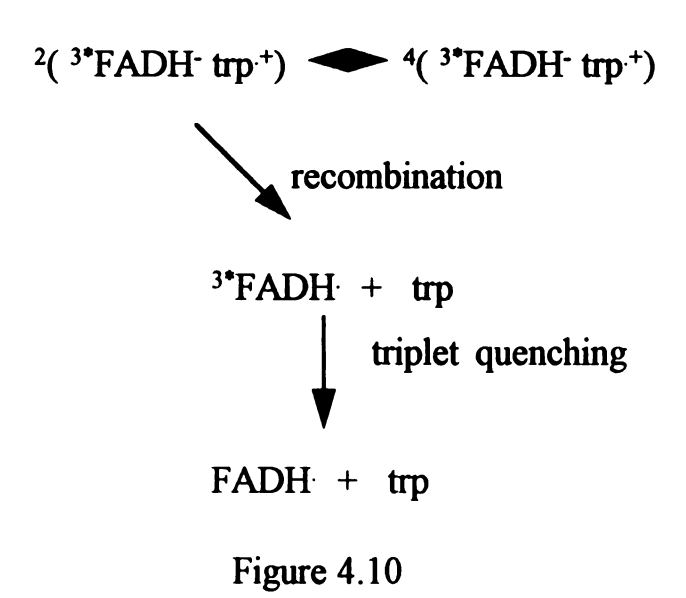
polarization (an A/E/A/E polarization pattern). The state that results from triplet quenching can recombine over several milliseconds to form the dark stable inactive form of photolyase. Figure 4.10b shows a mechanism in which the radical pair recombines directly from the excited triplet flavin state. In this mechanism the radical pair recombines by electron transfer to form a state that contains a diamagnetic tryptophan species and an excited ³ FADH radical that intersystem crosses to the ground state to form the inactive form of the enzyme. The mechanism in Figure 4.10b should also show quartet precursor spin polarization because only the doublet states of the triplet-doublet radical pair are expected to recombine²⁹ when the product state is a doublet (FADH). Both mechanisms predict a second polarization that is opposite in phase to the one that is observed in Figure 4.1a, but instrumental limitations have prevented us from observing this second polarization. Direct detection EPR measurements (faster time resolution) should allow us to observe this second phase in the future. The difference between the mechanism in Figure 4.10a and Figure 4.10b is the time at which triplet quenching and recombination will occur. Recombination of the doublet trp radical and the flavin species has been reported to occur over several milliseconds². Excited flavin triplet lifetimes have been measured in a photolyase sample that was catalytically active and are reported to be approximately 1 µs³⁰. Activity of the enzyme is not expected to influence the lifetime of the excited triplet flavin radical which suggests that the lifetime of the radical will be the same in the inactive form of the enzyme. The lifetimes predicted above suggest that intersystem crossing precedes recombination of the radical pair as is shown in Figure 4.10a.

Figure 4.10. Possible mechanisms for recombination during DNA photolyase photoreduction.

a) Recombination from the ground state



b) Recombination from the excited state



New mechanism for photoreduction in photolyase. The previously proposed mechanism for photolyase¹⁸ shown in Figure 3.8 is inconsistent with the formation of doublet precursor polarization. If electron abstraction from trp₃₀₆ occurs after the excited flavin intersystem crosses to the quartet as is shown in Figure 3.8, the radicals formed would be ³*FADH and ²trp. due to conservation of spin. The polarization pattern would arise from a quartet precursor (⁴*FADH) which is inconsistent with an E/A/E/A pattern with a positive exchange interaction.

A different reaction scheme shown in Figure 4.11 can account for the polarization pattern that is shown in Figure 4.1a. If electron transfer from trp₃₀₆ to ²*FADH occurs before any intersystem crossing by the flavin, the radical pair members are ²trp⁺ and ¹*FADH because of spin conservation. The singlet flavin (¹*FADH) is quenched to form a triplet-doublet radical pair (²trp⁺ and ³*FADH) that shows a doublet precursor polarization pattern (Figure 4.1a). Quenching of the triplet in doublet state radical pairs produces excess quartet states and a quartet precursor polarization results. Recombination occurs over several milliseconds to reform the dark stable inactive form of the enzyme (FADH).

We have proposed a new triplet-doublet radical pair mechanism that is analogous to CRPP for doublet-doublet radical pairs. Figure 4.11 shows the complete mechanism for the photoreduction reaction in photolyase. The presence of the exchange interaction causes an alternating emissive and absorptive pattern. The close similarity between the polarization patterns in photolyase and the photosynthetic reaction centers and the fact that both reactions involve radical pairs that are protein-bound suggest that the mechanism

Figure 4.11. Mechanism for photoreduction in photolyase that includes doublet precursor spin polarization.

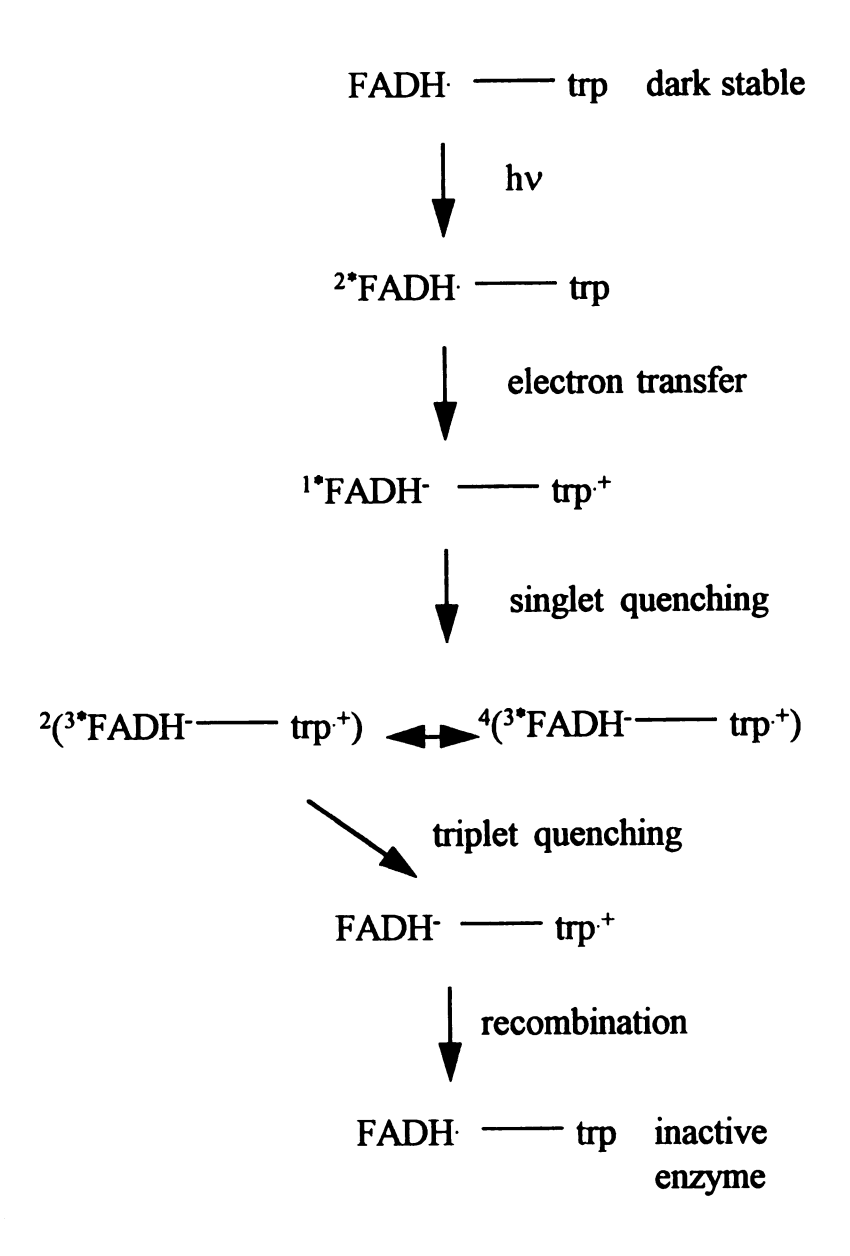


Figure 4.11

that we are proposing is not a special but rather a general case of spin polarization in proteins. The phenomena we observe is probably present in other proteins that function through electron transfer mechanisms. As more proteins and their reactions are discovered, we expect to see other cases of CRPP and CTDRPP surface.

References

- 1. Kim, S.T.; Sancar, A.; Essenmacher, C. and Babcock, G.T. Proc. Natl. Acad. Sci. USA 1993, 90, 8023.
- 2. Heelis, P.F.; Okamura, T. and Sancar, A. Biochemistry 1990, 29, 5694.
- 3. Okamura, T.A.; Sancar, A.; Heelis, P.F.; Hirata, Y. and Mataga, N. J. Am. Chem. Soc. 1989, 111, 5967.
- 4. Li, Y.F.; Heelis, P.F. and Sancar, A. Biochemistry 1991, 30, 6322.
- 5. Essenmacher, C.; Kim S.T.; Atamian, M.; Babcock, G.T. and Sancar, A. J. Am. Chem. Soc. 1993, 115, 1602.
- 6. Heelis, P.F.; Payne, G. and Sancar, A. Biochemistry 1987, 26, 4634.
- 7. Blättler, C.; Jent, F. and Paul, H. Chem. Phys. Lett. 1990, 166, 375.
- 8. Kawai, A.; Okutsa, T. and Obi, K. J. Phys. Chem. 1991, 95, 9130.
- 9. Kawai, A. and Obi, K. J. Phys. Chem. 1992, 96, 52.
- 10. Norris, J.R.; Morris, A.L.; Thurnauer, M.C. and Tang, J. J. Chem. Phys. 1990, 92, 4239.
- 11. Snyder, S.W. and Thurnauer, M.C. Electron Spin Polarization in Photosynthetic Reaction Centers: The Photosynthetic Reaction Center 1993, Vol.2 ed. Deisenhofer, J. and Norris, J.R. (Academic Press, SanDiego) p. 285.
- 12. Sancar, A. and Sancar, G.B. J. Biol. Chem. 1984, 172, 223.
- 13. Sancar, G.B.; Smith, F.W.; Reid, R.; Payne, G.; Levy, M. and Sancar, A. J. Biol. Chem. 1987, 262, 478.
- 14. Yerkes, C. Ph.D. dissertation 1982, Michigan State University, East Lansing, MI.
- 15. Hoganson, C.W. and Babcock, G.T. Biochemistry 1988, 27, 5848.
- 16. Jenks, W.S. and Turro, N.J. Rev. Chem. Int. 1990, 13, 237.
- 17. Adrian, F.J. Rev. Chem. Int. 1986, 7, 173.

- 18. Kim, S.T.; Heelis, P.F.; Okamura, T.; Hirata, Y.; Mataga, N. and Sancar, A. Biochemistry 1991, 30, 11262
- 19. Lhoste, J.M.; Haug, A. and Hemmerich, P. Biochemistry 1966, 5, 3290.
- 20. Heelis, P.F. and Sancar, A. Biochemistry 1986, 25, 8163.
- 21. Bock, C.; Stehlik, D. and Thurnauer, M.C. Israel J. Chem. 1988, 28, 177.
- 22. Snyder, S.W.; Morris, A.L.; Bondeson, S.R.; Norris, J.R. and Thurnauer, M.C. J. Am. Chem. Soc. 1993, 115, 3774.
- 23. Marcus, R.A. and Sutin, N. Biochim. Biophys. Acta 1985, 811, 265.
- 24. Moser, C.C.; Keske, J.M.; Warncke, K.; Farid, R.S. and Dutton, P.L. *Nature* 1992, 355, 796.
- 25. Woodhouse, J.H. and Dziewonski A.M. J. Geophys. Res. 1984, 89, 5953.
- Ito, E. and Yamada, H. High-Pressure Research in Mineral Physics 1982, ed.
 Akimoto, S. and Manghnani, M.H. (Center for Academic Publications, Tokyo) pp. 405-419.
- 27. Hoijtink, G.J.; Velthorst, N.H. and Zandstra Mol. Phys. 1960, 3, 543.
- 28. Batchelor, S.N.; Heikkilä, H.; Kay, C.W.M.; McLauchlan, K.A. and Shkrob, I.A. *J. Chem. Phys.* 1992, 162, 29.
- 29. Schulten, K. J. Chem. Phys. 1984, 80, 3668.
- 30. Heelis, P.F.; Rolley-Williams, C.A.; Hartman, R.F. and Rose, S.D. J. Photochem. Photobiol. B: Biol. 1994, 23, 155.

Chapter 5

Simulation of the Transient Tryptophan EPR Signal that Occurs during Photoreduction of Inactive Photolyase

Introduction

Inactive DNA photolyase can be photoreduced to produce an active enzyme that is capable of repairing UV-damaged DNA^{1,2,3}. Photoreduction of inactive photolyase produces a transient tryptophan radical that exhibits electron spin polarization^{4,5}, as discussed in Chapter 4. A current model for photoreduction of the inactive enzyme that accounts for spin polarization of the tryptophan radical as discussed in Chapter 4 is shown in Figure 4.11 and is discussed briefly below. Photoexcitation of the dark stable FADH radical produces an excited flavin doublet radical ^{2*}FADH. Electron transfer from tryptophan-306 to ^{2*}FADH produces an excited singlet flavin anion species (^{1*}FADH) and a tryptophan cation radical (trpH⁺). Intersystem crossing of ^{1*}FADH to the triplet produces a triplet-doublet radical pair that exhibits electron spin polarization. ^{3*}FADH intersystem crosses to the ground singlet state to form a diamagnetic FADH species that recombines over several milliseconds with trpH⁺ to reform the inactive, FADH containing enzyme when exogenous donors are absent. When exogenous donors are present, trpH⁺ is reduced to form the active FADH containing enzyme³ (see Chapter 3).

During the photoreduction reaction of inactive photolyase an intense EPR signal is observed transiently, and we have identified the origin of this signal as a tryptophan cation radical⁵ (see Chapter 3). The EPR spectrum of this transient signal is shown in Figure 4.1,

radical⁵ (see Chapter 3). The EPR spectrum of this transient signal is shown in Figure 4.1, and shows that some transitions are emissive which suggests that the tryptophan radical in photolyase is spin polarized. In Chapter 4 a possible mechanism for spin polarization in photolyase was proposed. State mixing between the energy levels of the doublet and quartet is responsible for the observed spin polarization. State mixing in the basis set of the triplet-doublet radical pair is induced through a difference in hyperfine coupling frequencies of the two radical pair members, as discussed in Chapter 4. The presence of an exchange interaction between the two radical pair members causes each transition to split into an emissive-absorptive pair where each transition in the pair is split in energy by the exchange interaction. The resulting EPR spectrum shows an alternating emission and absorption pattern with no net polarization.

In this chapter the experimentally observed spectrum in Figure 4.1 will be simulated in order to test the validity of the model for spin polarization in photolyase that was proposed in Chapter 4. A description of the program that was used to simulate the spectrum and the parameters that were used in the simulation will be presented. The results show that the simulated spectrum fits quite well with the experimentally observed spectrum and give support for the model that was suggested in Chapter 4.

Materials and Methods

The simulation program was written in the C++ programming language and uses the Object Windows Library (Borland International Inc., Scotts Valley, CA) and the

Microsoft Windows 3.1[©] Application Programming Interface (Microsoft Corporation, Redmond, WA) for certain portions of the program. The program requires the installation of Microsoft Windows 3.1[©] in order to run the program. Compilation of the source code was done with Borland C++ 3.1 for Windows and Application Frameworks (Borland International Inc., Scotts Valley, CA), and this code is shown in Appendix A. The simulation routine is a modified version of a BASIC program that was written by Dr. Curt Hoganson to simulate EPR spectra^{6,7}. The original simulation program was converted to C++ and spectral parameters that are necessary in order to introduce spin polarization were added to the simulation routine.

Even though the program is able to calculate EPR spectra for crystals, partially oriented membranes, and powder samples; the only case that will be discussed here will be the solution one because there is not enough experimental data to warrant any other type of simulation at this time. The flow chart and EPR stick diagrams that are shown in Figure 5.1 show the procedure that the simulation program uses to generate an EPR spectrum for a radical whose energy levels are populated according to a Boltzman distribution^{6,7}. The user must enter the g-value, microwave frequency, magnetic field limits and linewidth for the experimental spectrum that is to be simulated. If there is hyperfine coupling present in the spectrum, the user must also enter the coupling constant and nuclear spin for each coupled nucleus in the experimental spectrum. The program determines the magnetic field at which resonance occurs in the absence of hyperfine coupling by equation 5.1.

$$H = (hv) / (g\beta)$$

equation 5.1

where H is the magnetic field, h is Planck's constant, g is the electronic g-factor, β is the Bohr magnetron, and ν is the microwave frequency. The transition resonant from equation 5.1 is split by hyperfine coupling according to equation 5.2

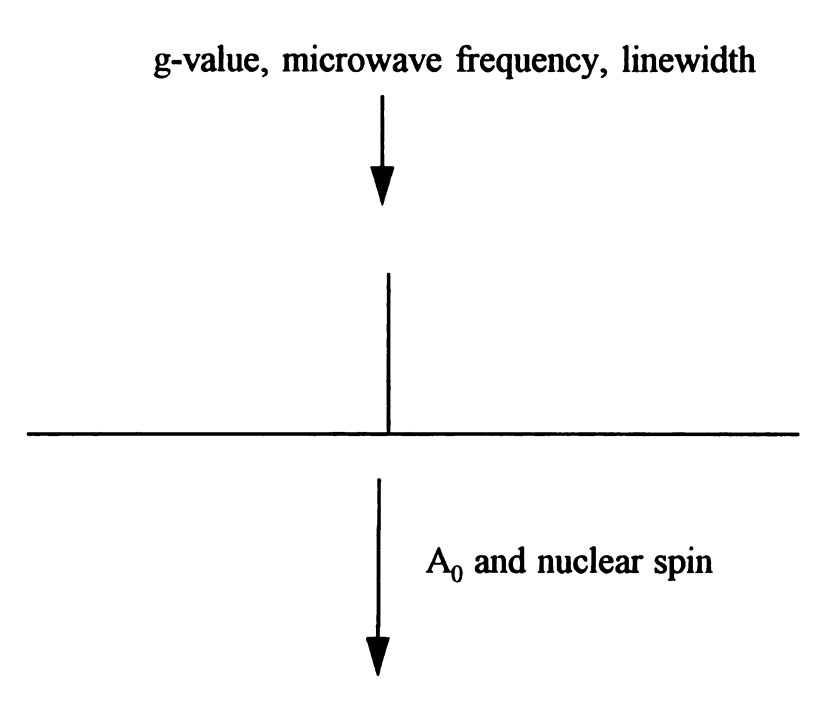
$$H = (hv - hA_0SI) / (g\beta)$$
 (equation 5.2)

where H, h, g, ν , and β are the same as in equation 5.1, and A_0 is the hyperfine coupling constant, S is the electron spin quantum number, and I is the nuclear spin quantum number. The program applies equation 5.2 for each coupled nucleus in the EPR spectrum and assigns equal intensity for each line that results from the splitting. The EPR stick diagram is shown for the case of hyperfine coupling to a spin 1/2 nucleus in Figure 5.1. The resulting EPR stick diagram has a first-derivative gaussian lineshape with a linewidth applied to it that is specified by the user, and the result is a simulated EPR spectrum with spectral parameters that were input by the user.

Figure 5.2 shows EPR stick diagrams of the simulation procedure when spin polarization is introduced into the calculation. The user must enter the precursor state, the exchange coupling between the doublet and triplet radicals, and the largest ratio of the transitions in an exchange-split doublet. The precursor state determines whether the polarization pattern begins in emission or absorption. As discussed in Chapter 4, a doublet precursor with a positive exchange interaction will begin in emission. If either the precursor state or the sign of the exchange interaction is reversed, the pattern will

Figure 5.1. Simulation of EPR spectra that are in thermal equilibrium.

a) Simulation of the center field transition



b) Simulation of hyperfine coupling

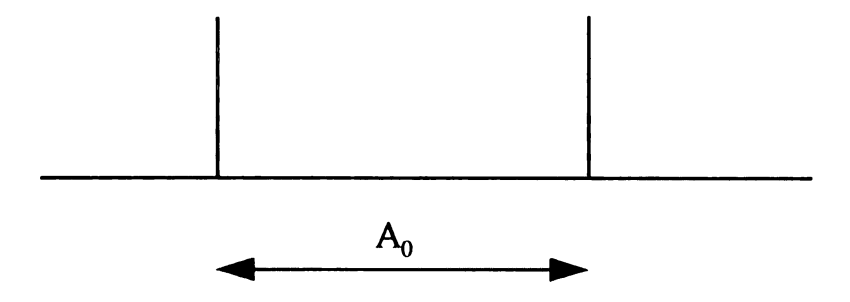


Figure 5.1

Figure 5.2. Simulation of a spin polarized radical.

a) thermalized radical with coupling to nuclear spin =1

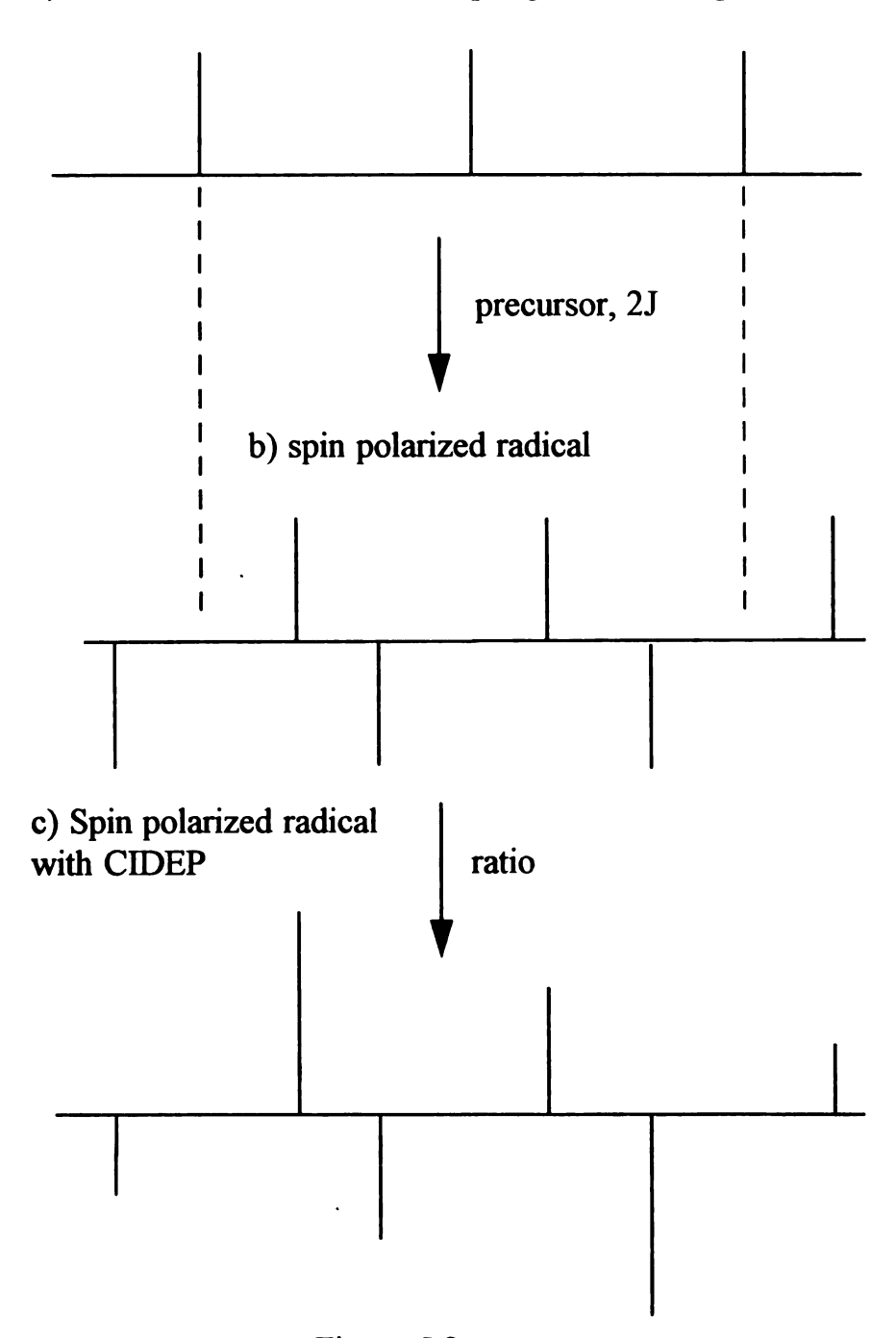


Figure 5.2

begin in absorption⁸. Figure 5.2a shows an EPR stick diagram for a thermalized doublet radical that shows hyperfine coupling to one spin = 1 nucleus. The pattern has three lines that are equal in intensity and split by the hyperfine coupling constant A_0 . The magnetic field positions once spin polarization is introduced into the spectrum is shown in Figure 5.2b. The exchange coupling splits each line in the thermalized spectrum into two lines as shown below in equation 5.3^8 .

$$H = H_t \pm (2J) / 2$$
 (equation 5.3)

where H_t is the magnetic field position for a transition in the thermalized spectrum, H is the new field position in the spin polarization spectrum, and 2J is the exchange interaction between the two radicals of the radical pair. Equation 5.3 is applied to each transition in the thermalized spectrum. The phase of each transition is determined by the sign of the exchange interaction and the precursor state as discussed above. For example, in Figure 5.2 the pattern is E/A/E/A/E/A because the precursor state is a doublet and the exchange interaction is positive^{8,9}. For the case in Figure 5.2b, the lower energy transition in the exchange split pair is in emission and the higher energy transition is in absorption^{8,9}.

Figure 5.2c shows how the simulation program assigns intensities to each transition in the spin polarized spectrum. According to equation 4.4, the amount of state mixing that occurs in a triplet-doublet radical pair is proportional to the difference in precessional frequencies of the two radical pair members⁸. Therefore, the transitions that are farthest away from center magnetic field of the spectrum which is calculated by equation 5.1 will

show the largest ratio of transitions in the exchange split pair. The program first calculates from equation 5.2 the transition that is farthest away from the center of the spectrum. For a doublet precursor with a positive exchange interaction, all transitions that are at a lower magnetic field than the center field will have intensities that obey equations 5.4 and 5.5

$$I_l = I_t / \{ (R - 1) * [(H - H_c) / (H_l - H_c)] + 2 \}$$
 (equation 5.4)

$$I_h = I_t - I_l \qquad (equation 5.5)$$

where I_l is the intensity of the lower field transition in the exchange split pair, and I_h is the intensity of the higher field transition. I_t is the relative intensity of the transition that was calculated in the thermalized spectrum, H is the field value of the transition that is calculated by equation 5.1, H_l is the field value of the farthest transition from the center field H_c , and R is the ratio that is entered by the user. For transitions that are at a higher field value than the center frequency the equations for I_l and I_h are reversed.

Equations 5.4 and 5.5 are based upon the assumption that there is a linear relationship between the amount of net polarization that occurs in an exchange split pair and the difference in precessional frequencies of the two radical pair members. Equation 4.4 shows that the amount of state mixing in triplet-doublet radical pairs is proportional to the difference in precessional frequencies of the two radical pair members. The amount of state mixing is proportional to the net polarization that is observed in an exchange split

doublet. It is well known from spin polarized doublet radicals in solution that the center exchange split doublet should show no net polarization 10,11,12,13, and equations 5.4 and 5.5 assume that the ratio of the two transitions will vary linearly from one at the center of the spectrum to the ratio that the user enters at the far edges of the spectrum where equation 4.4 will have the largest value. The ratio that the user enters is an entirely empirical parameter because the ratio cannot be calculated at the present with the current data that are available. In order to calculate the ratio of the two transitions in an exchange split doublet, it is necessary to have kinetic data on the lifetime of the triplet-doublet radical pair 8,9. At the present time we do not know the true kinetics of spin polarization in photolyase because of the use of 100 kHz modulation. Consequently, we cannot calculate the ratio of the two transitions in an exchange split doublet until the true kinetics of spin polarization in photolyase are known.

The simulation program whose source code is shown in Appendix A assumes that the only contribution to the difference in precessional frequencies of the two radical pair members is a difference in hyperfine coupling frequencies (see equation 4.4) of the two radicals. This assumption is reasonable for spin polarization in photolyase if a comparison of the g-values of the two radical pair members is considered. The excited triplet flavin anion radical is expected to have a g-value that is close to the dark stable doublet flavin radical whose g-value is 2.0039¹⁴. The tryptophan doublet cation radical whose absorption spectrum is shown in Figure 4.1a has an apparent g-value of 2.0028. The difference in magnetic field units between these two g-values is only 2 G. The difference in hyperfine coupling frequencies of the two radical pair members is at least 15 G which is

much larger than the g-value difference of the two radicals⁴. Further evidence for hyperfine coupling differences rather than g-value differences are driving spin polarization in photolyase is the polarization pattern for photolyase that is shown in Figure 4.1a. The first exchange split doublet shows net absorption, the second shows no net polarization. and the third doublet shows net emission⁴. The overall spectrum shows no net polarization because the amount of net absorption in the first exchange split doublet is offset by the amount of net emission in the third exchange split doublet. The polarization pattern of the exchange split doublets in Figure 4.1a is typical of a spin polarization that originates from a difference in hyperfine coupling frequencies (multiplet effect) rather than a difference in g-values (net effect) of the two radical pair members. If spin polarization in photolyase arises from a net effect, the polarization pattern would show either net emission or net absorption. In Chapter 2, we showed that the transient EPR signal in photolyase arises from only one member of the radical pair. In order to observe net effect spin polarization, one radical of the radical pair must show net emission and the other net absorption^{10,11}. The absence of net polarization in photolyase excludes net effect spin polarization as a possible mechanism because the transient EPR signal would have to show net polarization that arises from one member of the radical pair. Therefore, spin polarization in photolyase must arise from a multiplet effect as the simulation program in Appendix A assumes.

Another assumption of the simulation program in Appendix A is that the initial population distribution of nuclear spin states is equal for all nuclei in the other radical pair member. The manifestation of this assumption is in the difference in hyperfine coupling

frequencies of the two radical pair members as shown in equation 4.4. The transition that occurs at the lowest magnetic field in Figure 4.1a has a hyperfine coupling of approximately 15 G. In order to calculate the hyperfine coupling frequency difference for this particular transition, the difference in frequency must be taken for each nuclear spin state in the other radical of the triplet-doublet radical pair^{8,9}. For example, if the other radical pair member has hyperfine coupling to a single proton the frequency difference for the low field transition in Figure 4.1a will be as shown in equation 5.6.

$$\Delta \omega_t = 15 \text{ G} - (1/2)n_{1/2}A_0 + (1/2)n_{1/2}A_0$$
 (equation 5.6)

where Δ ω_t is the difference in precessional frequencies of the two radical pair members for the low field transition, n is the number of radicals that show hyperfine coupling to the particular nuclear spin state that is shown as a subscript, and A_0 is the hyperfine coupling constant in Gauss for this proton. The simulation program in Appendix A assumes that $n_{1/2} = n_{-1/2}$ and the result is that the low field transition precessional frequency difference is equal to 15 G. The program assumes for hyperfine couplings to the simulated radical that the frequency difference is simply the hyperfine coupling that is observed for the simulated radical, and the other radical does not contribute to this frequency difference as is shown in the above example. At the present time, no theoretical work has been done on the initial population distribution of nuclear spin states in spin polarized systems, and as a result, the only practical approach that the simulation program can take at this time is that a random statistical distribution of nuclear spin states is formed.

Results and Discussion

Figure 5.3a shows the experimental time-resolved EPR spectrum (top) of a photolyase sample that contains natural abundance tryptophan. Directly below this spectrum is the spectrum that is obtained with the simulation program that is shown in Appendix A. Figure 5.3b shows the experimental and simulated spectra for a photolyase sample that contains tryptophan which is isotopically labeled with deuterium on all the α -ring carbons. The parameters that were used to simulate the EPR spectra are shown in Table 5.1. The simulation parameters that are shown in Table 5.1 are quite reasonable because an estimate for the parameters was obtained from experimental data as discussed below. The determination of an appropriate g-value for the simulation was made by using the apparent g-value of the experimental spectra in Figure 4.1a and Figure 4.1b. Because all photolyase samples that were used were in solution, an isotropic g-value of 2,0028 was used for both the natural abundance and specifically deuterated samples⁴. As discussed in Chapters 2 and 3, the large hyperfine couplings in Figure 4.1a and Figure 4.1b have been assigned to hyperfine coupling to two equivalent nuclei that are the β-methylene protons on tryptophan⁵. The coupling is estimated to be 15-16 G by measuring A_{HB} in the figure. The best fit for the simulated spectra was obtained with a hyperfine coupling of 15.5 G as shown in Table 5.1. The experimental spectra in Figure 2.8a and Figure 2.8b were used to assign the smaller hyperfine coupling to a single α -ring proton with a coupling of 5 G⁵. This value was used to simulate the natural abundance spectrum in Figure 5.3a, and a

Figure 5.3. Comparison of simulated and experimental spectra: (a) shows the natural abundance spectra and (b) shows the α -ring deuterated spectra. The top spectrum in each figure is the experimental spectrum and the lower spectrum is the simulated one.

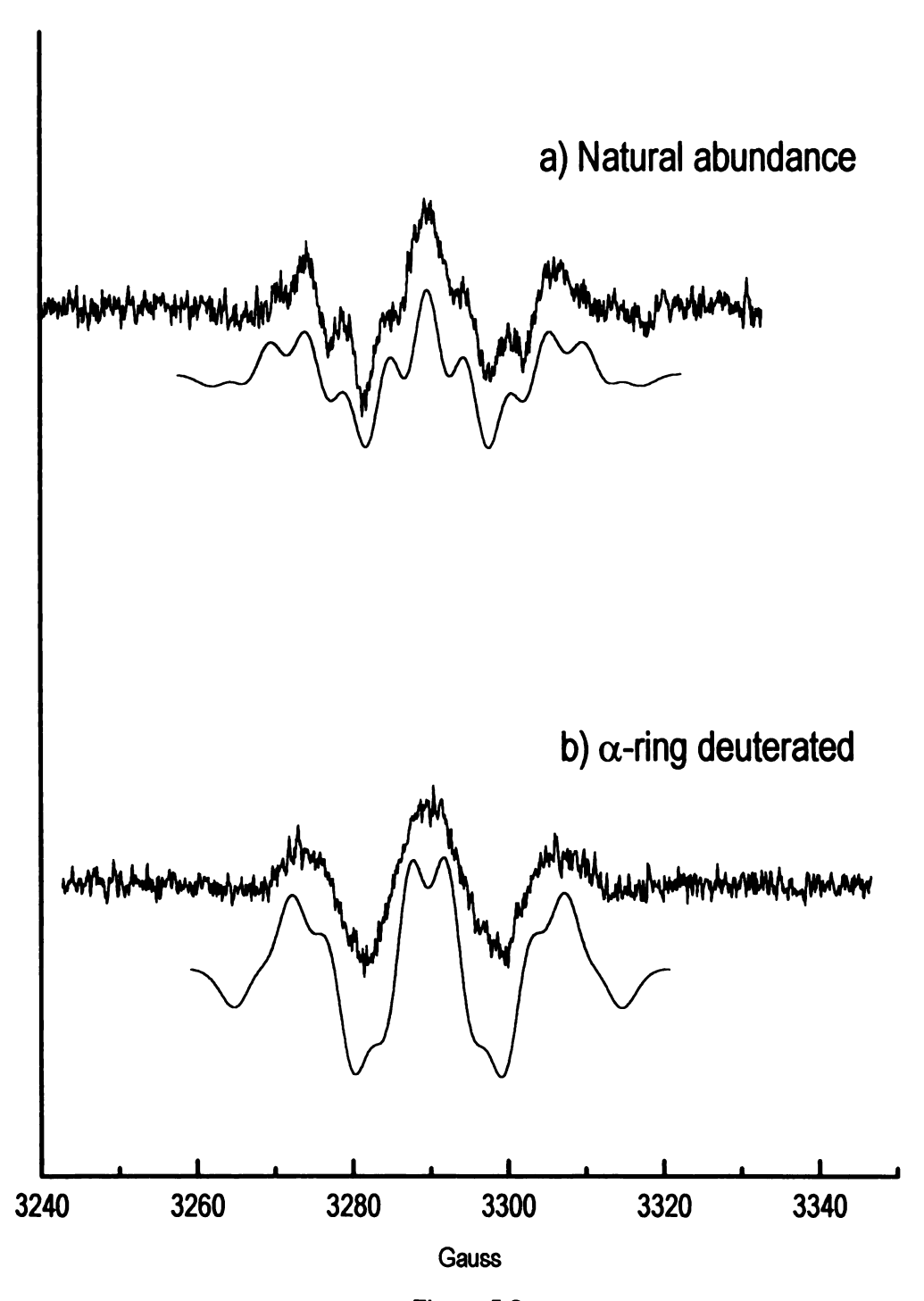


Figure 5.3

Table 5.1 Parameters used to simulate the spectra in Figure 5.3a and Figure 5.3b.

Parameters	Natural Abundance	Deuterated
g-value	2.0028	2.0028
Frequency (MHz)	9222.26	9222.26
Linewidth (G)	4.1	4.1
Exchange Coupling (G)	7.8	7.8
Ratio	3	2
Precursor State	Doublet	Doublet
2 β-methylene protons hyperfine coupling (G)	15.6	15.6
C(2) proton hyperfine coupling (G)	4.8	0.8
N(1) nitrogen hyperfine coupling	4.1	4.1

hyperfine coupling of 0.8 G (one-sixth of 5 G) was used to simulate deuterium labeled sample. Figure 3.3b shows the transient EPR spectrum for a photolyase sample that contains ¹⁵N-labeled tryptophan⁵. From a comparison with the natural abundance spectrum, an estimate of less than 5 G is estimated for hyperfine coupling to the nitrogen on the tryptophan ring. Table 5.1 shows that the best fit to the experimental spectra was obtained with a hyperfine coupling of 3.8 G for the tryptophan ring nitrogen. The exchange interaction is estimated to be 7-8 G in photolyase from a measurement of 2J in Figure 4.1a. The simulation used 7.5 G for the exchange interaction, which is within the predicted range for it. An estimate of the ratio of the low field exchange split pair can be made by examining Figure 4.1a. The figure shows that the ratio of the emissive to the absorptive transition in the exchange split pair is at least two. The best fit to the transient spectra was obtained with a ratio of 3.5 as shown in Table 5.1. The linewidth was estimated to be 4 G from the half width at half height of the transitions in Figure 4.1a.

The simulation of the natural abundance transient spectrum that is shown in Figure 5.3a agrees quite well with the experimental spectrum, which is shown directly above. The three major transitions that show hyperfine coupling of 15 G in a 1:2:1 ratio in the experimental spectrum are also present in the simulation as well as the smaller splittings that arise from a single ring proton. A comparison of the magnetic field where a transition occurs in each spectrum shows that the simulation shows transitions that are at the same field as the experimental spectrum. The intensity of each transition does not agree as well with the experimental spectrum, but it is probably due to a lack of experimental data such

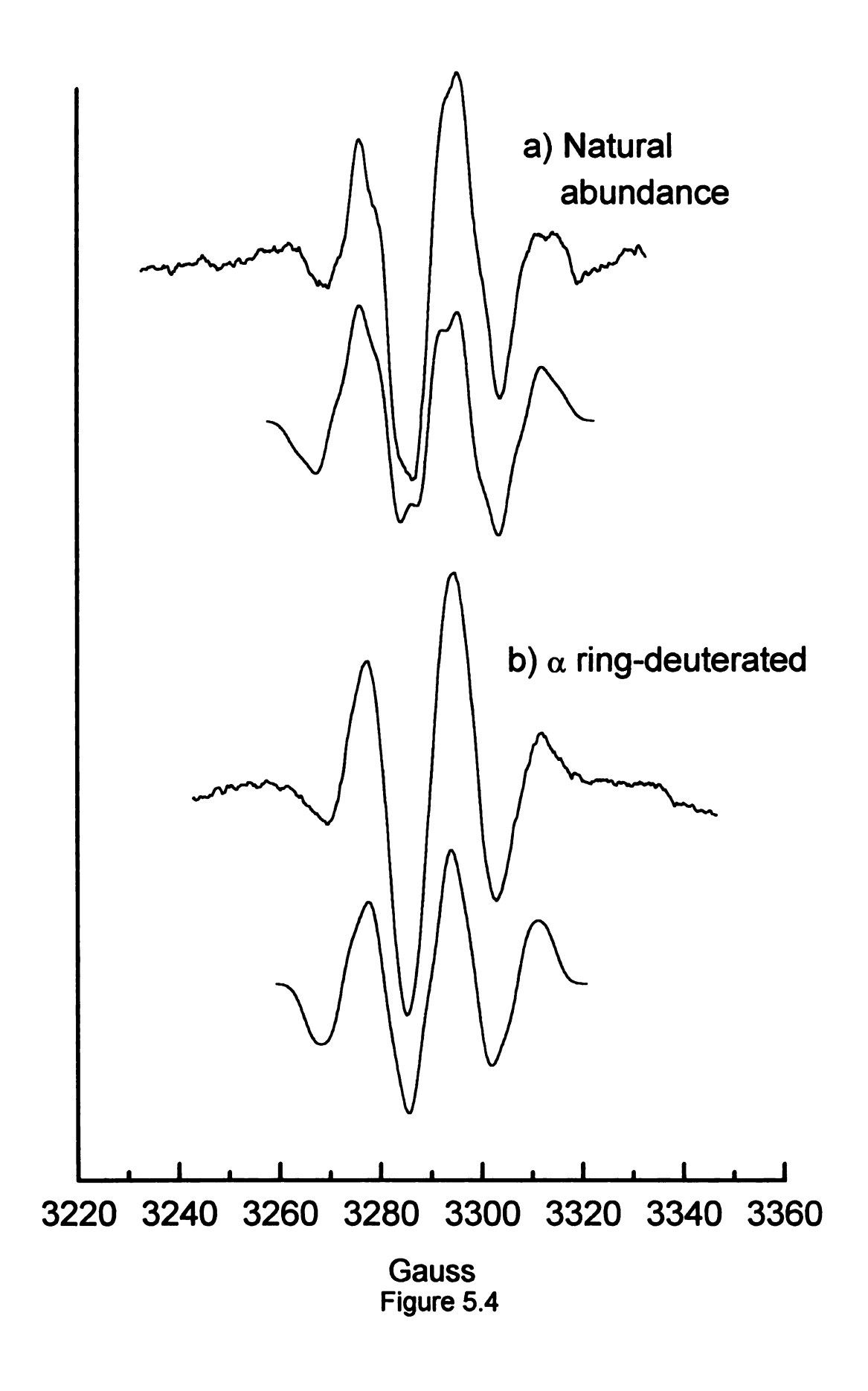
as anisotropy in the g and hyperfine tensors, accurate hyperfine couplings, and the relative orientations of the g and hyperfine axes rather than a limitation of the simulation program.

The simulation of the ring deuterated tryptophan transient spectrum that is shown in Figure 5.3b is also qualitatively similar to the experimental spectrum that is shown above. The simulation shows the same large hyperfine couplings as the experimental spectrum, and the intensity and magnetic field position of each transition are the same in each spectrum. The simulation does show small splittings that are not present in the experimental spectrum, but this error is again probably due to a lack of experimental data.

Figure 5.4a shows the integrated absorption spectrum of the spectra in Figure 5.3a for the natural abundance sample, and Figure 5.4b shows the integrated absorption spectra of the spectra in Figure 5.3b for the deuterated sample. The simulation in each case agrees very well with the experimental spectra in the figure. The simulations show the same six line polarization pattern that alternates between absorption and emission. The splitting between each exchange split pair and the splitting within the pair are also simulated very well when compared to the experimental spectra. The net polarization of each exchange split pair is also preserved in each simulation.

The simulation results in this chapter give strong support for the proposed mechanism of spin polarization in photolyase that was presented in Chapter 4. The simulation program is able to reproduce the experimental spectra to a high degree of accuracy, and the results are quite good for a first attempt at simulating spin polarization in photolyase. When better experimental data such as anisotropy in the g and hyperfine tensors, more accurate hyperfine couplings, and the relative orientation of the g and hyperfine axes is available; the simulation program should be able to better reproduce the transient spectra

Figure 5.4. Comparison of simulated and experimental absorption spectra for photolyase. (a) is the natural abundance spectrum and (b) is the deuterated spectra. The top spectrum in each figure is the experimental spectrum and the bottom one is the simulated one.



in photolyase.

References

- 1. Sancar, A. *Photolyase:* In *Advances in Electron Transfer Chemistry*; Mariano, P.E., Ed.; JAI Press: London, 1992; Vol. 2, pp. 215-272.
- 2. Kim, S.T.; Malhotra, K. and Sancar, A. In *Biological Responses to Ultraviolet Radiation*; Urbach, F., Ed.; Valdenmar: Overland Park, KS, 1992.
- 3. Heelis, P.F.; Okamura, T. and Sancar, A. Biochemistry 1990, 29, 5694.
- 4. Essenmacher, C.; Kim, S.T.; Atamian, M.; Babcock, G.T. and Sancar, A. J. Am. Chem. Soc. 1993, 115, 1602.
- 5. Kim, S.T.; Sancar, A.; Essenmacher, C. and Babcock, G.T. *Proc. Natl. Acad. Sci. USA* 1993, 90, 8023.
- 6. Brok, M.; Babcock, G.T.; DeGroot, A. and Hoff, A.J. J. Magn. Res. 1986, 70, 368.
- 7. Hoganson, C.W. and Babcock, G.T. Biochemistry 1992, 31, 11874.
- 8. Norris, J.R.; Morris, A.L.; Thurnauer, M.C. and Tang, J. J. Chem. Phys. 1990, 92, 4239.
- 9. Snyder, S.W. and Thurnauer, M.C. Electron Spin Polarization in Photosynthetic Reaction Centers: The Photosynthetic Reaction Center 1993, Vol.2 ed. Deisenhofer, J. and Norris, J.R. (Academic Press, SanDiego) p. 285.
- 10. Jenks, W.S. and Turro, N.J. Rev. Chem. Int. 1990, 13, 237.
- 11. Adrian, F.J. Rev. Chem. Int. 1986, 7, 173.
- 12. Kawai, A.; Okutsa, T. and Obi, K. J. Phys. Chem. 1991, 95, 9130.
- 13. Kawai, A. and Obi, K. J. Phys. Chem. 1992, 96, 52.
- 14. Lhoste, J.M.; Haug, A. and Hemmerich, P. Biochemistry 1966, 5, 3290.

APPENDIX

APPENDIX

Listing of program to simulate spin polarized EPR spectra

#include "polhead.h" char FileName[MAXPATH]; char FileName1[MAXPATH]; char FileName2[MAXPATH]; PRINTDLG pd; **BOOL PrevSave = FALSE**; int SimType=1; float HMin, HMax; float xepr [1024]; float yepr [1024]; float spec [512]; int DataNumber; PTFileWindow ImportFileWindow; PTWindow ParamWindow; float Freq = 9400; int NumberGroups = 0; float gx = 2.0023; float gy = 2.0023; float gz = 2.0023; int StepSize = 15; int NoDiv = 5; float Dalpha = 30; float MemTheta = 0; float MemPhi = 0; float Omega = 0; float Wobble = 5; float Linewidth = 2; float CrystalTheta = 0; float CrystalPhi = 0; float AHyp [3][3][8]; float NuclearSpin [8]; int NucleiPerGroup [8]; float Theta[8]; float Phi[8]; float Psi[8]; **BOOL AccurGen = TRUE**; BOOL SpecCRPP = FALSE; float Exchange = 5.0; float Ratio = 5.0; **BOOL PrecurDou = TRUE**;

```
BOOL SimTrue = FALSE:
BOOL ExperLoaded = FALSE;
int DrawMode = 0:
HPEN PaintPen;
float Back 1=0;
float Tilt=0:
BOOL FileSaved = TRUE;
PTScroller GlobalScroller;
BOOL Integrate = FALSE;
HDC PolarDC: // Device context for main window
void DrawSpectrum (HDC DrawDC)
{
 SetCursor(LoadCursor(NULL,IDC WAIT));
 float dspec[512];
 float yint[1024];
 if (!Integrate && ExperLoaded)
   for (int g=0;g<1024;++g)
    yint[g] = yepr[g];
 if (Integrate && ExperLoaded)
  float Back=0;
   for (int f=5;f<55;++f)
   Back += yepr[f];
   Back /= 50;
   for (int g=0;g<1024;++g)
   yint[g] = 0;
   for (int d=1;d<DataNumber;++d)
    yint[d] = yint[d-1] + ((yepr[d]-Back-Back1-(Tilt*d))*(xepr[DataNumber-1]-xepr[0])/1022);
 if (DrawMode != 2)
 int istart.iend;
 float w,a,b,c,br,d1,d2;
 float gaussperch = (HMax - HMin) / 511;
 w = Linewidth / gaussperch;
 a = pow(w,3);
 b = 2 * pow(w,2);
 c = 4 * w;
 for (int d = 0; d < 512; ++d)
  dspec[d] = 0;
 for (int e=0; e<512; ++e)
   if (spec[e] != 0)
    istart = e - c;
```

```
iend = e + c;
    if (istart < 0)
         istart = 0;
    if (iend > 511)
         iend = 511:
    for (int f = istart; f < iend + 1:++f)
         d1 = f - e:
        d2 = pow(d1,2);
        br = -d1 / a*exp(-d2/b);
        dspec[f] += br * spec[e];
if (Integrate && SimTrue)
 for (int a=1;a<512;++a)
  dspec[a] = dspec[a-1] + dspec[a]*(HMax-HMin)/511;
 }
if (DrawMode == 1)
SetMapMode(DrawDC,MM_ANISOTROPIC);
RECT WindowRect:
HWND MainHandle = GetActiveWindow():
GetClientRect(MainHandle, & WindowRect);
SetWindowExt(DrawDC,681,1200);
SetViewportExt(DrawDC, WindowRect.right, -WindowRect.bottom);
float dspecmax = dspec[0];
float dspecmin = dspec[0];
float hfl.ds:
for (int g=0;g<512;++g)
 if(dspec[g] < dspecmin)
  dspecmin = dspec[g];
 if(dspec[g] > dspecmax)
  dspecmax = dspec[g];
SetWindowOrg(DrawDC,-85,1000);
MoveTo(DrawDC,0,800);
LineTo(DrawDC,0,0);
LineTo(DrawDC,511,0);
float dstemp = (dspec[0]-dspecmin)*800/(dspecmax-dspecmin);
MoveTo(DrawDC,0,dstemp);
for (int h=1;h<512;++h)
 hfl = h:
 ds = (dspec[h]-dspecmin)*800/(dspecmax-dspecmin);
 LineTo(DrawDC,hfl,ds);
MoveTo(DrawDC,0,0);
LineTo(DrawDC,0,-20);
```

```
MoveTo(DrawDC,511/3,-20);
 LineTo(DrawDC,511/3,0):
 MoveTo(DrawDC,511*2/3,-20);
LineTo(DrawDC,511*2/3.0):
MoveTo(DrawDC,511,0);
LineTo(DrawDC,511,-20);
char FieldText [7];
RECT FormatField;
FormatField.top = -25:
FormatField.bottom = -80:
FormatField.left = -20:
FormatField.right=80;
gcvt(HMin,5,FieldText);
DrawText(DrawDC,FieldText,-1,&FormatField,DT_TOP | DT_LEFT);
OffsetRect(&FormatField,511/3,0);
gcvt((HMax-HMin)/3+HMin,5,FieldText);
DrawText(DrawDC,FieldText,-1,&FormatField,DT_TOP | DT_LEFT);
OffsetRect(&FormatField,511/3,0);
gcvt((HMax-HMin)*2/3+HMin,5,FieldText):
DrawText(DrawDC,FieldText,-1,&FormatField,DT TOP | DT LEFT);
OffsetRect(&FormatField,511/3,0);
gcvt(HMax,5,FieldText);
DrawText(DrawDC,FieldText,-1,&FormatField,DT_TOP | DT_LEFT);
OffsetRect(&FormatField,-511/2 - 50,930);
FormatField.right = 400;
DrawText(DrawDC, "Simulated Spectrum", 18, & FormatField, DT_TOP | DT_LEFT);
if (DrawMode == 2)
HWND MainHandle = GetActiveWindow():
RECT WindowRect:
GetClientRect(MainHandle, & WindowRect):
SetMapMode(DrawDC,MM ANISOTROPIC);
SetWindowExt(DrawDC,681,1200);
SetViewportExt(DrawDC, WindowRect.right, -WindowRect.bottom);
float specmin = vint[0];
float specmax = vint[0]:
for (int a=1;a<DataNumber;++a)
 if (yint[a] < specmin)
 specmin = yint[a];
 if (yint[a] > specmax)
 specmax = yint[a];
SetWindowOrg(DrawDC,-85,1000);
MoveTo(DrawDC,0,800);
LineTo(DrawDC.0.0):
LineTo(DrawDC,511,0);
float YConv = 800/(specmax-specmin);
float XConv = 511/(xepr[DataNumber-1] - xepr[0]);
MoveTo(DrawDC,0,(yint[0]-specmin)*YConv);
for (int b=1;b<DataNumber;++b)
 LineTo(DrawDC,(xepr[b]-xepr[0])*XConv,(yint[b]-specmin)*YConv);
```

```
MoveTo(DrawDC.0.0):
 LineTo(DrawDC.0.-20):
 MoveTo(DrawDC,511/3,-20);
 LineTo(DrawDC.511/3.0):
 MoveTo(DrawDC.511*2/3.-20):
 LineTo(DrawDC,511*2/3,0);
 MoveTo(DrawDC.511.0):
 LineTo(DrawDC,511,-20);
 char FieldText [7];
 RECT FormatField:
 FormatField.top = -25;
 FormatField.bottom = -80:
 FormatField.left = -20:
 FormatField.right=80;
 gcvt(xepr[0],5,FieldText);
 DrawText(DrawDC,FieldText,-1,&FormatField,DT_TOP | DT_LEFT);
 OffsetRect(&FormatField,511/3,0);
 gcvt((xepr[DataNumber-1]-xepr[0])/3+xepr[0],5,FieldText);
 DrawText(DrawDC,FieldText,-1,&FormatField,DT TOP | DT LEFT);
 OffsetRect(&FormatField,511/3,0);
 gcvt((xepr[DataNumber-1]-xepr[0])*2/3+xepr[0],5,FieldText);
 DrawText(DrawDC,FieldText,-1,&FormatField,DT TOP | DT LEFT);
 OffsetRect(&FormatField,511/3,0);
 gcvt(xepr[DataNumber-1],5,FieldText);
 DrawText(DrawDC,FieldText,-1,&FormatField,DT TOP | DT LEFT);
 OffsetRect(&FormatField,-511/2 - 50,930);
 FormatField.right = 400:
 DrawText(DrawDC, "Experimental Spectrum", 21, & FormatField, DT TOP | DT LEFT);
if (DrawMode == 3)
 HWND MainHandle = GetActiveWindow();
 RECT WindowRect;
 GetClientRect(MainHandle,&WindowRect);
 SetMapMode(DrawDC,MM ANISOTROPIC);
 SetWindowExt(DrawDC,681,1200);
 SetViewportExt(DrawDC, WindowRect.right, - WindowRect.bottom);
 float specmin = yint[0];
 float specmax = yint[0];
 for (int a=1;a<DataNumber;++a)
  if (yint[a] < specmin)
  specmin = yint[a];
  if (yint[a] > specmax)
  specmax = yint[a];
 float dspecmin = dspec[0];
 float dspecmax = dspec[0];
 for (int b=1;b<512;++b)
  if (dspec[b] < dspecmin)</pre>
  dspecmin = dspec[b];
  if (dspec[b] > dspecmax)
```

```
dspecmax = dspec[b];
 SetWindowOrg(DrawDC,-85,1000);
 MoveTo(DrawDC,0,800);
 LineTo(DrawDC,0,0);
 LineTo(DrawDC,511,0);
 float YConv = 800/(specmax-specmin);
float XConv = 511/(xepr[DataNumber-1] - xepr[0]);
 MoveTo(DrawDC,0,(yint[0]-specmin)*YConv);
 for (int e=1;e<DataNumber;++e)
  LineTo(DrawDC,(xepr[e]-xepr[0])*XConv,(yint[e]-specmin)*YConv);
 YConv = 800/(dspecmax-dspecmin);
 SelectObject(DrawDC,GetStockObject(BLACK PEN));
 PaintPen = CreatePen(PS SOLID, 1,0x000000FF);
 SelectObject(DrawDC, PaintPen);
MoveTo(DrawDC,(HMin-xepr[0])*XConv,(dspec[0]-dspecmin)*YConv);
 for (int c=1;c<512;++c)
 {
  LineTo(DrawDC,((HMin+c*(HMax-HMin)/511)-xepr[0])*XConv,(dspec[c]-dspecmin)*YConv);
MoveTo(DrawDC,0,0);
LineTo(DrawDC.0,-20);
MoveTo(DrawDC,511/3,-20);
LineTo(DrawDC,511/3,0);
MoveTo(DrawDC,511*2/3,-20);
LineTo(DrawDC,511*2/3,0);
MoveTo(DrawDC,511,0);
LineTo(DrawDC,511,-20);
char FieldText [7]:
RECT FormatField:
FormatField.top = -25:
FormatField.bottom = -80;
FormatField.left = -20;
FormatField.right=80;
 gcvt(xepr[0],5,FieldText);
DrawText(DrawDC,FieldText,-1,&FormatField,DT TOP | DT LEFT);
 OffsetRect(&FormatField,511/3,0);
 gcvt((xepr[DataNumber-1]-xepr[0])/3+xepr[0],5,FieldText);
DrawText(DrawDC,FieldText,-1,&FormatField,DT TOP | DT LEFT);
OffsetRect(&FormatField,511/3,0);
 gcvt((xepr[DataNumber-1]-xepr[0])*2/3+xepr[0],5,FieldText);
DrawText(DrawDC,FieldText,-1,&FormatField,DT TOP | DT LEFT);
OffsetRect(&FormatField,511/3,0);
 gcvt(xepr[DataNumber-1],5,FieldText);
DrawText(DrawDC,FieldText,-1,&FormatField,DT TOP | DT LEFT);
 OffsetRect(&FormatField,-511/2 - 50,930);
FormatField.right = 400;
DrawText(DrawDC, "Overlaid Spectra", 16,&FormatField, DT TOP | DT LEFT);
if (DrawMode == 4)
HWND MainHandle = GetActiveWindow();
```

```
RECT WindowRect:
GetClientRect(MainHandle,&WindowRect):
SetMapMode(DrawDC,MM ANISOTROPIC):
SetWindowExt(DrawDC,681,1200);
SetViewportExt(DrawDC, WindowRect.right, -WindowRect.bottom);
float specmin = yint[0];
float specmax = vint[0];
for (int a=1;a<DataNumber;++a)
 if (vint[a] < specmin)
 specmin = yint[a];
 if (yint[a] > specmax)
 specmax = yint[a];
float dspecmin = dspec[0];
float dspecmax = dspec[0];
for (int b=1;b<512;++b)
{
 if (dspec[b] < dspecmin)
 dspecmin = dspec[b];
 if (dspec[b] > dspecmax)
 dspecmax = dspec[b];
SetWindowOrg(DrawDC,-85,1000);
MoveTo(DrawDC,0,800);
LineTo(DrawDC,0,0);
LineTo(DrawDC,511,0);
float YConv = 800/(specmax-specmin);
float XConv = 511/(xepr[DataNumber-1] - xepr[0]);
MoveTo(DrawDC,0,(yint[0]-specmin)*YConv);
for (int e=1;e<DataNumber;++e)
 LineTo(DrawDC,(xepr[e]-xepr[0])*XConv,(yint[e]-specmin)*YConv);
YConv = 800/(dspecmax-dspecmin);
MoveTo(DrawDC,0,(dspec[0]-dspecmin)*YConv-1200);
for (int c=1;c<512;++c)
 LineTo(DrawDC,c,(dspec[c]-dspecmin)*YConv-1200);
MoveTo(DrawDC,0,0);
LineTo(DrawDC.0,-20);
MoveTo(DrawDC,511/3,-20);
LineTo(DrawDC,511/3,0);
MoveTo(DrawDC,511*2/3,-20);
LineTo(DrawDC,511*2/3,0);
MoveTo(DrawDC,511,0);
LineTo(DrawDC,511,-20);
char FieldText [7];
RECT FormatField;
FormatField.top = -25;
FormatField.bottom = -80;
FormatField.left = -20;
FormatField.right=80;
```

```
gcvt(xepr[0],5,FieldText);
 DrawText(DrawDC,FieldText,-1,&FormatField,DT TOP | DT LEFT);
 OffsetRect(&FormatField,511/3,0);
 gcvt((xepr[DataNumber-1]-xepr[0])/3+xepr[0],5,FieldText);
 DrawText(DrawDC,FieldText,-1,&FormatField,DT TOP | DT LEFT);
 OffsetRect(&FormatField,511/3,0):
 gcvt((xepr[DataNumber-1]-xepr[0])*2/3+xepr[0],5,FieldText);
 DrawText(DrawDC,FieldText,-1,&FormatField,DT_TOP | DT_LEFT);
 OffsetRect(&FormatField,511/3,0);
 gcvt(xepr[DataNumber-1],5,FieldText);
 DrawText(DrawDC,FieldText,-1,&FormatField,DT TOP | DT LEFT);
 OffsetRect(&FormatField,-511/2 - 50,930);
 FormatField.right = 400;
 DrawText(DrawDC, "Experimental Spectrum", 21, & FormatField, DT TOP | DT LEFT);
 MoveTo(DrawDC,0,-1200);
 LineTo(DrawDC,0,-1220);
 MoveTo(DrawDC,511/3,-1220);
 LineTo(DrawDC,511/3,-1200);
 MoveTo(DrawDC,511*2/3,-1220);
 LineTo(DrawDC,511*2/3,-1200);
 MoveTo(DrawDC,511,-1200);
 LineTo(DrawDC,511,-1220);
 MoveTo(DrawDC,0,-400);
 LineTo(DrawDC,0,-1200);
 LineTo(DrawDC,511,-1200);
 FormatField.top = -1225:
 FormatField.bottom = -1280;
 FormatField.left = -20;
 FormatField.right=80;
 gcvt(HMin,5,FieldText);
 DrawText(DrawDC, FieldText, -1, & FormatField, DT TOP | DT LEFT);
 OffsetRect(&FormatField,511/3,0);
 gcvt(HMin+(HMax-HMin)/3,5,FieldText);
 DrawText(DrawDC,FieldText,-1,&FormatField,DT TOP | DT LEFT);
 OffsetRect(&FormatField,511/3,0);
 gcvt(HMin+(HMax-HMin)*2/3,5,FieldText);
 DrawText(DrawDC,FieldText,-1,&FormatField,DT TOP | DT LEFT);
 OffsetRect(&FormatField,511/3,0);
 gcvt(HMax,5,FieldText);
 DrawText(DrawDC,FieldText,-1,&FormatField,DT TOP | DT LEFT);
 OffsetRect(&FormatField,-511/2 - 50,930);
 FormatField.right = 600;
 DrawText(DrawDC, "Simulated Spectrum", 18,&FormatField,DT TOP | DT LEFT);
if (DrawMode == 10)
 HWND MainHandle = GetActiveWindow():
 ofstream exportos(FileName2);
 if (!exportos.bad())
  for (int s=0; s<512; ++s)
       exportos << (HMin + s*(HMax-HMin)/511) << " " << dspec[s] << "\n";
```

```
}
 else
 MessageBox(MainHandle, "File cannot be opened", "Disk Error",
               MB_OK | MB_ICONSTOP );
 exportos.close();
if (DrawMode == 11)
 POINT PageSize, OffsetSize;
 Escape(DrawDC,GETPHYSPAGESIZE,NULL,NULL,&PageSize);
 Escape(DrawDC,GETPRINTINGOFFSET,NULL,NULL,&OffsetSize);
 SetMapMode(DrawDC,MM ANISOTROPIC);
 SetWindowExt(DrawDC,690,1200);
 SetViewportExt(DrawDC,PageSize.x - 2*OffsetSize.x,-(PageSize.y-2*OffsetSize.y));
 SetWindowOrg(DrawDC,-85,1000);
 SetViewportOrg(DrawDC,-OffsetSize.x,-OffsetSize.y);
float dspecmax = dspec[0];
 float dspecmin = dspec[0];
 for (int v=1; v<512; ++v)
  if (dspec[v] < dspecmin)
      dspecmin = dspec[v];
  if (dspec[v] > dspecmax)
      dspecmax = dspec[v];
 float YConv = 800/(dspecmax-dspecmin);
 Escape(DrawDC,STARTDOC,6,"SimDoc",NULL);
 MoveTo(DrawDC,0,800);
LineTo(DrawDC,0,0);
LineTo(DrawDC,511,0);
LineTo(DrawDC,511,-20);
 MoveTo(DrawDC,511/3*2,0);
LineTo(DrawDC,511/3*2,-20);
 MoveTo(DrawDC,511/3,0);
LineTo(DrawDC,511/3,-20);
 MoveTo(DrawDC,0,(dspec[0]-dspecmin)*YConv);
 for (int y=1;y<512;++y)
  LineTo(DrawDC,y,(dspec[y]-dspecmin)*YConv);
char FieldPrint [10];
 RECT FieldRect;
 FieldRect.left = -20;
 FieldRect.right = 80;
 FieldRect.top = -25;
 FieldRect.bottom = -85;
 gcvt(HMin,6,FieldPrint);
 DrawText(DrawDC,FieldPrint,-1,&FieldRect,DT TOP | DT LEFT);
 OffsetRect(&FieldRect,511/3,0);
 gcvt((HMin+(HMax-HMin)/3),6,FieldPrint);
 DrawText(DrawDC,FieldPrint,-1,&FieldRect,DT_TOP | DT_LEFT);
 OffsetRect(&FieldRect,511/3,0);
 gcvt((HMin+(HMax-HMin)*2/3),6,FieldPrint);
 DrawText(DrawDC,FieldPrint,-1,&FieldRect,DT TOP | DT LEFT);
```

```
OffsetRect(&FieldRect,511/3,0);
  gcvt(HMax,6,FieldPrint);
  DrawText(DrawDC,FieldPrint,-1,&FieldRect,DT TOP | DT LEFT);
  OffsetRect(&FieldRect,-511/2-10,-40):
  DrawText(DrawDC, "Gauss", 5, & FieldRect, DT TOP | DT LEFT);
  FieldRect.left = 511/2-70:
  FieldRect.right = 511/2 + 200;
  FieldRect.top = 900;
  FieldRect.bottom = 820:
  DrawText(DrawDC, "Simulated Spectrum", 18, & FieldRect, DT_TOP | DT_LEFT);
  Escape(DrawDC, NEWFRAME, 0, NULL, NULL);
  Escape(DrawDC, ENDDOC, 0, NULL, NULL);
 SetCursor(LoadCursor(NULL,IDC ARROW));
// define the application class derived from TApplication
class TPolarization :public TApplication
 public:
  TPolarization (LPSTR AName, HANDLE hInstance, HANDLE
    hPrevInstance, LPSTR lpCmdLine, int nCmdShow):
    TApplication ( AName, hInstance, hPrevInstance,
                   lpCmdLine, nCmdShow) {};
  virtual void InitMainWindow ();
};
// Construct a Window class for main window derived from TWindow
class TPolarWindow: public TWindow
 public: // Data members for TPolarWindow
    PTWindow ImportWindow, PolParamWindow;
    PTWindow FieldWindow:
    HPEN PaintPen;
    BOOL helpb:
    // Declare functions for the file menu choices
    virtual void CMFileNew (RTMessage Msg) = [CM FIRST + CM FILENEW];
    virtual void CMFileOpen (RTMessage Msg) = [CM FIRST + CM FILEOPEN];
    void CMFileImport (RTMessage Msg) = [CM FIRST + CM IMPORT];
    virtual void CMFileSave (RTMessage Msg) = [CM FIRST + CM FILESAVE];
    virtual void CMFileSaveAs (RTMessage Msg) = [CM FIRST + CM FILESAVEAS];
    void CMFileExport (RTMessage Msg) = [CM FIRST + CM EXPORT];
    void CMPrint (RTMessage Msg) = [CM FIRST + CM PRINT];
    void CMPrintSetup (RTMessage Msg) = [CM FIRST + CM PRINTSETUP];
    virtual void CMExit (RTMessage Msg) = [CM FIRST + CM EXIT];
    virtual BOOL CanClose():
    virtual LPSTR GetClassName();
    virtual void GetWindowClass(WNDCLASS& AWndClass);
 // Declare functions for View menu choices
    void CMViewExper (RTMessage Msg) = [CM FIRST + CM VIEWEXPER];
    void CMViewSim (RTMessage Msg) = [CM FIRST + CM VIEWSIM];
    void CMViewBoth (RTMessage Msg) = [CM FIRST + CM VIEWBOTH];
    void CMViewPaged (RTMessage Msg) = [CM_FIRST + CM_VIEWPAGED];
```

```
// Declare functions for simulate menu choices
   void CMSimulate (RTMessage Msg) = [CM FIRST + CM SIMSPEC];
   void CMSimParam (RTMessage Msg) = [CM FIRST + CM SIMPARAM];
   void CMSimPolParam (RTMessage Msg) = [CM FIRST + CM SIMPOLPARAM];
   void CMSimLineChange (RTMessage Msg) = [CM FIRST + CM SIMLINE];
// Declare integrate menu functions
   void CMIntegDrawInteg (RTMessage Msg) = [CM FIRST + CM DRAWINTEG];
   void CMIntegEPR (RTMessage Msg) = [CM FIRST + CM INTEGEPR];
   void CMIntegBase (RTMessage Msg) = [CM_FIRST + CM_INTEGBASE];
   void CMIntegBaseOrg (RTMessage Msg) = [CM_FIRST + CM_INTEGBASEORG];
 // Declare various utility functions that are need
   void OpenFile();
   virtual void Paint(HDC PDC, PAINTSTRUCT& PS);
   void FileSave();
   void CMHelpIndex(RTMessage Msg) = [CM FIRST + 901];
   void CMCommands(RTMessage Msg) = [CM FIRST + 903];
   void CMHelpOnHelp(RTMessage Msg) = [CM_FIRST + 902];
// Constructor for TPolarWindow
   TPolarWindow (PTWindowsObject AParent, LPSTR ATitle);
   ~TPolarWindow()
   if (helpb)
   WinHelp(HWindow, "simhelp.hlp", HELP QUIT, 0);
};
TPolarWindow::TPolarWindow (PTWindowsObject AParent, LPSTR ATitle):
   TWindow (AParent, ATitle)
helpb = FALSE;
Attr.X = 10;
Attr.Y = 10;
 Attr.W = 620;
 Attr.H = 460:
 Attr.Style |= WS VSCROLL;
 Scroller = new TScroller(this, 1, 23, 2, 19):
 AssignMenu("MENU 1");
 GlobalScroller = Scroller;
 PolarDC = GetDC(HWindow);
 long int begin = GetCurrentTime();
BITMAP bm:
HBITMAP OldBit;
HDC BitmapDC = CreateCompatibleDC(PolarDC);
 HBITMAP IntroBitmap = LoadBitmap(GetApplication()->hInstance, "BITMAP_1");
 GetObject(IntroBitmap,sizeof(BITMAP),&bm);
 OldBit = SelectObject(BitmapDC,IntroBitmap);
 BitBlt(PolarDC, 160, 80, bm. bmWidth, bm. bmHeight, BitmapDC, 0, 0, SRCCOPY);
start:
 long int end = GetCurrentTime();
 if ((end-begin) < 4000 \parallel (end-begin) < 0)
 goto start;
 SelectObject(BitmapDC.OldBit);
```

```
DeleteObject(OldBit);
 DeleteObject(IntroBitmap);
 InvalidateRect(HWindow, NULL, TRUE);
 DeleteDC(BitmapDC);
 ReleaseDC(HWindow,PolarDC);
}
//Define class to create the parameter window
class TParamWindow:public TWindow
public:
char FreqText [10];
char NumberGroupsText [3];
char gxText [10];
char gvText[10];
char gzText[10];
char StepSizeText[5];
char NoDivText [5];
char DalphaText[10];
char MemThetaText[10];
char MemPhiText[10];
char OmegaText[10];
char WobbleText[10];
char LinewidthText[10];
char CrystalThetaText[10];
char CrystalPhiText[10];
PTComboBox SimTypeCombo;
PTWindow GroupsWindow;
PTEdit LinewidthEdit, NoDivEdit, DalphaEdit, WobbleEdit, OmegaEdit;
PTEdit CrystalThetaEdit,CrystalPhiEdit,MemThetaEdit,MemPhiEdit;
PTButton OKButton. CanButton:
PTListBox AccurListBox:
PTEdit FreqEdit,NoGroupsEdit,gxEdit,gyEdit,gzEdit,StepSizeEdit;
virtual void SetupWindow():
void HandleCancelButton (RTMessage Msg) = [ID FIRST + 28];
void HandleOKButton (RTMessage Msg) = [ID FIRST + 27];
TParamWindow(PTWindowsObject AParent, LPSTR ATitle);
// define a class to enter hyperfine values for each group
class TNumberGroupWindow:public TWindow
public:
char AxText[8], AyText[8], AzText[8];
char PhiText[8], ThetaText[8], PsiText[8];
char NoNucleiText[8];
char NuclearSpinText[8];
char GroupNumber [2];
PTEdit AxEdit [8];
PTEdit AyEdit [8];
PTEdit AzEdit [8];
PTEdit PhiEdit [8];
PTEdit PsiEdit [8];
PTEdit ThetaEdit [8]:
PTEdit NoNucleiEdit [8]:
```

```
PTEdit NuclearSpinEdit [8];
PTButton OKButton, CancelButton;
void HandleButtonOK(RTMessage Msg) = [ID FIRST + 94];
void HandleButtonCancel (RTMessage Msg) = [ID FIRST + 95];
TNumberGroupWindow(PTWindowsObject AParent,LPSTR ATitle);
};
// Define class to query the user to choose H field values for simulation
class TFieldWindow:public TWindow
public:
char HMAX [10], HMIN [10];
float amax;
float atemp:
float gmax;
float gmin;
void SimulateSpectrum ();
void goniomf(float Theta1,float Phi1,float Alpha,float Hohm,float &X1,float &Y1,
    float &Z1);
void HandleYesButtonField (RTMessage Msg) = [ID FIRST + 150];
void HandleNoButtonField (RTMessage Msg) = [ID FIRST + 151];
TFieldWindow(PTWindowsObject AParent,LPSTR ATitle);
};
// Define a class to create an import window
class TImportWindow:public TWindow
public:
  char delimiter:
  int FileBeginRead, FileEndRead;
  PTGroupBox DelimGroupBox; // Creates a group of radio buttons
  PTGroupBox LineGroupBox; // another group
  PTRadioButton ImportRadio;
  PTRadioButton ImportRadio1;
  PTRadioButton ImportRadio2:
  PTRadioButton ImportRadio3:
  PTRadioButton ImportRadio4;
  PTStatic ImportStatic:
  PTButton ImportButton;
  PTButton ImportButton1;
  virtual void SetupWindow():
  void HandleButtonOKImport (RTMessage Msg) = [ID FIRST + 5];
  void HandleButtonCanImport (RTMessage Msg) = [ID FIRST + 6];
  void HandleRadioOtherImport (RTMessage Msg) = [ID FIRST + 4];
  void HandleRadioOtherLinesImport (RTMessage Msg) = [ID FIRST + 8];
  TImportWindow(PTWindowsObject AParent, LPSTR ATitle):
    TWindow(AParent, ATitle)
  FileBeginRead = 1;
   FileEndRead = -1;
  DisableAutoCreate();
   Attr.Style |= WS_POPUP | WS_CAPTION;
   Attr.X = 20;
   Attr.Y = 20;
   Attr.W = 600;
```

```
Attr.H = 210;
  // Creation of the groupbox
DelimGroupBox = new TGroupBox(this, 1, "Delimiter in File",
                          10,10,185,120);
 // Creation of radiobuttons
ImportRadio = new TRadioButton(this, 2, "whitespace",
               30,30,100,30,DelimGroupBox);
ImportRadio->Attr.Style |= WS TABSTOP;
ImportRadio1 = new TRadioButton(this,3,"comma",
          30,60,100,30,DelimGroupBox);
ImportRadio2 = new TRadioButton(this, 4, "other",
               30,90,100,30,DelimGroupBox);
 // creation of another groupbox
LineGroupBox = new TGroupBox(this, 9, "Lines to Input",
                196,10,250,120);
 // Creation of radiobuttons for LineGroupbox
ImportRadio3 = new TRadioButton(this,7,"All",
               215,40,100,30,LineGroupBox);
ImportRadio3->Attr.Style |= WS TABSTOP;
ImportRadio4 = new TRadioButton(this,8,"Other",
               215,80,100,30,LineGroupBox);
 // Create static text in the window
ImportStatic = new TStatic(this,-1,"View of the file",
 0,140,580,30,17);
ImportStatic->Attr.Style = ImportStatic->Attr.Style & ~SS LEFT | SS CENTER;
// MAKE A PUSH BUTTON FOR USER TO MAKE A CHOICE
ImportButton = new TButton(this,5,"OK",500,30,70,30,TRUE);
ImportButton->Attr.Style |= WS TABSTOP | BS DEFPUSHBUTTON;
ImportButton1 = new TButton(this,6, "Cancel",500,70,70,30,TRUE);
ImportButton1->Attr.Style |= WS TABSTOP;
EnableKBHandler(); // Enables the tab key
 }
// Make a window for the polarization parameters
class TPolParamWindow:public TWindow
public:
PTGroupBox, PolGroup1Box;
PTEdit PolEdit, PolEdit1;
PTRadioButton PolCheckBox, PolCheck1Box;
PTRadioButton PolCheck2Box, PolCheck3Box;
PTButton PolButton.PolButton1:
char CIDEPRatio [9];
char EXCHANGE [9];
virtual void SetupWindow();
void HandleOKPolButton (RTMessage Msg) = [ID FIRST + 168];
void HandleCanPolButton (RTMessage Msg) = [ID FIRST + 169];
TPolParamWindow(PTWindowsObject AParent,LPSTR ATitle):
}:
TPolParamWindow:TPolParamWindow (PTWindowsObject AParent, LPSTR ATitle):
                                TWindow(AParent, ATitle)
 DisableAutoCreate();
```

```
Attr.Style |= WS POPUP | WS CAPTION;
 Attr.X = 50;
 Attr.Y = 120;
 Attr.W = 540;
 Attr.H = 240:
 gcvt(Exchange, 5, EXCHANGE);
 gcvt(Ratio,5,CIDEPRatio);
 PolGroupBox = new TGroupBox(this, 160, "Spectrum Type", 10, 10, 125, 70);
 PolCheckBox = new TRadioButton(this, 161, "Normal", 40, 30, 80, 20, PolGroupBox);
 PolCheck1Box = new TRadioButton(this, 162, "CRPP", 40, 50, 80, 20, PolGroupBox);
 PolGroup1Box = new TGroupBox(this, 163, "Precursor", 145, 10, 125, 70);
 PolCheck2Box = new TRadioButton(this, 164, "Doublet", 175, 30, 80, 20, PolGroup1Box);
 PolCheck3Box = new TRadioButton(this, 165, "Quartet", 175,50,80,20, PolGroup1Box);
 new TStatic(this,-1,"Ratio of peaks with largest coupling",20,100,150,40,36);
 PolEdit = new TEdit(this, 166, CIDEPRatio, 30, 150, 70, 25, 6, FALSE);
 PolEdit->Attr.Style |= WS_TABSTOP;
 new TStatic(this,-1,"Exchange value(Gauss)",305,10,125,50,21);
 PolEdit1 = new TEdit(this, 167, EXCHANGE, 305, 55, 100, 25, 6, FALSE);
 PolEdit1->Attr.Style |= WS TABSTOP;
 PolButton = new TButton(this, 168, "OK", 450, 10, 70, 30, TRUE);
 PolButton->Attr.Style |= BS DEFPUSHBUTTON | WS TABSTOP;
 PolButton1 = new TButton(this, 169, "Cancel", 450, 50, 70, 30, TRUE);
 PolButton1->Attr.Style |= WS_TABSTOP;
}
void TPolParamWindow::SetupWindow()
 TWindow::SetupWindow();
 if (!SpecCRPP)
 PolCheckBox->Check();
 PolCheck1Box->Check();
 if (PrecurDou)
 PolCheck2Box->Check();
 else
 PolCheck3Box->Check();
}
// function that handles ok response for polarization parameters
void TPolParamWindow::HandleOKPolButton (RTMessage)
 if (PolCheckBox->GetCheck() == BF_CHECKED)
 SpecCRPP = FALSE;
 if (PolCheck1Box->GetCheck() == BF CHECKED)
  SpecCRPP = TRUE;
 if (PolCheck2Box->GetCheck() == BF CHECKED)
  PrecurDou = TRUE;
 if (PolCheck3Box->GetCheck() == BF_CHECKED)
  PrecurDou = FALSE;
 PolEdit->GetLine(CIDEPRatio, 6, 1);
 Ratio = atof(CIDEPRatio);
 PolEdit1->GetLine(EXCHANGE,6,1);
 Exchange = atof(EXCHANGE):
 CloseWindow();
```

```
}
// Function to handle a cancel response in the polarization parameter window
void TPolParamWindow::HandleCanPolButton (RTMessage)
 CloseWindow();
}
TFieldWindow::TFieldWindow (PTWindowsObject AParent,LPSTR ATitle):
                           TWindow(AParent, ATitle)
 Attr.Style |= WS_POPUP | WS_CAPTION;
 Attr.X = 100;
 Attr.W = 400;
 Attr.Y = 100;
 Attr.H = 240:
 // Function to calculate hmax and hmin for simulation
 gmax=gx;
 gmin=gx;
 if (gmax < gy)
  gmax=gy;
 if (gmax < gz)
  gmax=gz;
 if (gmin > gy)
  gmin = gy;
 if (gmin > gz)
  gmin = gz;
 HMax = Freq*0.714484/gmin;
 HMin = Freq *0.714484/gmax;
 amax = 0;
 if (NumberGroups > 0)
  for (int i=0;i<NumberGroups;++i)
   for (int j=0; j<3; ++j)
        atemp = AHyp [j][j][i];
        if (atemp < 0)
         atemp = -atemp;
        if (atemp > amax)
          amax = atemp;
   HMin -= amax * NucleiPerGroup [i] * NuclearSpin [i];
   HMax += amax * NucleiPerGroup [i] * NuclearSpin [i];
   amax = 0:
  }
 HMax = HMax + 5 * Linewidth;
 HMin = HMin - 5 * Linewidth;
 gcvt(HMax,6,HMAX);
 gcvt(HMin,6,HMIN);
 new TStatic(this,-1,"The Calculated Value for Hmin is ",10,10,290,20,
   33);
 new TStatic(this,-1,HMIN,300,10,60,20,sizeof HMIN);
 new TStatic(this,-1,"The Calculated Value for Hmax is ",10,50,290,20,
```

```
33);
 new TStatic(this,-1,HMAX,300,60,60,20,sizeof HMAX);
 new TStatic(this,-1,"Do you wish to use these values?",30,100,290,20,
 new TButton(this, 150, "Yes", 150, 140, 70, 30, FALSE);
 new TButton(this, 151, "No", 250, 140, 70, 30, FALSE);
TParamWindow::TParamWindow (PTWindowsObject AParent,LPSTR ATitle):
        TWindow(AParent, ATitle)
 DisableAutoCreate();
 Attr.Style |= WS POPUP | WS CAPTION;
 Attr.X=1:
 Attr.Y=1:
 Attr.W=639;
 Attr.H=479;
 gcvt(Freq,6,FreqText);
 gcvt(NumberGroups,2,NumberGroupsText);
 gcvt(gx,6,gxText);
 gcvt(gy,6,gyText);
 gcvt(gz,6,gzText);
 itoa(StepSize, StepSizeText, 10);
 itoa(NoDiv, NoDivText, 10);
 gcvt(Dalpha,6,DalphaText);
 gcvt(MemTheta,6,MemThetaText);
 gcvt(MemPhi,6,MemPhiText);
 gcvt(Omega,6,OmegaText);
 gcvt(Wobble,6,WobbleText);
 gcvt(Linewidth*2,6,LinewidthText);
 gcvt(CrystalTheta,6,CrystalThetaText);
 gcvt(CrystalPhi,6,CrystalPhiText);
 new TStatic (this,-1,"Sim. Type",50,1,90,20,9);
 SimTypeCombo = new TComboBox(this, 10,50,22,90,95,
   CBS DROPDOWNLIST, 10);
 SimTypeCombo->Attr.Style |= WS TABSTOP;
 new TStatic (this,-1,"Freq. (MHz)",50,174,90,20,11);
 FreqEdit = new TEdit(this,11,FreqText,50,196,90,25,9,FALSE);
 FreqEdit->Attr.Style |= WS TABSTOP;
 new TStatic (this,-1,"Accuracy", 190, 1,90,20,8);
 AccurListBox = new TListBox(this, 12, 190, 22, 90, 35);
 AccurListBox->Attr.Style |= WS TABSTOP;
 new TStatic (this,-1,"Linewidth",190,174,90,20,9);
 LinewidthEdit = new TEdit(this, 13, LinewidthText, 190, 196, 90, 25, 9, FALSE);
 LinewidthEdit->Attr.Style |= WS TABSTOP;
 new TStatic(this,-1,"gx-value",50,87,90,20,8);
 new TStatic(this,-1,"gy-value",190,87,90,20,8);
 new TStatic(this,-1,"gz-value",330,87,90,20,8);
 new TStatic(this,-1,"# of groups",330,1.90,20,11);
 gxEdit = new TEdit(this, 14, gxText, 50, 109, 90, 25, 9, FALSE);
 gxEdit->Attr.Style |= WS_TABSTOP;
 gyEdit = new TEdit(this, 15, gyText, 190, 109, 90, 25, 9, FALSE);
 gyEdit->Attr.Style |= WS TABSTOP;
 gzEdit = new TEdit(this, 16, gzText, 330, 109, 90, 25, 9, FALSE);
```

```
gzEdit->Attr.Style |= WS TABSTOP;
NoGroupsEdit = new TEdit(this, 17, NumberGroupsText, 330, 22, 90, 25, 2, FALSE);
NoGroupsEdit->Attr.Style |= WS TABSTOP;
new TStatic(this,-1,"Step Size",330,174,90,20,9);
new TStatic(this,-1,"# div.",470,174,90,20,6);
StepSizeEdit = new TEdit(this, 18, StepSizeText, 330, 196, 90, 25, 4, FALSE);
StepSizeEdit->Attr.Style |= WS TABSTOP;
NoDivEdit = new TEdit(this, 19, NoDivText, 470, 196, 90, 25, 5, FALSE);
NoDivEdit->Attr.Style |= WS TABSTOP;
new TStatic(this.-1."dalpha",50,261,90,20,6);
new TStatic(this,-1,"omega",190,261,90,20,5);
new TStatic(this,-1,"wobble",330,261,90,20,6);
DalphaEdit = new TEdit(this, 20, DalphaText, 50, 283, 90, 25, 9, FALSE);
DalphaEdit->Attr.Style |= WS TABSTOP;
OmegaEdit = new TEdit(this,21,OmegaText,190,283,90,25,9,FALSE);
OmegaEdit->Attr.Style |= WS TABSTOP;
 WobbleEdit = new TEdit(this, 22, WobbleText, 330, 283, 90, 25, 9, FALSE);
 WobbleEdit->Attr.Style |= WS TABSTOP;
new TStatic(this,-1,"Mem. Theta",50,348,90,20,10);
new TStatic(this,-1,"Mem. Phi",190,348,90,20,8);
new TStatic(this,-1,"Cry. Theta",330,348,90,20,10);
new TStatic(this,-1,"Cry. Phi",470,348,90,20,8);
 MemThetaEdit = new TEdit(this,23,MemThetaText,50,370,90,25,9,FALSE);
MemThetaEdit->Attr.Style |= WS_TABSTOP;
MemPhiEdit = new TEdit(this,24,MemPhiText,190,370,90,25,9,FALSE);
 MemPhiEdit->Attr.Style |= WS TABSTOP;
 CrystalThetaEdit = new TEdit(this,25,CrystalThetaText,330,370,90,25,9,FALSE);
 CrystalThetaEdit->Attr.Style |= WS_TABSTOP;
 CrystalPhiEdit = new TEdit(this.26, CrystalPhiText, 470, 370, 90, 25, 9, FALSE);
 CrystalPhiEdit->Attr.Style |= WS TABSTOP;
 OKButton = new TButton(this,27,"OK",500,30,70,30,TRUE);
 CanButton = new TButton(this, 28, "Cancel", 500, 70, 70, 30, TRUE);
EnableKBHandler();
void TParamWindow::SetupWindow()
 TWindow::SetupWindow();
 SimTypeCombo->AddString("Powder");
 SimTypeCombo->AddString("Oriented");
 SimTypeCombo->AddString("Crystal");
 SimTypeCombo->AddString("Solution");
 if (SimType == 1)
 SimTypeCombo->SetSelIndex(2);
 if (SimType == 2)
 SimTypeCombo->SetSelIndex(1);
 if (SimType == 3)
 SimTypeCombo->SetSelIndex(0);
 if (SimType == 4)
 SimTypeCombo->SetSelIndex(3);
 AccurListBox->AddString("General");
 AccurListBox->AddString("Approx.");
 if (AccurGen)
 AccurListBox->SetSelIndex(1);
 else
```

```
AccurListBox->SetSelIndex(0);
// Handles the ok choice in the parameter window
void TParamWindow::HandleOKButton (RTMessage)
 FreqEdit->GetLine(FreqText,7,1);
 Freq = atof(FreqText);
 if (Freq < 0)
 Freq = -Freq;
 if (Freq == 0)
 Freq = 9400:
 if (SimTypeCombo->GetSelIndex() == 0)
 SimType = 3:
 if (SimTypeCombo->GetSelIndex() == 1)
 SimType = 2;
 if (SimTypeCombo->GetSelIndex() == 2)
 SimType = 1;
 if (SimTypeCombo->GetSelIndex() == 3)
 SimType = 4;
 if (AccurListBox->GetSelIndex() == 0)
 AccurGen = FALSE;
 else
 AccurGen = TRUE;
 NoGroupsEdit->GetLine(NumberGroupsText,3,1);
 NumberGroups = atof (NumberGroupsText);
 if (NumberGroups > 8)
 NumberGroups = 8;
 if (NumberGroups < 0)
 NumberGroups = 0:
 gxEdit->GetLine(gxText,7,1);
 gx = atof(gxText);
 if (gx < 0)
 gx = -gx;
 if (gx == 0)
 gx = 2.0023;
 gyEdit->GetLine(gyText,7,1);
 gy = atof(gyText);
 if (gy < 0)
 gy = -gy;
 if (gy == 0)
 gy = 2.0023;
 gzEdit->GetLine(gzText,7,1);
 gz = atof(gzText);
 if (gz < 0)
 gz = -gz;
 if (gz == 0)
 gz = 2.0023;
 StepSizeEdit->GetLine(StepSizeText, 5, 1);
 StepSize = atoi(StepSizeText);
 if (StepSize < 0)
 StepSize = -StepSize;
 if (StepSize < 1 || StepSize > 180)
 StepSize = 15;
 NoDivEdit->GetLine(NoDivText, 5, 1);
```

```
NoDiv = atoi(NoDivText);
if (NoDiv < 0)
NoDiv = -NoDiv;
if (NoDiv == 0)
NoDiv = 5;
DalphaEdit->GetLine(DalphaText, 6, 1);
Dalpha = atof(DalphaText);
if (Dalpha == 0)
Dalpha = 30;
MemThetaEdit->GetLine(MemThetaText,6,1);
MemTheta = atof(MemThetaText);
MemPhiEdit->GetLine(MemPhiText,6,1);
MemPhi = atof(MemPhiText);
OmegaEdit->GetLine(OmegaText,6,1);
 Omega = atof(OmegaText);
 WobbleEdit->GetLine(WobbleText,6,1);
 Wobble = atof(WobbleText);
 CrystalThetaEdit->GetLine(CrystalThetaText,6,1);
 CrystalTheta = atof(CrystalThetaText);
 CrystalPhiEdit->GetLine(CrystalPhiText,6,1);
 CrystalPhi = atof(CrystalPhiText);
LinewidthEdit->GetLine(LinewidthText, 6, 1);
Linewidth = atof(LinewidthText);
Linewidth /= 2;
 if (Linewidth < 0.05)
Linewidth = 0.05;
 if (NumberGroups == 0)
 CloseWindow();
 if (NumberGroups > 0)
 GroupsWindow = new TNumberGroupWindow(this, "Group Parameters");
 GetApplication()->MakeWindow(GroupsWindow);
 }
void TParamWindow::HandleCancelButton(RTMessage)
 CloseWindow();
//Constructor for TNumberGroupWindow
TNumberGroupWindow::TNumberGroupWindow(PTWindowsObject AParent,
   LPSTR ATitle):TWindow(AParent, ATitle)
{
Attr.Style |= WS_POPUP | WS_CAPTION;
Attr.X = 5;
Attr.Y = 10;
Attr.W = 635;
Attr.H = 469;
new TStatic(this,-1,"Group",10,80,70,20,5);
new TStatic(this,-1,"Ax",80,80,70,20,2);
new TStatic(this,-1,"Ay",151,80,70,20,2);
new TStatic(this,-1,"Az",222,80,70,20,2);
new TStatic(this,-1,"Phi",293,80,70,20,3);
new TStatic(this,-1,"Theta",364,80,70,20,5);
new TStatic(this,-1,"Psi",435,80,70,20,3);
```

```
new TStatic(this,-1,"# Nuc",506,80,70,20,5);
new TStatic(this,-1,"Spin",577,80,50,20,4);
for (int i =0;i<NumberGroups;++i)
 itoa(i+1, Group Number, 10);
 new TStatic(this,-1, GroupNumber, 10, 100+i*25, 70, 25, size of GroupNumber);
 gcvt(AHyp[0][0][i],7,AxText);
 gcvt(AHyp[1][1][i],7,AyText);
 gcvt(AHyp[2][2][i],7,AzText);
 gcvt(Phi[i],6,PhiText);
 gcvt(Theta[i],6,ThetaText);
 gcvt(Psi[i],6,PsiText);
 itoa(NucleiPerGroup[i], NoNucleiText, 4);
 gcvt(NuclearSpin[i],4,NuclearSpinText);
 AxEdit[i] = new TEdit(this, 30+i, AxText, 80, 100+i*25, 70, 25, 7, FALSE);
 AxEdit[i]->Attr.Style |= WS_TABSTOP;
 AyEdit[i] = new TEdit(this, 38+i, AyText, 151, 100+i*25, 70, 25, 7, FALSE);
 AyEdit[i]->Attr.Style |= WS TABSTOP;
 AzEdit[i] = new TEdit(this,46+i,AzText,222,100+i*25,70,25,7,FALSE);
 AzEdit[i]->Attr.Style |= WS TABSTOP;
 PhiEdit[i]= new TEdit(this,54+i,PhiText,293,100+i*25,70,25,7,FALSE);
 PhiEdit[i]->Attr.Style |= WS_TABSTOP;
 ThetaEdit[i] = new TEdit(this,62+i,ThetaText,364,100+i*25,70,25,7,FALSE);
 ThetaEdit[i]->Attr.Style |= WS TABSTOP;
 PsiEdit[i] = new TEdit(this,70+i,PsiText,435,100+i*25,70,25,7,FALSE);
 PsiEdit[i]->Attr.Style |= WS TABSTOP;
 NoNucleiEdit[i] = new TEdit(this,78+i,NoNucleiText,506,100+i*25,70,25,7,FALSE);
 NoNucleiEdit[i]->Attr.Style |= WS_TABSTOP;
 NuclearSpinEdit[i]=new TEdit(this,86+i,NuclearSpinText,577,100+i*25,50,25,7,FALSE);
 NuclearSpinEdit[i]->Attr.Style |= WS_TABSTOP;
 OKButton = new TButton(this, 94, "OK", 500, 10, 70, 30, TRUE);
 CancelButton = new TButton(this,95,"Cancel",500,45,70,30,TRUE);
 EnableKBHandler();
void TNumberGroupWindow::HandleButtonOK(RTMessage)
for (int i=0;i<NumberGroups;++i)
 AxEdit[i]->GetLine(AxText,8,1);
 AHyp[0][0][i] = atof(AxText);
 AyEdit[i]->GetLine(AyText,8,1);
 AHyp[1][1][i] = atof(AyText);
 AzEdit[i]->GetLine(AzText,8,1);
 AHyp[2][2][i] = atof(AzText);
 PhiEdit[i]->GetLine(PhiText,8,1);
 Phi[i] = atof(PhiText);
 PsiEdit[i]->GetLine(PsiText, 8, 1);
 Psi[i] = atof(PsiText);
 ThetaEdit[i]->GetLine(ThetaText, 8, 1);
 Theta[i]=atof(ThetaText);
 NoNucleiEdit[i]->GetLine(NoNucleiText, 8, 1);
 NucleiPerGroup[i]=atoi(NoNucleiText);
 NuclearSpinEdit[i]->GetLine(NuclearSpinText, 8, 1);
```

```
NuclearSpin[i]=atof(NuclearSpinText);
CloseWindow():
ParamWindow->CloseWindow();
void TNumberGroupWindow::HandleButtonCancel(RTMessage)
CloseWindow();
ParamWindow->CloseWindow();
// Actual setup of the controls in the import window
void TImportWindow::SetupWindow()
TWindow::SetupWindow();
ImportRadio->SetCheck(BF CHECKED);
ImportRadio3->SetCheck(BF_CHECKED);
}
// Make response function for ok command in the import window
void TImportWindow::HandleButtonOKImport (RTMessage)
 SetCursor(LoadCursor(NULL,IDC WAIT));
 // Get the data from the file
 ifstream is(FileName);
  if (!is.bad())
   if (ImportRadio2->GetCheck()==BF_CHECKED)
    char xeprchar [10], yeprchar [10];
    if (FileEndRead==-1 && FileBeginRead != 1)
         for (int d=1;d<FileBeginRead;++d)
      is.ignore(80,\n');
         int c=0:
         while (!is.eof())
          is.getline(xeprchar, 10, delimiter);
          is.getline(yeprchar, 10);
          xepr[c] = atof(xeprchar);
          yepr[c] = atof(yeprchar);
      ++c;
     DataNumber = c;
    else if (FileBeginRead != 1 || FileEndRead != -1)
         for (int e=1;e<FileBeginRead;++e)
         is.ignore(80,\n');
         for(int f=0;f < (FileEndRead - FileBeginRead + 1);++f)
          is.getline(xeprchar, 10, delimiter);
          is.getline(yeprchar, 10);
          xepr[f] = atof(xeprchar);
```

```
yepr[f] = atof(yeprchar);
  DataNumber = FileEndRead - FileBeginRead + 1;
 else
 {
  int g=0;
      while (!(is.eof()))
       is.getline(xeprchar, 10, delimiter);
       is.getline(yeprchar, 10);
       xepr[g] = atof(xeprchar);
       yepr[g] = atof(yeprchar);
       ++g;
  DataNumber = g;
else if (ImportRadio1->GetCheck()==BF_CHECKED)
 char xeprchar [10], yeprchar [10];
 if (FileEndRead==-1 && FileBeginRead != 1)
      for (int d=1;d<FileBeginRead;++d)
   is.ignore(80,\n');
      int c=0;
      while (lis.eof())
       is.getline(xeprchar, 10,',');
       is.getline(yeprchar, 10);
       xepr[c] = atof(xeprchar);
       yepr[c] = atof(yeprchar);
   ++c;
  DataNumber = c;
 else if (FileBeginRead != 1 || FileEndRead != -1)
      for (int e=1;e<FileBeginRead;++e)
      is.ignore(80,\n');
      for(int f=0;f < (FileEndRead - FileBeginRead + 1);++f)</pre>
       is.getline(xeprchar, 10,',');
       is.getline(yeprchar, 10);
       xepr[f] = atof(xeprchar);
       yepr[f] = atof(yeprchar);
  DataNumber = FileEndRead - FileBeginRead + 1;
 }
 else
  int g=0;
      while (!(is.eof()))
```

```
is.getline(xeprchar, 10,',');
      is.getline(yeprchar, 10);
      xepr[g] = atof(xeprchar);
      yepr[g] = atof(yeprchar);
      ++g;
  DataNumber = g;
 }
}
else
 if (FileEndRead==-1 && FileBeginRead != 1)
     for (int d=1;d<FileBeginRead;++d)
   is.ignore(80,\n');
  int c=0;
     while (!is.eof())
      is >> xepr[c] >> yepr[c];
   ++c;
     DataNumber = c-1;
 else if (FileBeginRead != 1 || FileEndRead != -1)
     for (int e=1;e<FileBeginRead;++e)
     is.ignore(80,\n');
     for(int f=0;f < (FileEndRead - FileBeginRead + 1);++f)
      is >> xepr[f] >> yepr[f];
  DataNumber = FileEndRead - FileBeginRead + 1;
 }
 else
  int g=0;
     while (lis.eof())
      is >> xepr[g] >> yepr[g];
      ++g;
  DataNumber = g-1;
 }
is.close();
ImportFileWindow->CloseWindow();
CloseWindow();
ExperLoaded = TRUE;
HMENU MainMenu = GetMenu(Parent->HWindow);
EnableMenuItem(MainMenu,CM VIEWEXPER,MF BYCOMMAND | MF ENABLED);
EnableMenuItem(MainMenu, CM_IMPORT, MF_BYCOMMAND | MF_GRAYED);
EnableMenuItem(MainMenu, CM INTEGBASE, MF BYCOMMAND | MF ENABLED);
EnableMenuItem(MainMenu,CM INTEGBASEORG, MF BYCOMMAND | MF ENABLED);
EnableMenuItem(MainMenu,CM INTEGEPR,MF BYCOMMAND | MF GRAYED);
```

```
EnableMenuItem(MainMenu,CM_DRAWINTEG,MF_BYCOMMAND | MF_ENABLED);
   if (SimTrue)
    EnableMenuItem(MainMenu,CM VIEWBOTH,MF BYCOMMAND | MF ENABLED);
    EnableMenuItem(MainMenu, CM_VIEWPAGED, MF_BYCOMMAND | MF_ENABLED);
   }
   else
   is.close();
   HWND ImportWndHandle = GetActiveWindow();
   MessageBox(ImportWndHandle, "Cannot Open File", "File Error", IDOK);
 SetCursor(LoadCursor(NULL,IDC ARROW));
void TImportWindow::HandleButtonCanImport (RTMessage)
 ImportFileWindow->CloseWindow();
 CloseWindow();
// function that prompts user to enter a delimiter character
void TImportWindow::HandleRadioOtherImport (RTMessage)
char delim [5] = "";
// Displays a dialog box for the user
 if (GetApplication()->ExecDialog(new TInputDialog(this, "Delimiter Character"
   ,"Enter the delimiter character in the file:".delim.sizeof
   delim) = IDOK)
 sscanf(delim, "%c", &delimiter);
 }
// function that prompts the user to enter file lines to read
void TImportWindow::HandleRadioOtherLinesImport (RTMessage )
// Displays the input boxes
char begin [10] = "1";
char end [10] = "end";
if (GetApplication()->ExecDialog(new TInputDialog(this, "Begin Line",
 "Enter the line to begin reading", begin, size of begin)) == IDOK)
 FileBeginRead = atoi(begin);
if (GetApplication()->ExecDialog(new TInputDialog(this."End Line".
  "Enter the line to end reading", end, size of end)) == IDOK)
 if (!strcmp(end, "end"))
 FileEndRead = -1;
 else
 FileEndRead = atoi(end);
}
void TFieldWindow::goniomf(float Theta1,float Phi1,float Alpha,
             float Hohm, float &X1, float &Y1, float &Z1)
{
```

```
float const convert = 0.017453292:
 X1 = (cos(Hohm*convert) * sin(Theta1*convert) * cos(Phi1*convert));
 X1 = (X1 + \sin(Hohm * convert) * \sin(Alpha * convert) * \sin(Phi1 * convert));
 X1 = (X1 - \sin(Hohm + convert) + \cos(Alpha + convert) + \cos(Theta1 + convert) +
       cos(Phil*convert));
 Y1 = (cos(Hohm*convert) * sin(Theta1*convert) * sin(Phi1*convert));
 Y1 = (Y1 - sin(Hohm*convert) * sin(Alpha*convert) * cos(Phi1*convert));
 Y1 = (Y1 - \sin(Hohm*convert)*cos(Alpha*convert)*cos(Theta1*convert)*
        sin(Phi1*convert));
 Z1 = (\cos(Hohm*convert) * \cos(Theta1*convert));
 Z1 = (Z1 + \sin(Hohm*convert) * \cos(Alpha*convert) * \sin(Theta1*convert));
// Definition of TFieldWindow functions
void TFieldWindow::HandleYesButtonField (RTMessage)
CloseWindow():
DrawMode = 0;
SimulateSpectrum();
if (SimTrue)
FileSaved = FALSE;
Integrate = FALSE;
DrawMode=1:
GlobalScroller->ScrollTo(1.0);
InvalidateRect(Parent->HWindow, NULL, TRUE);
UpdateWindow(Parent->HWindow);
HMENU MainMenu = GetMenu(Parent->HWindow);
EnableMenuItem(MainMenu.CM SIMLINE.MF BYCOMMAND | MF ENABLED):
EnableMenuItem(MainMenu, CM_VIEWSIM, MF_BYCOMMAND | MF_ENABLED);
EnableMenuItem(MainMenu,CM FILESAVE,MF BYCOMMAND | MF ENABLED);
EnableMenuItem(MainMenu,CM FILESAVEAS,MF BYCOMMAND | MF ENABLED);
EnableMenuItem(MainMenu,CM EXPORT,MF BYCOMMAND | MF ENABLED);
EnableMenuItem(MainMenu, CM_PRINT, MF_BYCOMMAND | MF_ENABLED);
EnableMenuItem(MainMenu,CM FILEOPEN,MF BYCOMMAND | MF GRAYED);
EnableMenuItem(MainMenu,CM INTEGEPR,MF BYCOMMAND | MF GRAYED);
EnableMenuItem(MainMenu,CM DRAWINTEG,MF BYCOMMAND | MF ENABLED);
if (ExperLoaded)
 {
 EnableMenuItem(MainMenu,CM VIEWBOTH,MF_BYCOMMAND | MF_ENABLED);
 EnableMenuItem(MainMenu, CM VIEWPAGED, MF BYCOMMAND | MF ENABLED);
DrawMenuBar(Parent->HWindow);
 }
else
 {
 FileSaved = TRUE;
 DrawMode = 0:
 GlobalScroller->ScrollTo(1,0);
 HMENU MainMenu = GetMenu(Parent->HWindow);
 EnableMenuItem(MainMenu, CM SIMLINE, MF BYCOMMAND | MF GRAYED);
EnableMenuItem(MainMenu, CM_VIEWSIM, MF_BYCOMMAND | MF_GRAYED);
EnableMenuItem(MainMenu,CM FILESAVE,MF BYCOMMAND | MF GRAYED);
EnableMenuItem(MainMenu, CM FILESAVEAS, MF BYCOMMAND | MF GRAYED);
```

```
EnableMenuItem(MainMenu, CM EXPORT, MF BYCOMMAND | MF GRAYED);
EnableMenuItem(MainMenu, CM_PRINT, MF_BYCOMMAND | MF_GRAYED);
 EnableMenuItem(MainMenu, CM VIEWBOTH, MF BYCOMMAND | MF GRAYED);
 EnableMenuItem(MainMenu, CM VIEWPAGED, MF BYCOMMAND | MF GRAYED);
 EnableMenuItem(MainMenu,CM FILEOPEN,MF BYCOMMAND | MF ENABLED);
DrawMenuBar(Parent->HWindow);
}
void TFieldWindow::HandleNoButtonField (RTMessage )
gcvt(HMin,6,HMIN);
gcvt(HMax,6,HMAX);
if (GetApplication()->ExecDialog(new TInputDialog(this, "Minimum H",
"Input a new minimum H", HMIN, sizeof HMIN)) == IDOK)
HMin = atof(HMIN);
if (GetApplication()->ExecDialog(new TInputDialog(this, "Maximum H",
"Input a new maximum H", HMAX, sizeof HMAX)) == IDOK)
HMax = atof(HMAX);
CloseWindow();
DrawMode = 0:
SimulateSpectrum();
if (SimTrue)
FileSaved = FALSE;
Integrate = FALSE:
DrawMode = 1;
GlobalScroller->ScrollTo(1,0);
InvalidateRect(Parent->HWindow, NULL, TRUE);
UpdateWindow(Parent->HWindow);
HMENU MainMenu = GetMenu(Parent->HWindow);
EnableMenuItem(MainMenu,CM SIMLINE,MF BYCOMMAND | MF ENABLED);
EnableMenuItem(MainMenu,CM VIEWSIM,MF BYCOMMAND | MF ENABLED);
EnableMenuItem(MainMenu,CM FILESAVE,MF BYCOMMAND | MF ENABLED);
EnableMenuItem(MainMenu, CM FILESAVEAS, MF BYCOMMAND | MF ENABLED);
EnableMenuItem(MainMenu, CM EXPORT, MF BYCOMMAND | MF ENABLED);
EnableMenuItem(MainMenu,CM PRINT,MF BYCOMMAND | MF ENABLED);
EnableMenuItem(MainMenu,CM FILEOPEN,MF BYCOMMAND | MF GRAYED);
EnableMenuItem(MainMenu, CM_INTEGEPR, MF_BYCOMMAND | MF_GRAYED);
EnableMenuItem(MainMenu,CM DRAWINTEG,MF BYCOMMAND | MF ENABLED);
if (ExperLoaded)
 EnableMenuItem(MainMenu, CM VIEWBOTH, MF BYCOMMAND | MF ENABLED);
 EnableMenuItem(MainMenu,CM_VIEWPAGED, MF_BYCOMMAND | MF_ENABLED);
DrawMenuBar(Parent->HWindow);
}
else
 FileSaved = TRUE:
 DrawMode = 0;
 GlobalScroller->ScrollTo(1,0);
 HMENU MainMenu = GetMenu(Parent->HWindow);
EnableMenuItem(MainMenu, CM_SIMLINE, MF_BYCOMMAND | MF_GRAYED);
```

```
EnableMenuItem(MainMenu,CM VIEWSIM,MF BYCOMMAND | MF GRAYED);
EnableMenuItem(MainMenu, CM FILESAVE, MF BYCOMMAND | MF GRAYED);
EnableMenuItem(MainMenu,CM FILESAVEAS,MF BYCOMMAND | MF GRAYED);
EnableMenuItem(MainMenu,CM EXPORT,MF BYCOMMAND | MF GRAYED);
EnableMenuItem(MainMenu,CM PRINT,MF BYCOMMAND | MF GRAYED);
 EnableMenuItem(MainMenu,CM VIEWBOTH,MF BYCOMMAND | MF GRAYED):
 EnableMenuItem(MainMenu, CM VIEWPAGED, MF BYCOMMAND | MF GRAYED);
 EnableMenuItem(MainMenu,CM FILEOPEN,MF BYCOMMAND | MF ENABLED);
DrawMenuBar(Parent->HWindow);
}
// DEFINITION OF FILE MENU FUNCTIONS BEGINS HERE
        // this command erases the screen and clears the experimental and
        // simulated spectrum from memory after prompting the user to
     // save their work
void TPolarWindow::CMFileNew (RTMessage)
 BOOL Clear = TRUE;
 if (!FileSaved)
  if (MessageBox(HWindow,"Do you wish to save?", "File not Saved",
        MB YESNO | MB ICONQUESTION) == IDYES)
   Clear = FALSE:
 if (Clear)
  DrawMode = 0;
  Scroller->ScrollTo(1,0):
  InvalidateRect(HWindow,NULL,TRUE);
  UpdateWindow(HWindow);
  Freq = 9400;
  SimType = 1;
  NumberGroups = 0;
  gx = 2.0023;
  gy = 2.0023;
  gz = 2.0023;
  StepSize = 15;
  NoDiv = 5:
  MemTheta = 0;
  MemPhi = 0:
  CrystalPhi = 0;
  CrystalTheta = 0;
  Dalpha = 30:
  Omega = 0;
  Wobble = 5:
  Linewidth = 2;
  Integrate = FALSE;
  Back 1 = 0;
  Tilt = 0:
  AccurGen = TRUE;
  PrevSave = FALSE;
  FileSaved = TRUE:
```

```
PrecurDou = TRUE:
 SpecCRPP = FALSE;
 Ratio = 5:
 Exchange = 5;
 for (int a=0:a<1024:++a)
 {
  xepr[a] = 0;
  yepr[a] = 0;
 for (int b=0;b<512;++b)
  spec[b] = 0:
 SimTrue = FALSE;
 ExperLoaded = FALSE:
 for (int c=0;c<8;++c)
  NucleiPerGroup[c] = 0:
  NuclearSpin[c] = 0;
  Theta[c] = 0:
  Phi[c] = 0;
  Psi[c] = 0:
  for (int d=0;d<3;++d)
      for (int e=0; e<3; ++e)
       AHyp[e][d][c] = 0;
  }
 HMENU MainMenu = GetMenu(HWindow);
 EnableMenuItem(MainMenu,CM FILESAVE,MF_BYCOMMAND | MF_GRAYED);
 EnableMenuItem(MainMenu,CM FILESAVEAS,MF BYCOMMAND | MF GRAYED);
 EnableMenuItem(MainMenu,CM IMPORT,MF BYCOMMAND | MF ENABLED);
 EnableMenuItem(MainMenu, CM EXPORT, MF BYCOMMAND | MF GRAYED);
 EnableMenuItem(MainMenu.CM FILEOPEN.MF BYCOMMAND | MF ENABLED);
 EnableMenuItem(MainMenu, CM PRINT, MF BYCOMMAND | MF GRAYED);
 EnableMenuItem(MainMenu, CM VIEWEXPER, MF BYCOMMAND | MF GRAYED);
 EnableMenuItem(MainMenu, CM VIEWSIM, MF BYCOMMAND | MF GRAYED);
 EnableMenuItem(MainMenu, CM VIEWBOTH, MF BYCOMMAND | MF GRAYED);
 EnableMenuItem(MainMenu,CM VIEWPAGED,MF BYCOMMAND | MF GRAYED);
 EnableMenuItem(MainMenu, CM VIEWEXPER, MF BYCOMMAND | MF GRAYED);
 EnableMenuItem(MainMenu,CM INTEGBASE, MF BYCOMMAND | MF GRAYED);
  EnableMenuItem(MainMenu,CM INTEGBASEORG, MF BYCOMMAND | MF GRAYED);
  EnableMenuItem(MainMenu,CM INTEGEPR,MF BYCOMMAND | MF GRAYED);
  EnableMenuItem(MainMenu,CM DRAWINTEG,MF BYCOMMAND | MF GRAYED):
 EnableMenuItem(MainMenu, CM SIMLINE, MF_BYCOMMAND | MF_GRAYED);
 DrawMenuBar(HWindow):
}
}
       // this command opens a previously saved simulated spectrum along
       // with the experimental spectrum if one was saved
void TPolarWindow::CMFileOpen (RTMessage)
SetCursor(LoadCursor(NULL,IDC WAIT));
```

```
if (GetApplication()->ExecDialog(new TFileDialog(this,SD_FILEOPEN,
  strcpy(FileName1,"*.sim"))) == IDOK)
 ifstream ifs(FileName1);
 if (!ifs.bad())
  char VersionTest [30];
  ifs.getline(VersionTest,30);
  if (strcmp(VersionTest, "Sim Pol Program Version 1.0") == 0)
   ifs >> HMax >> HMin;
   ifs >> SimType >> Freq >> NumberGroups;
   ifs \gg gx \gg gy \gg gz;
   ifs >> StepSize >> NoDiv >> Dalpha;
   ifs >> MemTheta >> MemPhi >> Omega;
   ifs >> Wobble >> Linewidth >> CrystalTheta >> CrystalPhi;
   for (int a = 0; a < 8; ++a)
    ifs >> NucleiPerGroup[a] >> NuclearSpin[a];
   for (int b=0;b<8;++b)
    ifs >> Theta[b] >> Phi[b] >> Psi[b];
   for (int c=0; c<8; ++c)
    ifs >> AHyp[0][0][c] >> AHyp[1][1][c] >> AHyp[2][2][c];
   for (int d=0;d<512;++d)
    ifs >> spec[d];
   int Speccrrp;
   int Precurdou;
   ifs >> Speccrrp >> Precurdou >> Exchange >> Ratio;
   if (Speccrrp == 1)
        SpecCRPP = TRUE;
    SpecCRPP = FALSE;
   if (Precurdou == 2)
        PrecurDou = TRUE:
   else
        PrecurDou = FALSE;
   DrawMode = 1;
   Scroller->ScrollTo(1,0);
   InvalidateRect(HWindow, NULL, TRUE);
   PrevSave = TRUE;
   FileSaved = TRUE;
   SimTrue = TRUE;
   HMENU MainMenu = GetMenu(HWindow);
   EnableMenuItem(MainMenu, CM_SIMLINE, MF_BYCOMMAND | MF_ENABLED);
   EnableMenuItem(MainMenu,CM VIEWSIM,MF BYCOMMAND | MF ENABLED);
   EnableMenuItem(MainMenu, CM FILESAVE, MF_BYCOMMAND | MF_ENABLED);
   EnableMenuItem(MainMenu, CM_FILESAVEAS, MF_BYCOMMAND | MF_ENABLED);
```

```
EnableMenuItem(MainMenu, CM EXPORT, MF BYCOMMAND | MF ENABLED);
   EnableMenuItem(MainMenu,CM PRINT,MF BYCOMMAND | MF ENABLED);
   EnableMenuItem(MainMenu,CM FILEOPEN,MF BYCOMMAND | MF GRAYED);
   EnableMenuItem(MainMenu,CM VIEWEXPER, MF BYCOMMAND | MF GRAYED);
   EnableMenuItem(MainMenu.CM INTEGEPR,MF BYCOMMAND | MF GRAYED);
   EnableMenuItem(MainMenu,CM DRAWINTEG,MF BYCOMMAND | MF ENABLED);
   if (ExperLoaded)
    EnableMenuItem(MainMenu,CM VIEWBOTH,MF BYCOMMAND | MF ENABLED);
    EnableMenuItem(MainMenu,CM VIEWPAGED, MF BYCOMMAND | MF ENABLED);
       EnableMenuItem(MainMenu,CM VIEWEXPER, MF BYCOMMAND | MF ENABLED);
       EnableMenuItem(MainMenu,CM INTEGBASE, MF BYCOMMAND | MF ENABLED);
       EnableMenuItem(MainMenu, CM INTEGBASEORG, MF BYCOMMAND | MF ENABLED);
   DrawMenuBar(HWindow);
   }
  else
   {
   MessageBox(HWindow, "File must be a *.sim file", "Incorrect File Format",
              MB OK | MB ICONSTOP);
   }
 }
 else
   MessageBox(HWindow, "File cannot be opened", "File Error",
              MB OK | MB ICONSTOP);
 }
SetCursor(LoadCursor(NULL,IDC_ARROW));
        // command to import an experimental spectrum to compare with a
        // simulated spectrum that will be created
void TPolarWindow::CMFileImport (RTMessage )
  // create a file selection box
if (GetApplication()->ExecDialog(new TFileDialog(this,
   SD FILEOPEN, strcpy(FileName, "*.DAT"))) == IDOK)
  // Actual creation of the Import window
ImportWindow = new TImportWindow(this, "Import File");
ImportFileWindow = new TFileWindow(this, "FileWindow",
       FileName);
// Import file window attributes
 ImportFileWindow->Attr.X=20;
ImportFileWindow->Attr.Y=230;
ImportFileWindow->Attr.W=600;
ImportFileWindow->Attr.H=240;
// Makes the import window interface elements
GetApplication()->MakeWindow(ImportFileWindow):
GetApplication()->MakeWindow(ImportWindow);
 }
```

}

// command that saves a simulated spectrum that has been

```
// previously saved
void TPolarWindow::CMFileSave (RTMessage)
 if (!PrevSave)
 if (GetApplication()->ExecDialog(new TFileDialog(this,SD FILESAVE,
                 strcpy(FileName1,"*.sim"))) == IDOK)
 FileSave();
 }
 else
 FileSave();
        // command that saves a spectrum that has not been saved
         // previously or to save under a different name
void TPolarWindow::CMFileSaveAs (RTMessage)
 if (GetApplication()->ExecDialog(new TFileDialog(this,SD_FILESAVE,
                   strcpy(FileName1,"*.sim"))) == IDOK)
 FileSave();
}
         // exports the simulated spectrum in an x,y ASCII format text file
void TPolarWindow::CMFileExport (RTMessage)
 if (GetApplication()->ExecDialog(new TFileDialog(this,SD_FILESAVE,
   strcpy(FileName2, "*.dat"))) == IDOK)
 int tempDrawMode = DrawMode;
 DrawMode = 10;
 PolarDC = GetDC(HWindow);
 DrawSpectrum(PolarDC);
 ReleaseDC(HWindow,PolarDC);
 DrawMode = tempDrawMode;
}
         // command to print a simulation and experimental spectrum
void TPolarWindow::CMPrint (RTMessage)
memset(&pd,0,sizeof(PRINTDLG));
pd.lStructSize = sizeof (PRINTDLG);
pd.hwndOwner = HWindow;
pd.Flags = PD_RETURNDC | PD_HIDEPRINTTOFILE | PD_NOPAGENUMS | PD_NOSELECTION |
         PD_ALLPAGES | PD_SHOWHELP;
if (PrintDlg(&pd) != 0)
 int tempDrawMode = DrawMode;
 DrawMode = 11;
 DrawSpectrum(pd.hDC);
 DrawMode = tempDrawMode;
 if (pd.hDevMode != NULL)
 GlobalFree(pd.hDevMode);
 if (pd.hDevNames != NULL)
```

```
GlobalFree(pd.hDevNames);
}
else
MessageBox(HWindow, "Unable to print!", "Printer Error", MB OK | MB ICONINFORMATION);
         // configures a printer to print
void TPolarWindow::CMPrintSetup (RTMessage )
memset(&pd,0,sizeof(PRINTDLG));
pd.1StructSize = sizeof(PRINTDLG);
pd.hwndOwner = HWindow;
pd.Flags = PD PRINTSETUP | PD SHOWHELP;
if (PrintDlg(\&pd) != 0)
 if (pd.hDevMode != NULL)
  GlobalFree(pd.hDevMode);
  if (pd.hDevNames != NULL)
  GlobalFree(pd.hDevNames);
 }
else
MessageBox(HWindow, "Printer is not initialized!", "Printer Initialization Error",
       MB_OK | MB_ICONEXCLAMATION);
         // exits the program after checking that all data is saved
void TPolarWindow::CMExit (RTMessage)
 CloseWindow();
// determines if the main window can be closed
BOOL TPolarWindow::CanClose()
{
 if (FileSaved)
 return TRUE;
 else if (MessageBox(HWindow, "Do you wish to save?", "File not saved",
         MB YESNO | MB ICONOUESTION) == IDNO)
 return TRUE;
 else
 return FALSE:
// THIS IS THE END OF THE FILE MENU FUNCTIONS
// VIEW MENU FUNCTIONS BEGIN HERE
         // Shows the experimental spectrum on the screen
void TPolarWindow::CMViewExper (RTMessage )
 DrawMode=2;
 Scroller->ScrollTo(1,0);
 InvalidateRect(HWindow,NULL,TRUE);
 UpdateWindow(HWindow);
}
```

```
// Shows the simulated spectrum on the screen
void TPolarWindow::CMViewSim (RTMessage)
 DrawMode=1;
 Scroller->ScrollTo(1.0):
 InvalidateRect(HWindow, NULL, TRUE);
 UpdateWindow(HWindow);
     // Shows both the simulated and experimental spectrum on the screen
void TPolarWindow::CMViewBoth (RTMessage)
 DrawMode=3:
 Scroller->ScrollTo(1.0);
 InvalidateRect(HWindow, NULL, TRUE);
 UpdateWindow(HWindow);
         // Shows both spectra but in different windows
void TPolarWindow::CMViewPaged (RTMessage)
 DrawMode=4;
 Scroller->ScrollTo(1,0);
 InvalidateRect(HWindow, NULL, TRUE);
 UpdateWindow(HWindow);
// END OF THE VIEW MENU FUNCTIONS
// BEGIN THE SIMULATION MENU FUNCTIONS
void TPolarWindow::CMSimParam (RTMessage)
 ParamWindow = new TParamWindow(this, "Simulation Parameters");
 GetApplication()->MakeWindow(ParamWindow);
// Does the actual simulation of the EPR spectrum
void TPolarWindow::CMSimulate(RTMessage)
 FieldWindow = new TFieldWindow(this, "Calculated Maximum and Minimum H values");
 GetApplication()->MakeWindow(FieldWindow);
// query the user for the polarization parameters
void TPolarWindow::CMSimPolParam(RTMessage)
 PolParamWindow = new TPolParamWindow(this, "Polarization Parmeters");
 GetApplication()->MakeWindow(PolParamWindow);
// Redraw the spectrum with new linewidth parameter
void TPolarWindow::CMSimLineChange(RTMessage)
 char LineText [10];
 float LineOld = Linewidth;
 gcvt(2*Linewidth,5,LineText);
```

```
if (GetApplication()->ExecDialog(new TInputDialog(this, "Linewidth",
    "Input a new linewidth", LineText, sizeof LineText)) == IDOK)
  Linewidth = atof(LineText)/2;
   HMax = HMax - 5*LineOld + 5*Linewidth;
   HMin = HMin + 5*LineOld - 5*Linewidth:
  FileSaved = FALSE:
 Scroller->ScrollTo(1.0):
 InvalidateRect(HWindow, NULL, TRUE);
 UpdateWindow(HWindow);
// Begin integrate menu functions
void TPolarWindow::CMIntegDrawInteg (RTMessage)
 Integrate = TRUE;
 HMENU MainMenu = GetMenu(HWindow);
 EnableMenuItem(MainMenu,CM DRAWINTEG,MF BYCOMMAND | MF GRAYED);
 EnableMenuItem(MainMenu,CM INTEGEPR,MF BYCOMMAND | MF ENABLED);
 Scroller->ScrollTo(1,0);
 InvalidateRect(HWindow,NULL,TRUE);
 UpdateWindow(HWindow);
void TPolarWindow::CMIntegEPR (RTMessage)
 Integrate = FALSE;
 HMENU MainMenu = GetMenu(HWindow);
 EnableMenuItem(MainMenu,CM DRAWINTEG,MF BYCOMMAND | MF ENABLED);
 EnableMenuItem(MainMenu, CM_INTEGEPR, MF_BYCOMMAND | MF_GRAYED);
 Scroller->ScrollTo(1,0);
 InvalidateRect(HWindow, NULL, TRUE);
 UpdateWindow(HWindow);
void TPolarWindow::CMIntegBase(RTMessage)
 char Background [5];
 gcvt(Back1,3,Background);
 char TiltText [10];
 gcvt (Tilt,6,TiltText);
 if (GetApplication()->ExecDialog(new TInputDialog(this, "Background",
        "Enter the amount to raise or lower the Background:", Background,
        sizeof Background)) == IDOK)
 {
  Integrate = TRUE;
  Back1 = atof(Background);
 if (GetApplication()->ExecDialog(new TInputDialog(this, "Tilt",
 "Enter the amount in degrees to tilt the baseline:", TiltText,
 sizeof TiltText)) == IDOK)
  Integrate = TRUE;
  Tilt = atof(TiltText);
  if (Tilt > 20)
```

```
Tilt = 20;
  Tilt = (xepr[DataNumber]-xepr[0])*tan(Tilt*0.174532);
  Tilt /= (DataNumber - 1);
 if (Integrate)
 HMENU 382X HMENU MainMenu = GetMenu(HWindow);
 EnableMenuItem(MainMenu,CM_DRAWINTEG,MF_BYCOMMAND | MF_GRAYED);
 EnableMenuItem(MainMenu, CM_INTEGEPR, MF_BYCOMMAND | MF_ENABLED);
 Scroller->ScrollTo(1,0);
 InvalidateRect(HWindow,NULL,TRUE);
 UpdateWindow(HWindow);
 }
void TPolarWindow::CMIntegBaseOrg (RTMessage)
 Tilt = 0;
 Back1 = 0;
 Integrate = TRUE;
 HMENU MainMenu = GetMenu(HWindow);
 EnableMenuItem(MainMenu, CM_DRAWINTEG, MF_BYCOMMAND | MF_GRAYED);
 EnableMenuItem(MainMenu, CM_INTEGEPR, MF_BYCOMMAND | MF_ENABLED);
 Scroller->ScrollTo(1,0);
 InvalidateRect(HWindow,NULL,TRUE);
 UpdateWindow(HWindow);
}
// Begin other utility functions that are used for program
// function that actually saves the file
void TPolarWindow::FileSave()
SetCursor(LoadCursor(NULL,IDC_WAIT));
ofstream of(FileName1);
if (!of.bad())
 of << "Sim Pol Program Version 1.0\n";
 of << HMax << " " << HMin << "\n";
 of << SimType << " " << Freq << " " << NumberGroups << "\n";
 of << g_X << " " << g_Y << " " << g_Z << " \n";
 of << StepSize << " " << NoDiv << " " << Dalpha << "\n";
 of << MemTheta << " " << MemPhi << " " << Omega << "\n";
 of << Wobble << " " << CrystalTheta << " " << CrystalPhi << "\n";
 for (int a = 0; a < 8; ++a)
  of << NucleiPerGroup[a] << " " << NuclearSpin[a] << "\n";
 for (int b=0;b<8;++b)
  of << Theta[b] << " " << Phi[b] << " " << Psi[b] << "\n";
 for (int c=0;c<8;++c)
  of << AHyp[0][0][c] << " " << AHyp[1][1][c] << " " << AHyp[2][2][c] << "\n";
```

```
for (int d=0;d<512;++d)
  of << spec[d] << "\n";
 if (SpecCRPP)
 of << "1";
 else
 of << "0";
 if (PrecurDou)
 of << " " << "2";
 of << " " << "4";
 of << " " << Exchange << " " << Ratio;
 of.close();
 FileSaved = TRUE;
SetCursor(LoadCursor(NULL,IDC_ARROW));
 // this function redraws the experimental spectrum
void TPolarWindow::Paint(HDC PDC,PAINTSTRUCT& )
 PaintPen = CreatePen(PS_SOLID, 1,0x00FF0000);
 SelectObject(PDC,PaintPen);
 if (ExperLoaded || SimTrue)
  if (DrawMode != 0 \parallel DrawMode > 9)
  DrawSpectrum(PDC);
 DeleteObject(PaintPen);
// Function that registers the window class
LPSTR TPolarWindow::GetClassName()
 return "PolarWindow";
}
// function that displays the help index for Polar Sim
void TPolarWindow::CMHelpIndex (RTMessage)
 WinHelp(HWindow, "simhelp.hlp", HELP_INDEX, 0);
 helpb = TRUE;
void TPolarWindow::CMHelpOnHelp(RTMessage)
 WinHelp(HWindow, "simhelp.hlp", HELP_HELPONHELP,0);
}
// function that displays help on commands in polar Sim
void TPolarWindow::CMCommands(RTMessage)
 WinHelp(HWindow, "simhelp.hlp", HELP CONTEXT, 500);
 helpb = TRUE;
```

```
}
// Function to change window characteristics
void TPolarWindow::GetWindowClass(WNDCLASS& AWndClass)
 TWindow::GetWindowClass(AWndClass);
 AWndClass.hIcon = LoadIcon(GetApplication()->hInstance, "ICON_1");
// Function that does the actual simulation of the spectrum
void TFieldWindow::SimulateSpectrum()
  SetCursor(LoadCursor(NULL,IDC WAIT));
  float hhfp[3],hhfm[3];
  float heffp[3],heffm[3];
  float magheffp=0;
  float magheffm=0;
  float CouplingMax=0;
  float htheta=0;
  const float factor = 658.2109:
  float Wobble 1=0, weight=0;
  float geff=0,h=0,bigsplit=0,smasplit=0,bigintens=0,smaintens=0,x=0;
  int h1=0.center=0:
  float const convert = 0.017453292;
  float x1=0,y1=0,z1=0;
  float ah1 [3][3];
  float dc[3],dcg[3];
  float ahrot[3][3][8];
  float thetatemp=0,phitemp=0,a=0;
  float tx[3][3];
  float strmos=0,endmos=0,hohm=0,steep=0,alpha=0;
  int nflag=0,oddint=0;
  float cph=0,sph=0,cth=0,sth=0,cps=0,sps=0;
  float t[3][3];
  float gaussperch=0;
  float r[512],rn[512];
  gaussperch = (HMax - HMin)/511;
  HWND MainHandle = GetActiveWindow();
  PolarDC = GetDC(MainHandle);
  MessageBox(MainHandle, "Press F4 to abort", "To cancel", MB_OK | MB_ICONINFORMATION);
  if (SpecCRPP)
 float couplingmax;
 float coupling = 0;
  if (NumberGroups > 0)
   for (int a=0;a<NumberGroups;++a)
    coupling = 0;
    for (int b=0;b<3;++b)
         couplingmax = AHyp[b][b][a] * NucleiPerGroup[a] * NuclearSpin[a];
         if (couplingmax > coupling)
     coupling = couplingmax;
```

```
CouplingMax += coupling;
CouplingMax /= gaussperch;
 for (int aa=0;aa< 3;++aa)
  dc[aa]=0;
  dcg[aa]=0;
  hhfp[aa]=0;
  hhfm[aa]=0;
  heffp[aa]=0;
  heffm[aa]=0;
  for (int bb=0;bb<3;++bb)
   ah1[aa][bb] = 0.0;
   tx [aa][bb] = 0.0;
   t [aa][bb] = 0.0;
   for (int cc=0;cc<8;++cc)
        ahrot[aa][bb][\infty] = 0.0;
  }
 for (int u = 0; u < 512; ++u)
  r[u] = 0.0;
  rn[u] = 0.0;
  spec [u] = 0.0;
 if (SimType == 1)
  thetatemp = 0;
  phitemp = 0;
 if (SimType == 2)
  if (Wobble == 0)
   Wobble 1 = 2;
   Wobble = 1;
  else
   if (Wobble < 45)
     Wobble 1 = 2 * Wobble;
   else
     Wobble 1 = 90;
  if (Omega < 0)
  Omega = -Omega;
  if (Omega == 0)
   if ((int)(NoDiv/2) == NoDiv/2)
```

```
NoDiv += 1;
  strmos = Omega - Wobble1;
  endmos = Omega + Wobble1;
  if (strmos >= 0)
   nflag = 0;
   steep = (cos(strmos*convert) - cos(endmos*convert))/ NoDiv;
  else
    nflag = 1;
    if (Omega == 0)
     steep = (2 - cos(strmos*convert) - cos(endmos*convert)) / NoDiv;
    else
     if (Omega >= fabs(strmos))
          strmos = -Omega;
         oddint = 1 + 2 * (NoDiv/2);
         steep = 2 / oddint * (1 - cos(strmos*convert));
         NoDiv = (2 - cos(endmos*convert) - cos(strmos*convert))/steep;
    }
   hohm = strmos;
   alpha = 0.0;
if (NumberGroups > 0)
 for (int b=0;b<NumberGroups;++b)
   for(int c=0;c<3;++c)
    ah1[c][c] = AHyp[c][c][b];
   cph = cos(Phi[b]*convert);
   sph = sin(Phi[b]*convert);
   cth = cos(Theta[b]*convert);
   sth = sin(Theta[b]*convert);
   cps = cos(Psi[b]*convert);
   sps = sin(Psi[b]*convert);
   t[0][0] = cps * cth * cph - sps * sph;
   t[0][1] = cps * cth * sph + sps * cph;
   t[0][2] = -cps * sth;
   t[1][0] = -sps * cth * cph - cps * sph;
   t[1][1] = -sps * cth * sph + cps * cph;
   t[1][2] = sps * sth;
   t[2][0] = sth * cph;
   t[2][1] = sth * sph;
   t[2][2] = cth;
   for (int x=0; x<3; ++x)
    for (int d=0;d<3;++d)
         a = 0.0;
```

```
for (int e=0; e<3; ++e)
          a = a + t[x][e] * ahl[e][d];
         }
         tx[x][d] = a;
    }
   }
   for (int f=0;f<3;++f)
    for (int g=0;g<3;++g)
    {
         a = 0.0;
         for (int h=0;h<3;++h)
          a = a + tx[f][h] * t[g][h];
         ahrot[f][g][b] = a;
    }
   }
 }
}
 top:
 if (SimType == 1)
   dc[0] = cos(phitemp*convert) * sin(thetatemp*convert);
   dc[1] = sin(phitemp*convert) * sin(thetatemp*convert);
  dc[2] = cos(thetatemp*convert);
 if (SimType == 2)
   weight = exp((-log(2) * pow((hohm - Omega),2)) / pow(Wobble,2)) / Wobble;
   goniomf(MemTheta,MemPhi,alpha,hohm,x1,y1,z1);
   dc[0] = x1;
   dc[1] = y1;
   dc[2] = z1;
 if (SimType == 3)
   dc[0] = cos(CrystalPhi*convert) * sin(CrystalTheta*convert);
   dc[1] = sin(CrystalPhi*convert) * sin(CrystalTheta*convert);
   dc[2] = cos(CrystalTheta*convert);
 if (SimType == 4)
   geff = sqrt((pow(gx,2) + pow(gy,2) + pow(gz,2)) / 3);
   h = 0.714484 * Freq / geff;
  h1 = (h-HMin) / gaussperch;
 }
 else
   geff = sqrt(pow((gx * dc[0]).2) + pow((gy*dc[1]).2) + pow((gz*dc[2]).2));
   h = 0.714484 * Freq / geff;
   h1 = (h - HMin) / gaussperch;
 }
```

```
if (h1 \ge 0 \&\& h1 < 511)
  if (SimType == 1)
   r[h1] = sin(thetatemp*convert) * geff;
   if (thetatemp == 0)
   r[h1] = 0.784 * geff;
  if (SimType == 2)
  r[h1] = weight * geff;
  if (SimType == 3)
  r[h1] = 100;
  if (SimType == 4)
  r[h1] = 100;
 else
 MessageBox(GetActiveWindow(), "Transition is not within the spectral limits",
           "Magnetic Field Limit Error", MB ICONSTOP | MB OK);
if (NumberGroups > 0)
 if (SimType < 4)
  dcg[0] = gx * dc[0] / geff;
  dcg[1] = gy * dc[1] /geff;
  dcg[2] = gz * dc[2] / geff;
 for (int k=0;k<NumberGroups;++k)
  if (NucleiPerGroup[k] > 0)
   if (SimType < 4)
        a = 0:
        if (NuclearSpin[k] > 0.6)
        AccurGen = FALSE;
        if (!AccurGen)
        {
         for (int l=0; l<3; ++1)
           for (int m=0; m<3;++m)
            for (int n=0; n<3; ++n)
                 a = a + dcg[l]*ahrot[l][n][k]*ahrot[n][m][k]*dcg[m];
            }
           }
         bigsplit = sqrt(a) / gaussperch;
         bigintens = 1;
         smasplit = 0;
         smaintens = 0;
        }
        else
        {
```

```
for (int ll=0;ll<3;++ll)
      for (int mm=0;mm<3;++mm)
       a = a + dcg[mm]*ahrot[mm][ll][k];
      }
      hhfp[11] = a*(-0.5)*factor;
      hhfm[ll] = a*0.5*factor;
      a = 0:
     magheffp = 0;
 magheffm = 0;
     for (int p=0; p<3; ++p)
      heffp[p] = h * dc[p] + hhfp[p];
      heffm[p] = h * dc[p] + hhfm[p];
       magheffp = magheffp + pow(heffp[p], 2);
       magheffm = magheffm + pow(heffm[p],2);
     magheffp = sqrt(magheffp);
     magheffm = sqrt(magheffm);
     bigsplit = (magheffp + magheffm) / factor / gaussperch;
     smasplit = (magheffp - magheffm) / factor / gaussperch;
      htheta = heffp[0] + heffm[0] + heffp[1] + heffm[1] + heffp[2] + heffm[2]; 
     if (magheffp*magheffm > 0)
       htheta /= (magheffp*magheffm);
       if (htheta > 1)
       htheta = 0;
       else if (htheta < -1)
       htheta = 180;
       else if (htheta \ge -1 && htheta \le 1)
       htheta = 57.29608*acos(htheta);
     else
       htheta = 0;
     bigintens = pow(sin(htheta*convert/2),2);
      smaintens = pow(cos(htheta*convert/2),2);
    }
if (SimType == 4)
    smaintens = 0;
    smasplit = 0;
    bigintens = 1;
    bigsplit = 0;
    for (int l=0; l<3; ++1)
      bigsplit += AHyp[1][1][k] / 3;
 bigsplit /= gaussperch;
for (int l=0;l<NucleiPerGroup[k];++l)
```

```
for(int m=0; m<512; ++m)
          if (r[m] > 0)
          {
           center = m;
           if (NuclearSpin[k] < 1)
            float newintens = r[center] * bigintens;
            int newpos = center - (bigsplit / 2);
            if (newpos \geq 0 && newpos \leq 511)
              rn[newpos] += newintens;
         newpos = center + (bigsplit / 2);
            if (newpos \geq 0 \&\& newpos \leq 511)
              rn[newpos] += newintens;
            if (smaintens > 0)
             {
              newintens = r[center] * smaintens;
              newpos = center - (smasplit/2);
              if (newpos \geq 0 \&\& newpos \leq 512)
               rn[newpos] += newintens;
              newpos = center + (smasplit/2);
              if (newpos \geq 0 \&\& newpos \leq 512)
                  rn[newpos] += newintens;
            }
           }
           else
            float intens = r[center];
         int newpos;
             for (int g=-2*NuclearSpin[k];g<2*NuclearSpin[k]+1;g+=2)
             {
                 newpos = center + g/2 * bigsplit;
                 if (newpos \geq 0 && newpos \leq 512)
                  rn[newpos] += intens;
             }
           }
         }
    }
         for (int j=0; j<512;++j)
          r[j] = rn[j];
          rn[j] = 0;
   }
MSG Stopmessage;
BOOL SimStop = FALSE;
if (PeekMessage(&Stopmessage,MainHandle,WM_KEYDOWN,WM_KEYDOWN,PM_NOYIELD |
PM_REMOVE))
 if (Stopmessage.wParam == VK F4)
   SimStop = TRUE;
```

```
}
if (SpecCRPP)
 float tempratio=0;
 int count = Exchange/gaussperch;
 for(int k=0;k<512;++k)
  if (r[k] > 0)
   if((h1 - k > 0) \&\& PrecurDou)
        if (Exchange != 0)
         tempratio = (Ratio - 1)*(h1-k)/(CouplingMax)+1;
         if ((k-count/2 \ge 0) && (k-count/2 < 512))
          rn[k-count/2] = -1/(tempratio + 1)*r[k];
         if ((k+count/2 >= 0) && (k+count/2 < 512))
          rn[k+count/2] = tempratio/(tempratio + 1)*r[k];
        }
    else if ((h1-k > 0) && !PrecurDou)
        if (Exchange != 0)
         tempratio = (Ratio - 1)*(h1-k)/(CouplingMax)+1;
         if ((k-count/2 \ge 0) && (k-count/2 \le 512))
          rn[k-count/2] = 1/(tempratio + 1)*r[k];
         if ((k+count/2 >= 0) && (k+count/2 < 512))
          rn[k+count/2] = -tempratio/(tempratio + 1)*r[k];
         }
        else
        rn[k] = -r[k];
    else if ((h1 - k < 0) \&\& PrecurDou)
        if (Exchange != 0)
         tempratio = (Ratio - 1)*(k-h1)/(CouplingMax)+1;
         if ((k-count/2 \ge 0) && (k-count/2 < 512))
          rn[k-count/2] = -tempratio/(tempratio + 1)*r[k];
         if ((k+count/2 >= 0) && (k+count/2 < 512))
          rn[k+count/2] = 1/(tempratio + 1)*r[k];
         }
        else
        rn[k] = -r[k];
    else if ( (h1 - k < 0) && !PrecurDou)
        if (Exchange != 0)
          tempratio = (Ratio - 1)*(k-h1)/(CouplingMax)+1;
         if ((k-count/2 \ge 0) && (k-count/2 \le 512))
          rn[k-count/2] = tempratio/(tempratio + 1)*r[k];
```

```
if ((k+count/2 \ge 0) & (k+count/2 < 512))
          rn[k+count/2] = -1/(tempratio + 1)*r[k];
   else if (h1 - k == 0)
        if (Exchange !=0)
         if (PrecurDou)
           if ((k-count/2 \ge 0) && (k-count/2 < 512))
           rn[k-count/2] = -0.5*r[k];
           if ((k+count/2 \ge 0) & (k+count/2 < 512))
            rn[k+count/2] = 0.5*r[k];
          else
          if ((k-count/2 \ge 0) & (k-count/2 \le 512))
           rn[k-count/2] = 0.5*r[k];
          if ((k+count/2 \ge 0) && (k+count/2 < 512))
           rn[k+count/2] = -0.5*r[k];
 }
for (int j=0; j<512;++j)
if (!SpecCRPP)
 spec[j] += r[j];
 r[j] = 0;
 }
else
 spec[j] +=rn[j];
 r[j] = 0;
 rn[j] = 0;
}
}
 if (SimType == 1)
  char ThetaText[5];
  char PhiText[5];
  RECT Change;
  Change.left = 210;
  Change.top = 280;
  Change.right = 350;
  Change.bottom = 330;
  gcvt(thetatemp,4,ThetaText);
  gcvt(phitemp,4,PhiText);
  if (SimStop)
  goto bottom;
```

```
TextOut(PolarDC, 100, 150, "Calculating the stick spectrum", 30);
TextOut(PolarDC,200,250,"Theta is",8);
TextOut(PolarDC,400,250,"Phi is",6);
SetTextColor(PolarDC,0x00FFFFFF);
DrawText(PolarDC,ThetaText,-1,&Change,DT_TOP);
OffsetRect(&Change, 200, 0);
DrawText(PolarDC,PhiText,-1,&Change,DT_TOP);
gcvt(thetatemp+StepSize,4,ThetaText);
gcvt(phitemp+StepSize,4,PhiText);
SetTextColor(PolarDC,0x00000000);
OffsetRect(&Change, -200,0);
DrawText(PolarDC,ThetaText,-1,&Change,DT_TOP);
OffsetRect(&Change, 200, 0);
DrawText(PolarDC,PhiText,-1,&Change,DT_TOP);
if (thetatemp == 0)
 thetatemp = StepSize;
 phitemp = 0;
 goto top;
 }
phitemp += StepSize;
if (phitemp < 180)
  goto top;
phitemp = 0;
thetatemp += StepSize;
 if (thetatemp < 180)
  goto top;
if (SimType == 2)
 alpha += Dalpha;
 if (alpha < 360)
  goto top;
 alpha = 0;
 if (hohm \geq endmos * 1.03)
 goto bottom;
 if (nflag == 0)
  x = cos(hohm*convert) - steep;
  hohm = acos(x);
 }
 else
  x = cos(hohm*convert) + steep;
  if (x<1)
  {
       hohm = -acos(x);
  }
  else
  {
       nflag = 0;
       hohm = acos(2-x);
  }
 }
```

```
if (hohm < endmos * 1.03)
    goto top;
 bottom:
  InvalidateRect(MainHandle, NULL, TRUE);
  SetCursor(LoadCursor(NULL,IDC_ARROW));
  if (!SimStop)
   MessageBox(MainHandle, "Valid Stick Spectrum exists", "Status", MB_OK);
   MessageBox(MainHandle, "Drawing the EPR spectrum", "Status", MB_OK);
   SimTrue = TRUE;
  }
  else
   MessageBox(MainHandle,"A valid spectrum does not exist", "Status",
                MB_OK | MB_ICONSTOP);
   SimTrue = FALSE;
   for (int a=0;a<512;++a)
    spec[a] = 0;
   }
 ReleaseDC(MainHandle,PolarDC);
// Construct TPolarization's MainWindow Data member
void TPolarization :: InitMainWindow()
 MainWindow = new TPolarWindow(NULL, "Polarization Simulation Program");
// Main program function for windows programs
int PASCAL WinMain (HANDLE hInstance, HANDLE hPrevInstance,
   LPSTR lpCmdLine, int nCmdShow)
//Create an object of application class TPolarization
 TPolarization Polarization ("Polarization", hInstance,
                 hPrevInstance, lpCmdLine, nCmdShow);
 Polarization.Run();
 return Polarization. Status;
}
```

